Cape Peninsula University of Technology

A performance and energy evaluation of a fertiliser-drawn forward osmosis (FDFO) system

by

Rhynhardt Lambrechts

Thesis submitted in fulfilment of the requirements for the degree

Master of Engineering: Chemical Engineering

in the Faculty of

Engineering

at the

Cape Peninsula University of Technology

Supervisor: Associate Professor Marshall Sheldon

Cape Town

December 2018

DECLARATION

I, Rhynhardt Lambrechts, declare that the contents of this thesis represent my own unaided work and that the thesis has not previously been submitted for academic examination towards any qualification. Furthermore, it represents my own opinions and not necessarily those of the Cape Peninsula University of Technology.

November 2018

Signed **Date**

ABSTRACT

Globally, water is considered an essential resource as it sustains human, animal and plant life. Water is not only essential for all forms of life but imperative for economic growth. The world's population is increasing at a disquieting rate, which will result in an increased demand for fresh water and food security. The agricultural industry is the main consumer of global freshwater and utilises fertilisers in order to meet food demands. The demand for water in South Africa (SA) has increased considerably due to the rapid expansion of the agricultural industry, and of the municipal and industrial sectors. Agricultural developments in SA are affected greatly as the country is facing a current drought crisis as a result of low rainfall and large water demands. With an abundance of saline water globally, desalinisation will be a major contributor to solving the global freshwater crisis. With limited fresh water resources accompanied by the agricultural industry as a major consumer, alternative measures are required to desalinate water specifically for agricultural use.

Forward osmosis (FO) is a membrane technology that gained interest over the past decade because it has several advantages over pressure-driven membrane processes such as reverse osmosis (RO). FO technology is based on the natural osmotic process which is driven by a concentration gradient between two solutions separated by a semi-permeable membrane. Naturally, water will permeate through the membrane from a solution of low solute concentration or low osmotic pressure (OP) known as a feed solution (FS) to a solution of a higher concentration or higher OP also known as a draw solution (DS). Whilst various research studies have contributed to several advances in FO, several process limitations such as reverse solute flux (RSF), concentration polarisation (CP) and membrane fouling remain problematic, hindering FO for large-scale applications. Further investigation is therefore warranted and crucial in order to understand how to mitigate these limitations to develop/improve future processes.

The aim of this study was to evaluate a fertiliser-drawn forward osmosis (FDFO) system by investigating the effects of membrane orientation, system flow rate, DS concentration, and membrane fouling on an FDFO systems performance and energy consumption. The FS used was synthetic brackish water with a sodium chloride (NaCl) content of 5 g/L whereas a potassium chloride (KCl) synthetic fertiliser was used as a DS. The membrane utilised was a cellulose triacetate (CTA) membrane and was tested in forward osmosis mode (FO mode) and pressure retarded osmosis mode (PRO mode) whilst the system flow rate was adjusted between 100, 200 and 400 mL/min. Additionally, the DS concentration was altered from 0.5, 1 and 2 M KCl, respectively.

Experiments were performed using a bench scale FO setup which comprised of an i) FO membrane cell, ii) a double head variable peristaltic pump for transporting FS and DS's respectively, iii) a digital scale to measure the mass of the DS, iv) a magnetic stirrer to agitate the FS, v) two reservoirs for the FS and DS, respectively, vi) a digital multiparameter meter to determine FS electrical conductivity (EC) and vii) a digital electrical multimeter to measure system energy consumption. Each experiment comprised of seven steps i) pre-FDFO membrane control, ii) membrane cleaning, iii) FDFO experiment, iv) post-FDFO membrane control, v) membrane cleaning, vi) membrane damage dye identification and vii) membrane cleaning. Pre- and post-FDFO membrane control experiments operated for 5 h whilst each membrane cleaning procedure operated for 30 min. The FDFO experiment operated for 24 h whilst the membrane damage dye identification operated until a minimum of 10 mL water was recovered.

The process parameter which largely contributed to a beneficial system performance and specific energy consumption (SEC) was the increase in DS concentration. Water fluxes increased approximately threefold from a DS concentration increase from 0.5 to 1 M, followed by an additional 30 to 50 % rise in water flux at a DS concentration increase 1 to 2 M. SEC decreased by 58 and 53 % for FO and PRO modes, respectively, with a DS concentration increase from 0.5 to 1 M. An additional 35 and 37 % SEC reduction for FO and PRO modes was obtained for a DS concentration increase from 1 to 2 M. Altering the membrane from FO to PRO did not contribute to a beneficial system performance nor did it improve SEC. However, at a DS concentration of 0,5 M, the PRO mode obtained a 5.3 % greater water recovery compared to the FO mode. Conversely, at a DS concentration of 1 and 2 M, the FO mode achieved 5.4 and 7.0 % greater water recoveries compared to the PRO mode. The increase in flow rate also did not increase system performance significantly, however, a fluctuation in system SEC was observed. Throughout the study, no membrane fouling was observed, however, possible minute traces of membrane fouling could be observed from the membrane surface electron microscope (SEM) images. Additionally, minor changes in post- FDFO membrane control water recovery results were noticed which support the possible occurrence of membrane fouling during the FDFO experiment.

Keywords: Forward osmosis, fertiliser-drawn forward osmosis, energy consumption, membrane orientation, flow rate, draw solution concentration.

ACKNOWLEDGEMENTS

I wish to thank:

- My supervisor, Associate Professor Marshall Sheldon, for her guidance, support, scientific input and work ethic.
- Ms Robyn Augustine for her assistance and support throughout this study.
- Dr Debbie de Jager and Mr Mohammed Rahman for their assistance and support.
- Dr Charon de Villiers and Professor Muhammad Ali Dhansay for their constant moral support, advice and encouragements, not only during this project but throughout the years.
- The City of Cape Town (Athlone Waste Water Treatment Works) for the use of their facility.

The financial assistance of the National Research Foundation towards this research is acknowledged. Opinions expressed in this thesis and the conclusions arrived at, are those of the author, and are not necessarily to be attributed to the National Research Foundation.

DEDICATION

For my mom, whose unconditional love and support gave me the strength to follow my dreams. Thank you, mom.

TABLE OF CONTENTS

LIST OF APPENDIXES

LIST OF FIGURES

LIST OF TABLES

LIST OF SYMBOLS

Symbol	Description	Units
A	Pipe cross-sectional area	m^2
A_m	Effective membrane area	m^2
$C_{FS_{t_1}}$	Mass concentration of the FS at time interval 1	g/L
$C_{FS_{t_2}}$	Mass concentration of the FS at time interval 2	g/L
$D_{Internal}$	Pipe internal diameter	m
f	Friction factor	Dimensionless
g	Gravitational acceleration	m/s^2
H	Total pressure head	m
$H_{Dynamic}$	Dynamic head	m
$H_{Elevation}$	Elevation head	m
$H_{Friction}$	Friction head	m
$H_{Pressure}$	Pressure head	m
H_{Static}	Static head	m
$H_{Velocity}$	Velocity head	m
$h_{Discharge}$	Discharge height	m
$h_{Suction}$	Suction height	m
I_{Amp}	Electrical current (Ampere)	A
J_W	Water flux	$L/m^2.h$
J_S	Reverse solute flux	$g/m^2.h$
K	Equipment pressure drop	Dimensionless
L	Pipe length	m
$m_{DS_{t_1}}$	The mass of DS at time interval 1	g
$m_{DS_{t_2}}$	The mass of DS at time interval 2	g
PF	Power factor	Dimensionless
$P_{Hydraulic}$	Hydraulic power	W
P_{Motor}	Motor power	W
P_{Shaft}	Shaft power	W
ΔP	Difference in pressure	Pa

Q	Volumetric flow rate	m^3/s
t	Time	h
$V_{FS_{t_1}}$	The volume of FS at time interval 1	L
$V_{FS_{t_2}}$	The volume of FS at time interval 2	L
V_{Volt}	Electric potential (Voltage)	W/A

Greek symbols

Δ	Difference in	Dimensionless
ρ	Density	kg/m^3 or g/L
π	Osmotic pressure	kPa
ν	Fluid flow velocity	m/s
$\sum$	Sum of	Dimensionless
η	Efficiency	Dimensionless

LIST OF ABBREVIATIONS

Abbreviation	Description
AFO	Pressure-assisted forward osmosis
AL-DS	Active layer-draw solution
AL-FS	Active layer-feed solution
CA	Cellulose acetate
$Ca(NO_3)_2$	Calcium nitrate
CECP	Concentrative internal concentration polarisation
CICP	Concentrative internal concentration polarisation
CO_2	Carbon dioxide
CP	Concentration polarisation
CTA	Cellulose triacetate
DECP	Dilutive external concentration polarisation
DI	Deionised
DICP	Dilutive internal concentration polarisation
DS	Draw solution
EC	Electrical conductivity
ECP	External concentration polarisation
ED	Electrodialysis
FDFO	Fertiliser-drawn forward osmosis
FO	Forward osmosis
FS	Feed solution
GDP	Gross domestic product
KNO_3	Potassium nitrate
ICP	Internal concentration polarisation
KCl	Potassium chloride
$KHCO_3$	Potassium bicarbonate
K_2PO_4	Potassium sulphate
M	Molarity
MD	Membrane distillation
MED	Multi-effect distillation
$MgSO_4$	Magnesium sulphate

$MgCl_2$	Magnesium chloride
MSF	Multi-stage flash distillation
MVC	Mechanical vapour compression
NaCl	Sodium chloride
$NaNO_3$	Sodium nitrate
Na_2SO_4	Sodium sulphate
NF	Nanofiltration
NH_3	Ammonia
NH_4Cl	Ammonium chloride
NH_4HCO_3	Ammonium bicarbonate
$NH_4H_2PO_4$	Mono-ammonium phosphate
NH_4NO_3	Ammonium nitrate
$(NH_4)_2HPO_4$	Di-ammonium phosphate
$(NH_4)_2SO_4$	Ammonium sulphate
NP	Nanoparticles
OP	Osmotic pressure
PCR	Polymerase chain reaction
PRO	Pressure retarded osmosis
PWW	Primary wastewater
RO	Reverse osmosis
RSF	Reverse solute flux
SA	South Africa
SBW5	Synthetic brackish water 5 g/L
SEC	Specific energy consumption (kWh/m^3)
SRSF	Specific reverse solute flux (g/L)
SWW	Secondary wastewater
TDS	Total dissolved solids
TFC	Thin film composite
UF	Ultrafiltration
VNI	Value not indicated

GLOSSARY

Term	Description
Concentration polarisation	A concentration gradient at the interface of the membrane active layer due to permeation (Wang *et al.*, 2010; Cath *et al.*, 2006)
Draw solution	Highly concentrated solution exhibiting a high osmotic pressure located on the permeate side of a membrane (Cath *et al.*, 2006; Gray *et al.*, 2006)
External concentration polarisation	A concentration gradient located at the interface of the active layer of the membrane and a bulk solution (Cath *et al.*, 2006)
Feed solution	Lower concentrated solution exhibiting low osmotic pressure compared to the draw solution (Chung *et al.*, 2012) located on the retentate side of the membrane.
Fertigation	Application of dissolved fertilisers to agricultural farmland through an irrigation system (Phuntsho *et al.*, 2011)
Forward osmosis	Osmotically driven membrane process driven by an osmotic gradient for the permeation of water through a membrane (Tiraferri *et al.*, 2011)
Internal concentration polarisation	A concentration gradient located at the interface between the porous support layer and the active layer of the membrane (Wang *et al.,* 2010)
Membrane	The semi-permeable barrier that permits permeation based on species type (Seader *et al.,* 2011)

Membrane fouling	The adsorption of contaminants on a membrane surface (Shaffer *et al.,* 2015) resisting the net transport of water through a membrane.
Osmotic pressure	The pressure required to prevent the net flow of water through a membrane (Cath *et al.*, 2006)

CHAPTER 1
INTRODUCTION

1.1 Background

Worldwide, water is considered an essential resource as it sustains human, animal and plant life (WWAP, 2016). Water is not only crucial for all forms of life but is vital for global economic growth (WWAP, 2016). Even though water is in abundance, only 2.5% is fresh and of this, 68.9% remains frozen in glaciers and ice caps with a subsequent 30.8% located as groundwater (National Geographic, 2012). Therefore, only 0.3% of the total freshwater is accessible and suitable for human use (National Geographic, 2012). With the current world population increasing at an alarming rate, it is estimated that between 2011 and 2050 the population would increase from 7 billion to 9.3 billion (WWAP, 2016). This would account for a 33% increase in population with a corresponding 60% increase in food demand for the same period.

SA, a country with a population of approximately 55 million, is facing a current drought crisis as a result of low rainfall and large water demands. The demand for water in SA has increased considerably due to the rapid expansion of the agricultural industry, and of the municipal and industrial sectors (WWF-SA, 2017). It is projected that by 2030 the water demand will exceed the supply capacity by 17% (WWF-SA, 2017). That is, approximately 1% annually, from a demand of 15 billion m^3 in 2016 to 18 billion m^3 in 2030 (WWF-SA, 2017). With the demand exceeding the supply, SA is approaching physical water scarcity.

Agricultural development in SA accounts for approximately 63% of total water demand (WWF-SA, 2017). The industry contributes an average of 2.5% to the gross domestic product (GDP) and formally employs 5% of the population (AgriSETA, 2010). However, with the deterioration of water quality in SA (WWF-SA, 2016) and irregular rainfall, agricultural developments are affected greatly due to the lack of suitable water.

With the effects of climate change, population growth, urbanisation, industrial growth, agriculture, and energy production, the freshwater crisis will increase in the near future (Lotfi *et al.*, 2015). Since 97.5% of global water contains some degree of salt (Phuntsho *et al.*, 2012b), the process of desalination will be a major contributor to solving the freshwater crisis (Lotfi *et al.*, 2015; Phuntsho *et al.*, 2012a; Phuntsho *et al.*, 2011).

With freshwater resources limited and with the agricultural industry being a major consumer of freshwater, alternative measures are required to desalinate water specifically for agricultural use since conventional desalination technologies are considered uneconomical (Lotfi *et al.*, 2015). FO is a membrane technology that gained interest over the past decades as it exhibited strategic advantages over conventional desalination technologies. However, several process limitations, such as RSF, CP and membrane fouling, remain problematic, hindering the commercialisation of FO for large-scale operations. Therefore, the focus of this study is to evaluate factors that affect an FO system performance and energy consumption and to identify parameters in order to mitigate these process limitations.

1.2 Problem statement

Despite numerous advances in FO technology, several process limitations, such as RSF, CP and membrane fouling, remain a challenge. These limitations have the potential to restrict system performance and so increase system energy consumption.

1.3 Research questions

i. Which factors affect FDFO performance?
ii. Which factors affect FDFO energy consumption?

1.4 Aims and objectives

1.4.1 Aim

To evaluate an FDFO system by investigating the effects of process parameters (DS concentration, membrane orientation, and system flow rate) on the FDFO system performance and energy consumption.

1.4.2 Objectives

i. To evaluate the effect of DS concentration on system performance and energy consumption
ii. To evaluate the effect of membrane orientation on system performance and energy consumption.
iii. To evaluate the effect of flow rate on system performance and energy consumption.
iv. To evaluate the effect of fouling on system performance and energy consumption.

1.5 Significance

The findings from this study will contribute to the understanding in which membrane orientation and physicochemical properties of FS and DS contributed to the current challenges associated with FO (RSF, CP and membrane fouling) and how they affect the FDFO system performance and energy consumption.

1.6 Delineation

This study is subjected to agreed objectives and will not include the following:

- The energy consumption of solution preparations
- The effect of various draw solution types
- The effect of temperature
- The effect of membrane spacers
- The effect of flow direction (co-current or counter-current) with respect to the membrane
- System modelling

CHAPTER 2
LITERATURE REVIEW

2.1 The concept of water desalination

As freshwater resources are limited and with an abundance of saline water globally, in the future, the process of desalination will be a major contributor in solving the freshwater crisis (Lotfi *et al.*, 2015; Phuntsho *et al.*, 2012a; Phuntsho *et al.*, 2011). Water desalination is defined as the removal of salt from a solution in order to obtain clean water. However, water desalination is not a standardised process as various separation techniques are available. The method of separation is largely dependent on the nature of the saline water as various salt concentrations subsist.

The desalination of water has a variety of applications, such as for human consumption, for agricultural irrigation or for the reuse in industrial processes. However, product water should meet the regulatory standards of each of these applications in order to be used. Therefore, several desalination technologies are currently developed for desalinisation, however, the efficiency and carbon footprint of these processes deviate due to the type of separation technique used.

2.2 Water desalination for agricultural use

Global agricultural developments account for roughly 70% of the total freshwater withdrawal and can exceed 90% in some developing countries (WWAP, 2016). According to the Food and Agriculture Organisation of the United Nations, projected global freshwater withdrawals are at 3,928 km^3 per year, of which 1,492 km^3 are consumed by the agricultural sector (WWAP, 2017). Because the agricultural industry is one of the main consumers of fresh water globally (Lotfi *et al.*, 2015) and with an abundance of impaired water (saline water), it is sensible to investigate alternative measures to desalinate water specifically for agricultural use. Since advanced desalination technologies are already in existence, these processes are considered impractical for large-scale desalination, i.e. for the agricultural industry (Lotfi *et al.*, 2015). Subsequently, these processes have high capital and operational costs (Phuntsho *et al.*, 2016), which are uneconomical for large-scale operations (Lotfi *et al.*, 2015). Therefore, there is a need for a process utilised in the agricultural industry that is low energy intensive, with

reduced capital and operational cost, and which has the potential to desalinate impaired water to the required standards.

2.3 Desalination technologies

Several advanced desalination technologies are already in existence and can be classified into two main categories, namely thermal desalination and membrane desalination. Thermal desalination technologies such as multi-effect distillation (MED), multi-stage flash distillation (MSF) (Park *et al.*, 2011) and mechanical vapour compression (MVC) (Bahar *et al.*, 2004) are processes that utilise thermal energy to evaporate saline water (Ling *et al.*, 2010) which is then condense in order to obtain clean water. Membrane desalination technologies such as nanofiltration (NF), reverse osmosis (RO), pressure retarded osmosis (PRO), pressure-assisted forward osmosis (AFO) and forward osmosis (FO) incorporate a semipermeable membrane which allows water to permeate but retain solutes (salt) in order to produce clean water. For the relevance of this study, only osmosis type processes will be elaborated on.

2.4 Osmosis type membrane processes

There are various types of osmosis membrane processes, however, since osmosis refers to a natural phenomenon; the processes differ from one to the other. Osmosis is defined as the spontaneous movement of water molecules through a semi-permeable membrane due to the difference in osmotic pressure between the two solutions on either side of the membrane (Pardeshi *et al.*, 2016; Hawari *et al.*, 2016; Dabaghian & Rahimpour, 2015; Kumar & Pal, 2015; Phuntsho *et al.*, 2014; Phuntsho *et al.*, 2013; Cath *et al.*, 2006).

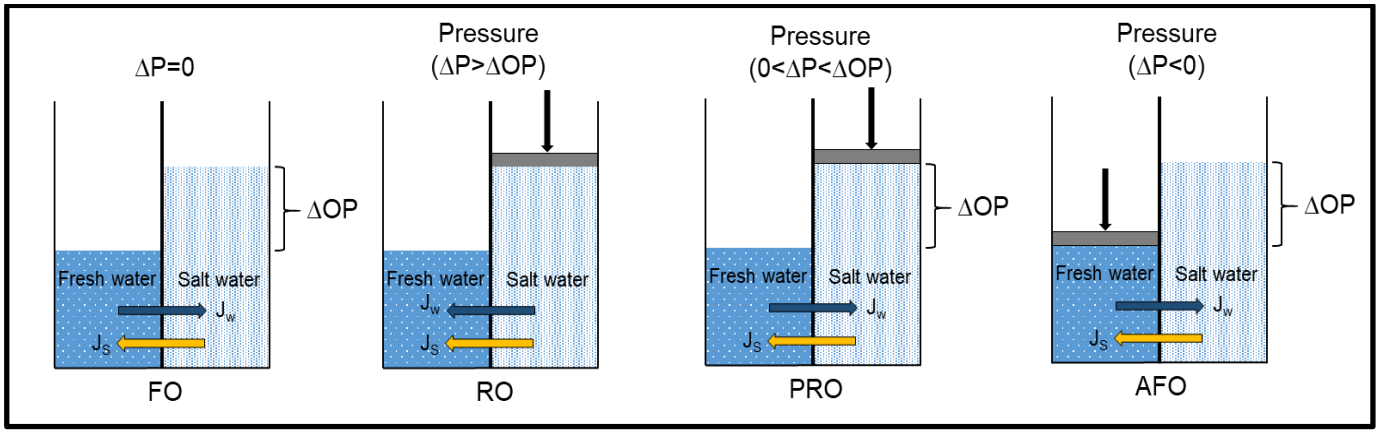

Figure 2.1: Types of osmosis processes: Forward Osmosis (FO); Reverse Osmosis (RO); Pressure Retarded Osmosis (PRO); Pressure Assisted Forward Osmosis (AFO) (Adapted from Korenak *et al*., 2017)

The process of FO requires no hydraulic pressure for the net movement of water molecules through the semi-permeable membrane (Korenak *et al.*, 2017). This process is based on the natural osmosis phenomenon and is solely driven by the difference in OP (ΔOP) between the two solutions on either side of the membrane (Korenak *et al.*, 2017). The most well-known osmosis type process is RO, as it is the leading desalination technology currently in operation (Figure 2.1) (Mazlan *et al.*, 2016; Dabaghian & Rahimpour, 2015; Lotfi *et al.*, 2015; McGovern & Lienhard, 2014). RO is a pressure driven membrane process by which the spontaneous movement of water molecules due to natural osmosis is counteracted by hydraulic pressure (Phuntsho *et al.*, 2012b; Ling *et al.*, 2010). The hydraulic pressure required should exceed that of the OP in order to force water molecules in the opposite direction through the semi-permeable membrane (Phuntsho *et al.*, 2012b). PRO is a combination of FO and RO processes. This process is driven by natural osmosis similar to FO, however, the water transport is retarded by the application of hydraulic pressure on the permeate side of the membrane (Korenak *et al.*, 2017; Achilli *et al.*, 2009) similar to RO. Nevertheless, the applied pressure on the permeate side does not exceed the OP like in RO. AFO, similar to PRO, is a combination of FO and RO processes. Yet, the difference between AFO and PRO is the pressurised stream. In an AFO process, the retentate side of the membrane is pressurised (Korenak *et al.*, 2017), unlike the permeate side in PRO. The application of hydraulic pressure to the retentate side of the membrane enhance the movement of water molecules through the membrane to the permeate side (Korenak *et al.*, 2017).

2.5 Forward osmosis technology

FO is defined as the spontaneous movement of water molecules through a semi-permeable membrane from a FS with low OP (high water chemical potential) to a DS of high OP (low water chemical potential) (Pardeshi *et al.*, 2016; Hawari *et al.*, 2016; Dabaghian & Rahimpour, 2015; Kumar & Pal, 2015; Phuntsho *et al.*, 2014; Phuntsho *et al.*, 2013; Cath *et al.*, 2006). Considering that the water molecules migrate from the FS to the DS, particulate such as organic matter, microorganisms and dissolved salts are retained in the feed stream (Phuntsho *et al.*, 2012b). The process of FO is therefore in agreement with the second law of thermodynamics (Qasim *et al.*, 2015) which state that the entropy of an isolated system will never decrease. Thus, in an isolated system such as an FO operation, the system will spontaneously evolve toward thermodynamic equilibrium (towards maximum entropy). In FO, the driving mechanism is solely due to the osmotic gradient, which is the ΔOP of the solutions on either side of the membrane (Lotfi *et al.*, 2015; Cath *et al.*, 2006) hence no external hydraulic pressure is required ($\Delta P=0$) for mass transport.

2.5.1 Advantages of forward osmosis

The process of FO has some distinct advantages compared to pressure-driven membrane processes which are the main reason for its widespread attention. The main advantages of FO are that it operates at low or no hydraulic pressure (Phuntsho *et al.*, 2016; Achilli *et al.*, 2010). Consequently, FO is considered less energy intensive than conventional pressure-driven membrane processes such as NF and RO (Phuntsho *et al.*, 2013; Phuntsho *et al.*, 2011). FO also exhibits lower fouling rates and lower irreversible membrane fouling. This is due to the less compact fouling layer when compared to pressure-driven membrane processes (Qasim *et al.*, 2015; Shaffer *et al.*, 2012). Therefore, a lower level of pre-treatment of the feed stream is required. Since FO withhold a lower irreversible membrane fouling propensity (Phuntsho *et al.*, 2011; Achilli *et al.*, 2010), straightforward membrane cleaning is therefore required. In addition, FO exhibits a high contaminant rejection (Achilli *et al.*, 2010) and can generate high recovery rates which in turn reduce the amount of concentrated FS discharge (Qasim *et al.*, 2015; McCutcheon *et al.*, 2006).

2.5.2 Factors affecting FO system performance

FO might have several advantages over pressure-driven membrane processes, however, FO also has several factors which affects the FO system performance.

2.5.2.1 Osmotic dilution

The purpose of the DS is to supply an OP greater than that of the FS, as a result ensuring an osmotic gradient (Korenak *et al.*, 2017). The osmosis phenomenon initiates the transport of water from the FS to DS, which inevitably becomes less concentrated as the system reaches osmotic equilibrium (DS OP = FS OP) (Phuntsho *et al.*, 2012a). As OP is proportional to concentration and so a colligative property (Phuntsho *et al.*, 2012b), it will decrease with the decline in the number of solutes per unit volume of solution. This osmotic dilution of the DS reduces the osmotic gradient and as a result system performance (Shaffer *et al.*, 2015; Phuntsho *et al.*, 2012a), which ultimately elevates system energy consumption.

2.5.2.2 Membrane fouling

In any membrane process, fouling is unavoidable and is defined as the adsorption of organic and inorganic compounds, colloidal particles and microbes to a membrane surface (Korenak *et al.*, 2017; Shaffer *et al.*, 2015; Qasim *et al.*, 2015). For that reason, membrane fouling refers to the action of organic solutes, whilst scaling refers to the action of inorganic solutes (Lotfi *et al.,* 2015). In FO, membrane fouling is dependent on FS, DS and membrane characteristics (Akther *et al.*, 2015; Lotfi *et al.*, 2015; Phuntsho *et al.*, 2014). Since inorganic solutes partially dissociate when dissolved, scaling of the membrane is possibly caused by two phenomena: (i) supersaturation of feed ions, or (ii) reverse solute ions that react with the feed ions, or both (Xiang *et al.*, 2017; Lotfi *et al.*, 2015; Phuntsho *et al.*, 2014). Nonetheless, various other factors regulates membrane fouling such as (i) membrane surface morphology determined by structural characteristics, (ii) the chemical interactions of solutes affecting foulant intermolecular adhesion forces and (iii) the hydrodynamic interactions such as permeate drag and shear forces which constitute to convective flow and membrane crossflow velocities (Mi & Elimelech, 2008). Fouling is a major contributor to the reduction in system performance given that it generates resistance to mass transport (water flux) and can affect the membrane lifespan. The ultimate result will be an escalation in system energy consumption and operational cost (Korenak *et al.*, 2017; Zou & He, 2016; Shaffer *et al.*, 2015; Qasim *et al.*, 2015; Phuntsho *et al.*, 2014). Given that typical FO membranes consist of two different layers,

membrane fouling occurs on different surfaces, dependent on the operational mode of the membrane (FO or PRO mode) (Mi & Elimelech, 2008). In FO mode, the active layer is facing the FS, thereby the fouling layer will be deposited on top of the active layer (Mi & Elimelech, 2008). Conversely, when the system operates in PRO mode, fouling will occur within the porous support layer of the membrane (Mi & Elimelech, 2008). Therefore, the common orientation in an FO process (i.e. wastewater treatment, water desalination etc.) is the FO mode (McCutcheon & Elimelech, 2006) as the fouling occurs on top of the membrane active layer instead of inside the membrane porous support layer. With the disadvantage of lower water fluxes compared to the PRO mode due to severe CP effects (Akther *et al.*, 2015), this orientation simplifies membrane cleaning.

2.5.2.3 Reverse solute flux

RSF is the passage of solutes from the DS to the FS as a result of the concentration gradient between the two solutions. Solutes will migrate spontaneously as the system tends to reach an osmotic equilibrium. Additionally, RSF is dependent on the concentration gradient between the FS and DS, the membranes structure as well as the solute rejection properties of the active layer (Phuntsho *et al.*, 2012b). An additional contributing factor to RSF is the charge of the membrane surface which could either attract or repel ions. Subsequently, this can result in increasing or decreasing RSF (Phuntsho *et al.*, 2011). RSF is considered one of the major challenges associated with FO (Qasim *et al.*, 2015; Phuntsho *et al.*, 2014) due to the effect on membrane fouling in addition to the reduction in the osmotic driving force. This is due to an increase of solutes in the FS which will upsurge the solutions OP and subsequently reduce the osmotic gradient between the FS and DS. Therefore RSF also contributes to an economic loss due to the additional cost for DS replenishment and later complicate concentrated FS disposal management (Korenak *et al.*, 2017; Zou & He, 2016; Phuntsho *et al.*, 2014; Achilli *et al.*, 2010). It is thus important to select an appropriate DS that produces a high water flux yet low RSF as it ultimately affects system performance and therefore system energy consumption.

2.5.2.4 Concentration Polarisation

The phenomenon of CP is primary to all membrane separation processes (McCutcheon & Elimelech, 2006). However, the complexity of this phenomenon is dependent on the membrane construction (Cath *et al.*, 2006) and in the case of FO, CP can occur on both sides of the membrane (McCutcheon & Elimelech, 2006). CP is the formation of a concentration gradient at the interface of the active layer of an FO membrane (Tiraferri *et al.*, 2011) as the active layer segregates solutes from solutions (Park *et al.*, 2011). In FO, actual water flux deviates considerably from theoretical water fluxes due to the effects of CP (Hawari *et al.*, 2016; Phuntsho *et al.*, 2013). CP, in general, is considered one of the major contributors to the decrease in water flux in FO (Hawari *et al.*, 2016). A study by McCutcheon and Elimelech (2006) concluded that an increase in solution temperature will reduce CP. This is because a rise in solution temperature will subsequently reduce the viscosity of the solution, decrease the solutes resistivity and surge the solution-diffusion coefficient. All these factors, in turn, result in an increase in water flux. However, at high solution temperatures, water flux will decrease as CP will become more dominant. Since typical FO membranes are asymmetric (Phuntsho *et al.*, 2013; Cath *et al.*, 2006), one side of the active layer is permanently adherent to the porous support layer, whilst the other is exposed to a bulk solution. This location of the active layer results in two types of CP phenomena known as internal concentration polarisation (ICP) and external concentration polarisation (ECP) (Hawari *et al.*, 2016; Phuntsho *et al.*, 2013).

2.5.2.4.1 Internal Concentration Polarisation

ICP is the formation of a strong concentration gradient at the interface of the active layer and the porous support layer of an FO membrane (Wang *et al.*, 2010). This concentration gradient occurs as the porous support layer operates as an inactive diffusive zone (Tiraferri *et al.*, 2011), and is impenetrable by system hydrodynamics (Qasim *et al.*, 2015; Phuntsho *et al.*, 2013; Park *et al.*, 2011; Gray *et al.*, 2006; McCutcheon *et al.*, 2006). ICP is essentially dependent on membrane structural parameters, which is the relationship between membrane thickness, tortuosity, and porosity (Korenak *et al.*, 2017; Park *et al.*, 2011). However, ICP is also dependent on solution physicochemical properties, i.e. solute diffusivity, ion/molecule size, and viscosity (Zhao & Zou, 2011). According to Zhao & Zou (2011), ICP will intensify in a high viscosity bulk solution complemented with, low solute diffusivity and a large solute molecule or ion size. These combined factors are determined by solute concentration. With OP being a colligative property (Phuntsho *et al.*, 2012b) and therefore directly proportional to

solute concentration, ICP is increased at high OPs. This is because high OPs result in a high water fluxes (Wang *et al.*, 2016; Zhao & Zou, 2011; Gray *et al.*, 2006; McCutcheon & Elimelech, 2006) which will convert as a self-limiting factor, creating a significant concentration gradient at the membrane boundary layers (Wang *et al.*, 2016; McCutcheon & Elimelech, 2006). ICP is a major contributor to water flux decline and is considered the main factor responsible for limiting system performance (Hawari *et al.*, 2016; Wang *et al.*, 2016; Dabaghian & Rahimpour, 2015; McGovern & Lienhard, 2014; Phuntsho *et al.*, 2011; Zhao & Zou, 2011; Achilli *et al.*, 2010). ICP can be subdivided into concentrative internal concentration polarisation (CICP) and dilutive internal concentration polarisation (DICP), depending on the operational mode of the FO membrane (FO or PRO mode) (Hawari *et al.*, 2016; Qasim *et al.*, 2015; Cath *et al.*, 2006).

CICP occurs when the FO system operates in the PRO mode (Figure 2.2b) (Hawari *et al.*, 2016; Qasim *et al.*, 2015; McCutcheon & Elimelech, 2006). As the FS propagates the porous support layer, it becomes more concentrated as water molecules permeate the active layer to the DS whilst solutes are retained (McCutcheon & Elimelech, 2006; Gray *et al.*, 2006). This increase in solute concentration at the interface of the active layer and porous support layer results in a concentration gradient (Zhao & Zou, 2011), which ultimately reduces the osmotic driving force (Zou & He, 2016; McCutcheon & Elimelech, 2006) and accordingly system performance (Qasim *et al.*, 2015).

DICP is similar to CICP. However, the difference is the operational mode of the FO membrane thus DICP occurs when the system operates in FO mode (Figure 2.2a) (Hawari *et al.*, 2016; Qasim *et al.*, 2015; McCutcheon & Elimelech, 2006). As the water permeates the active layer from the FS, propagated DS within the porous support layer becomes diluted due to convection (McCutcheon & Elimelech, 2006; Gray *et al.*, 2006). Thus, as with CICP, a concentration gradient forms at the interface of the active layer and porous support layer of the membrane which is considerably lower than the bulk DS (Gray *et al.*, 2006). This concentration gradient reduces system performance attributable to a lowered osmotic driving force (McCutcheon & Elimelech, 2006). DICP is considered one of the most severe CP effects in FO and can result up to 80% water flux regression (Qasim *et al.*, 2015).

2.5.2.4.2 External Concentration Polarisation

ECP is a CP phenomenon that transpires at the interface of the active layer of the membrane and bulk solutions during an FO operation, which reduces system performance (Hawari *et al.*, 2016; Wang *et al.*, 2016; Gray *et al.*, 2006) similarly to ICP. A study by Wang (2016) identified ECP to be intensified at high DS concentrations as it creates an elevated OP and therefore a greater water flux which will become self-limiting. However, ECP is less severe on system performance than ICP as this phenomenon is relatively easy to mitigate by system hydrodynamic optimisation (Korenak *et al.*, 2017; Qasim *et al.*, 2015; Wang *et al.*, 2010; Cath *et al.*, 2006). This occurrence can be described by the film theory by which fluctuating solution flow rate will alter the flow regime hence reducing the thickness of the mass transfer layer (concentration gradient) at the membrane surface (Wang *et al.*, 2016; Phuntsho *et al.*, 2013). ECP can be subdivided into concentrative external concentration polarisation (CECP) and dilutive external concentration polarisation (DECP) depending on the operational mode of the FO membrane (Hawari *et al.*, 2016; Qasim *et al.*, 2015; Cath *et al.*, 2006).

CECP ensues when an FO system operates in FO mode (Figure 2.2a) (Hawari *et al.*, 2016; Qasim *et al.*, 2015; McCutcheon & Elimelech, 2006). Considering that water permeates the active layer to the DS, the FS becomes more concentrated and a concentration gradient follows due to solute build-up at the active layer (Cath *et al.*, 2006). Therefore, CECP can be referred to as some form of membrane fouling (Qasim *et al.*, 2015; Cath *et al.*, 2006). One of the membranes scaling phenomena is the supersaturation of ions in the FS that adhere to the membrane surface (solute build-up) (Lotfi *et al.*, 2015) initiating a resistance to mass transport (water flux) and thus reducing system performance (Qasim *et al.*, 2015).

DECP, similar to CECP, occurs at the interface of the active layer of the membrane and a bulk solution when the system operates in PRO mode (Figure 2.2b) (Hawari *et al.*, 2016; Qasim *et al.*, 2015; McCutcheon & Elimelech, 2006). DECP transpires due to convective water permeation through the active layer (Gray *et al.*, 2006). This permeation creates a concentration gradient in the form of pure water at the interface of the active layer and bulk DS (Cath *et al.*, 2006), which reduces the osmotic driving force (McCutcheon & Elimelech, 2006) and subsequently system performance.

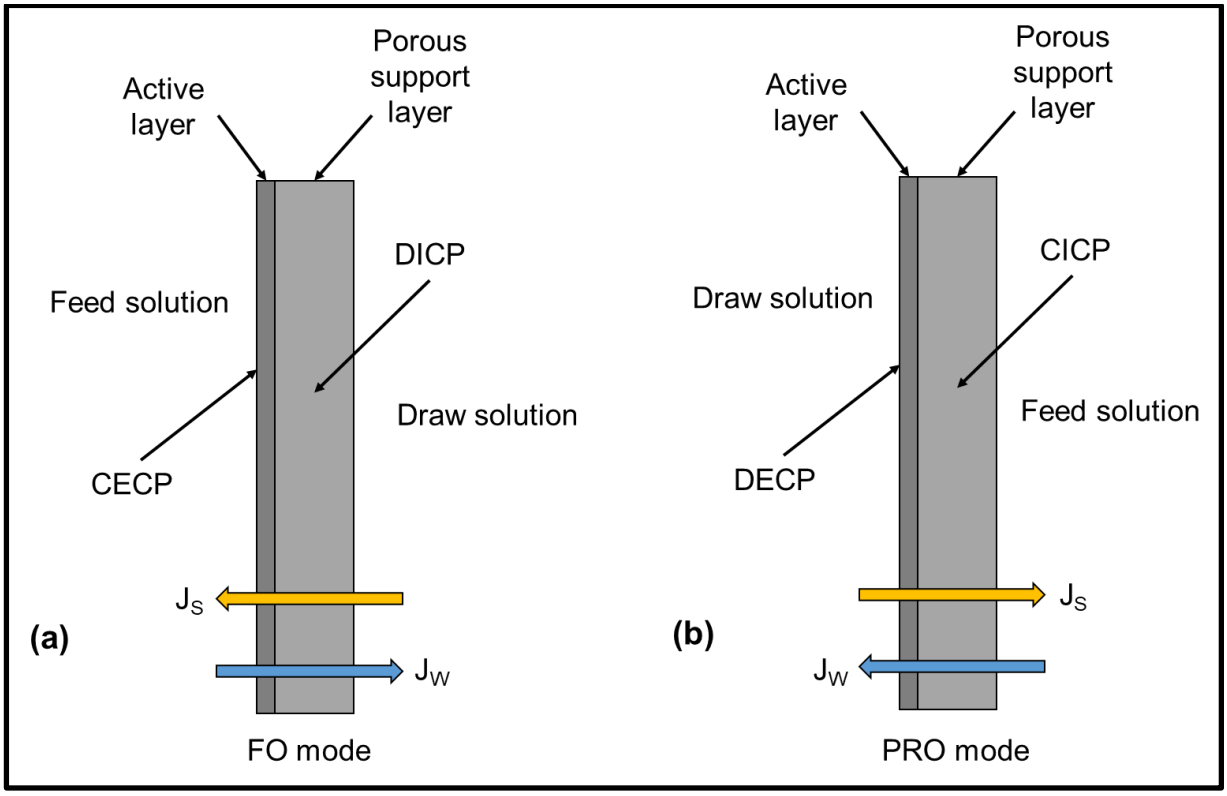

Figure 2.2: ICP and ECP representation during (a) FO mode; illustrating CECP and DICP and (b) PRO mode; illustrating DECP and CICP (Adapted from McCutcheon & Elimelech, 2006)

2.5.3 Feed solution

The FS utilised in FO consists of a higher water chemical potential with lower OP compared to that of the DS. A lower OP FS is vital to ensure an osmotic gradient that is the driving force in an FO operation. An FS is a typical stream which necessitates treatment and can range from regular saline water to more complex industrial waste streams (Kumar & Pal, 2015).

2.5.4 Draw solution

The DS utilised in FO comprise of a lower water chemical potential. Therefore, the DS is more concentrated with a higher OP compared to that of the FS. The elevated OP generated by the DS is crucial as it impacts mass transport and overall system efficiency (Korenak *et al.*, 2017; Kumar & Pal, 2015) and therefore forms an integral part of the FO process (Phuntsho *et al.*, 2012b). The ideal DS selected for an FO process should: (i) produce greater OP than that of the FS, (ii) be non-toxic, (iii) be water soluble, (iv) be inert and not react with the FS or membrane, (v) be inexpensive, (vi) be non-responsive to pH changes, and (vii) consist of relatively large molecule size to limit RSF but small enough to mitigate CP (Xiang *et al.*, 2017; Korenak *et al.*, 2017; Akther *et al.*, 2015; Shaffer *et al.*, 2015; Chung *et al.*, 2012; Phuntsho *et al.*, 2011; Zhao & Zou, 2011; Cath *et al.*, 2006).

2.5.4.1 Types of draw solutions used in forward osmosis

Several solutes have been reported to be utilised as DS in an FO operation and can be classified as responsive and non-responsive draw solutes (Table 2.1) (Cai & Hu, 2016). In responsive draw solutes, water affinity is affected by external stimuli whilst with non-responsive draw solutes, water affinity remains unaffected by external stimuli such as an electromagnetic field, temperature change, pH change etc. (Cai & Hu, 2016).

Table 2.1: Various types of responsive and non-responsive draw solutes (Adapted from Cai & Hu, 2016)

Responsive draw solutes	Non-responsive draw solutes
Nanoparticles	Inorganic salts
Hydrogels	Polymers
Metathesis perceptible salts	Organic salts
Soluble gasses	-
Volatile liquids	-
Switchable polarity solvents	-
Thermally responsive molecules	-

It can be observed from Table 2.1 that there is a wide variety of DS available for FO. However, FO still receives widespread criticism regarding its ability to desalinate seawater at a lower energy consumption than its counterpart RO (Cai & Hu, 2016). In addition, thermodynamics demonstrated that with the current FO technologies, FO desalination for potable use will exceed the energy demand of RO. This is primarily due to the lack of a DS which (i) produce high OP, (ii) is straightforward to separate from the extracted water and (iii) requires a low energy demanding draw regeneration process (Zou & He, 2016; Phuntsho *et al.*, 2016; Shaffer *et al.*, 2015; Phuntsho *et al.*, 2011; Ling *et al.*, 2010; Mi & Elimelech, 2008). Therefore, until significant breakthroughs are made in FO technology in order to compete with RO, FO is best suited for applications where no draw regeneration is required (Phuntsho *et al.*, 2012b) such as in the case of an FDFO system.

2.5.4.2 Fertiliser draw solutions

The concept of fertiliser DS in FO was first reported by Moody and Kessler in 1976 (Phuntsho *et al.*, 2012a). However, more recent studies by Phuntsho *et al.* (2011, 2012a) evaluated the performance of several commonly used inorganic fertilisers to determine their potential as a DS for direct fertigation. The study evaluated nine different fertilisers: ammonium chloride (NH_4Cl), ammonium nitrate (NH_4NO_3), ammonium sulphate ($(NH_4)_2SO_4$), calcium nitrate ($Ca(NO_3)_2$), di-ammonium phosphate (DAP) ($(NH_4)_2HPO_4$), mono-ammonium phosphate (MAP) ($NH_4H_2PO_4$), potassium chloride (KCl), potassium nitrate (KNO_3) and sodium nitrate ($NaNO_3$). Furthermore, the study incorporated a flat-sheet cellulose acetate (CA) membrane with deionised (DI) water as an FS and operated in FO mode.

Table 2.2: OP, pH, maximum solubility, water flux, RSF and SRSF for different fertilisers (Data adapted from Phuntsho *et al.,* 2012a; Phuntsho *et al.*, 2011)

Fertiliser name	Chemical formula	OP at 2 M (kPa)	pH at 2 M	Max. solubility (M)	J_W (L/m^2.h)	J_S (g/m^2.h)	SRSF (g/L)
Ammonium chloride	NH_4Cl	8886	4.76	7.35	19.25	4.64	0.24
Ammonium nitrate	NH_4NO_3	6576	4.87	101.9	15.04	15.15	1.01
Ammonium sulphate	$(NH_4)_2SO_4$	9332	5.46	5.80	19.41	0.14	0.01
Calcium nitrate	$Ca(NO_3)_2$	10994	4.68	22.04	18.08	0.30	0.02
DAP	$(NH_4)_2HPO_4$	9626	8.12	7.13	14.01	0.33	0.02
MAP	$NH_4H_2PO_4$	8744	3.93	4.56	15.66	1.83	0.12
Potassium chloride	KCl	9048	6.80	4.82	22.81	2.61	0.11
Potassium nitrate	KNO_3	6576	5.99	4.03	15.94	11.09	0.70
Sodium nitrate	$NaNO_3$	8217	5.98	10.95	20.54	4.13	0.20

The study determined that these fertilisers withhold a potential to be suitable DS as they generate high OP (Phuntsho *et al.*, 2011), which is essential in an FO operation. It can be seen from Table 2.2 that $Ca(NO_3)_2$ generated the highest OP followed by $(NH_4)_2HPO_4$, $(NH_4)_2SO_4$, KCl, NH_4Cl, $NH_4H_2PO_4$, $NaNO_3$, KNO_3 and NH_4NO_3. However, as the performance of a FO operation is determined based on specific reverse solute flux (SRSF) (Phuntsho *et al.*, 2013), $(NH_4)_2SO_4$ obtained the lowest SRSF followed by $Ca(NO_3)_2$, $(NH_4)_2HPO_4$, KCl, $NH_4H_2PO_4$, $NaNO_3$, NH_4Cl, KNO_3 and NH_4NO_3. It was reported that KCl obtained the highest water flux in comparison to all the other fertilisers tested.

There are reports by Achilli *et al.* (2010) on the evaluation of various inorganic based solutions for the application as DS in FO. From this variety of inorganic solutes tested, several can be implemented as fertilisers. These fertilisers included ammonium bicarbonate (NH_4HNO_3), ammonium chloride (NH_4Cl), ammonium sulphate ($(NH_4)_2SO_4$), calcium chloride ($CaCl_2$), calcium nitrate ($Ca(NO_3)_2$), magnesium chloride ($MgCl_2$), magnesium sulphate ($MgSO_4$), potassium chloride (KCl), potassium sulphate (K_2PO_4) and sodium sulphate (Na_2SO_4). The study incorporated a flat-sheet cellulose triacetate (CTA) membrane with ultrapure water as an FS and operated in FO mode.

Table 2.3: OP, water flux, RSF and SRSF for different fertilisers (Data adapted from Achilli *et al*., 2010)

Fertiliser name	Chemical formula	OP (kPa)	DS concentration (M)	J_W (L/m^2.h)	J_S (g/m^2.h)	SRSF (g/L)
Ammonium bicarbonate	NH_4HNO_3	2800	0.67	8.31	20.60	2.48
Ammonium chloride	NH_4Cl	2800	0.61	10.41	7.6	0.73
Ammonium sulphate	$(NH_4)_2SO_4$	2800	0.56	8.25	3.3	0.40
Calcium chloride	$CaCl_2$	2800	0.39	9.52	7.90	0.83
Calcium nitrate	$Ca(NO_3)_2$	2800	0.53	8.96	6.0	0.67
Magnesium chloride	$MgCl_2$	2800	0.36	8.42	4.80	0.57
Magnesium sulphate	$MgSO_4$	2800	1.17	5.71	1.20	0.21
Potassium chloride	KCl	2800	0.63	10.88	12.3	1.13
Potassium sulphate	K_2SO_4	2800	0.58	9.25	3.70	0.40
Sodium sulphate	Na_2SO_4	2800	0.60	7.5	2.7	0.36

It can be observed from the Table 2.3 that at an OP of 2800 kPa $MgSO_4$ obtained the lowest SRSF followed by Na_2SO_4, K_2SO_4, $MgCl_2$, $(NH_4)_2SO_4$, K_2SO_4, $MgCl_2$, $Ca(NO_3)_2$, NH_4Cl, $CaCl_2$, KCl and NH_4HNO_3. Achilli *et al.* (2010) also reported that the highest water flux was achieved when KCl was used as a DS.

The findings reported from the studies conducted by Phuntsho *et al.* and Achilli *et al.*, indicate that fertilisers do have the potential to be successfully utilised as DS in an FO operation. However, the performance of each fertiliser differs from the next due to factors such as physicochemical properties, membrane properties as well as FS and DS properties (Phuntsho *et al.*, 2012a; Phuntsho *et al.*, 2011). It is therefore essential selecting a DS that obtains minimal SRSF as it correlates to FO efficiency (Xiang *et al.*, 2017; Korenak *et al.*, 2017) which consequently relate to lower operational cost.

2.5.5 Fertiliser draw forward osmosis desalination

As global food insecurity intensifies, pressure on the agricultural sector remains constant. The additional limitation to agricultural land will require an increase in productivity to meet growing demands (Roberts, 2009). The use of commercial fertilisers accounts for approximately 40 to 60% of global food production (Roberts, 2009) and will increase in subsequent years because it forms an integral part of the global food security solution (Roberts, 2009).

The concept of fertigation is based on the application of fertilisers to crops, either in dissolved or suspended form via existing agricultural irrigation systems (Phuntsho *et al.*, 2012a). FDFO desalination for fertigation has elicited widespread attention as fertilisers were identified as suitable draw solutions (DS) (Phuntsho *et al.*, 2012a; Phuntsho *et al.*, 2011). It is considered a more efficient way of fertilising, is cost effective and requires no draw regeneration. It can, therefore, be directly utilised and provides nutrient-rich water to agricultural farmland if the fertiliser dilution is sufficient (Figure 2.3) (Zou & He, 2016; Lotfi *et al.*, 2015; McGovern & Lienhard, 2014; Phuntsho *et al.*, 2012a; Phuntsho *et al.*, 2011). The additional advantage of FDFO desalinisation is the minimisation of soil degradation that is caused by saline water irrigation and over fertilisation. A current challenge with FDFO is that fertiliser DS concentrations still remain above the desired nutrient concentration requirements of plants, creating direct fertigation problematic (Lotfi *et al.*, 2015) as high nutrient concentration could damage sensitive plants. Therefore, the fertiliser DS require additional dilution before it is suitable for use in the fertigation process.

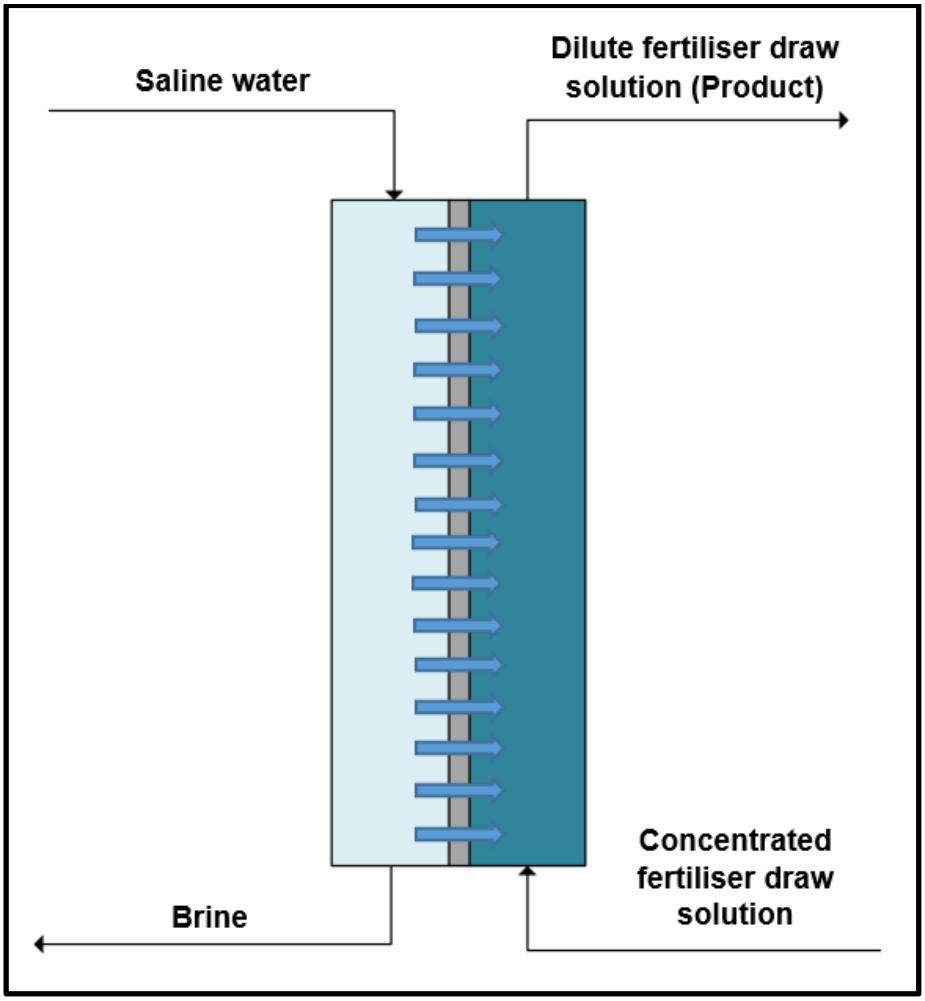

Figure 2.3: Schematic depiction of a basic fertiliser-drawn forward osmosis operation

2.5.6 Forward osmosis membranes

One of the current challenges limiting the commercialisation of FO is the lack of high-performance membranes (Chung *et al.*, 2012; Wang *et al.*, 2010). FO membranes are asymmetric and consist of two layers, a porous support layer to provide mechanical strength and a dense active layer for solute rejection (Hawari *et al.*, 2016; Qasim *et al.*, 2015; Phuntsho *et al.*, 2013; Achilli *et al.*, 2010). An ideal membrane utilised in FO should have: (i) high water flux due to reduced membrane structural parameter, (ii) high solute rejection, (iii) low CP, (iv) resistance to a widespread pH, (v) low fouling propensity, and (vi) good mechanical strength and (vii) a high chemical stability (Korenak *et al.*, 2017; Qasim *et al.*, 2015; Chung *et al.*, 2012; Zhao & Zou, 2011; Phillip *et al.*, 2010). The performance of a membrane is determined by the water transport from the FS to the DS (water flux) compared to the solute transport from the DS to the FS (RSF) (Korenak *et al.*, 2017; Qasim *et al.*, 2015). As the main purpose of the membrane active layer is to prevent RSF (Phuntsho *et al.*, 2013), this layer is still porous and

with the high concentration difference between the FS and DS, RSF is inevitable as the system tend to reach an equilibrium (Xiang *et al.*, 2017; Zou & He, 2016; Qasim *et al.*, 2015; Phuntsho *et al.*, 2011; Achilli *et al.*, 2010).

2.5.6.1 Type FO membranes

Various membrane types have been developed in an attempt to improve FO performance. Types range from (i) synthesising membranes with different materials i.e. based on cellulose, polyamide (including other polymers) and polyelectrolytes, (ii) fabrication of membrane modules and (iii) membrane coatings (active layer) (Korenak *et al.*, 2017). However, membrane development is best classified according to the method of fabrication, namely phase inversion formed membranes, thin film composite membranes (TFC) and chemically modified membranes (Qasim *et al.*, 2015). According to Korenak *et al.* (2017), a novelty in membrane development is the application of biomimetic membranes by which aquaporin's (biological water channel proteins) is utilised in separation processes such as FO.

2.5.6.2 Membrane orientation

Membranes in an FO operation can be arranged in two different orientations, either into forward osmosis (FO) mode or pressure retarded osmosis (PRO) mode (Hawari *et al.*, 2016; Park *et al.*, 2011). These orientations define the position of which the membrane dense active layer faces with respect to the FS or DS. FO mode, also known as the active layer feed solution (AL-FS), indicates that the membrane active layer is facing the FS (Hawari *et al.*, 2016) (Figure 2.4a). Similarly, PRO mode, also known as active layer draw solution (AL-DS), specifies that the membrane active layer is facing the DS (Hawari *et al.*, 2016) (Figure 2.4b). It has been reported that these orientations affect process performance (Phuntsho *et al.*, 2013) and is a key factor to be considered when selecting process objectives. A process operated in PRO mode tends to produce a greater water flux compared to a process operating in FO mode. Subsequently, an FO mode is more tolerant of membrane fouling than PRO mode (Korenak *et al.*, 2017; McGovern & Lienhard, 2014).

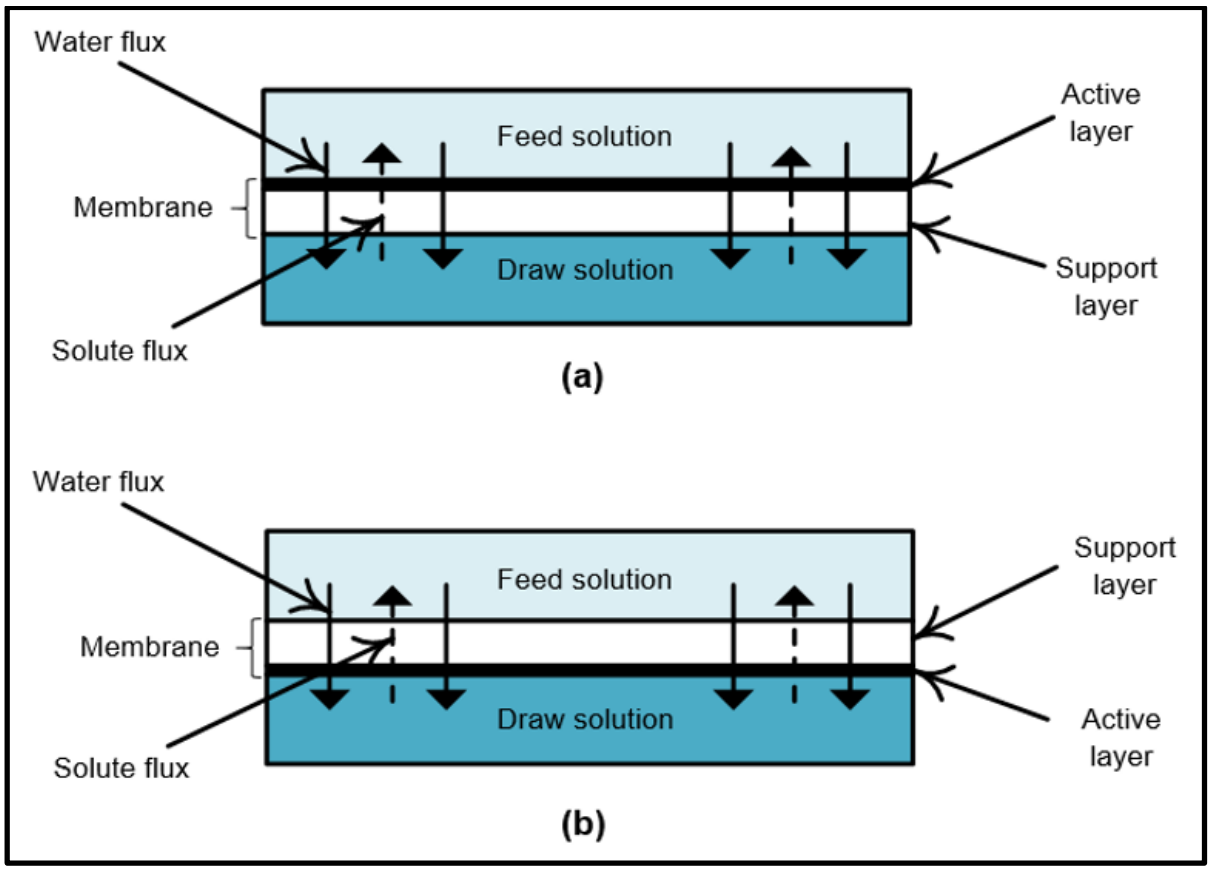

Figure 2.4: Schematic depiction of membrane operational modes: a) Active Layer - Feed Solution mode (AL-FS) (FO mode); b) Active Layer - Draw Solution mode (AL-DS) (PRO mode)

2.6 Forward osmosis energy evaluation

FO is considered a low energy consuming process, as no additional energy in the form of hydraulic pressure is required for the net transport of water molecules through the semi-permeable membrane (Phuntsho *et al.*, 2012a). FO, as a separate process, is considered a reliable alternative low energy consuming membrane process compared to other pressure-driven membrane processes such as microfiltration (MF), UF, NF and RO (Korenak *et al.*, 2017; Altaee *et al.*, 2014; Mi & Elimelech, 2008; McCutcheon & Elimelech, 2006). However, the application of FO in certain process environments can contradict FO as a replacement for pressure-driven membrane processes as the energy consumption depends on the use of the final product (Phuntsho *et al.*, 2013). The only energy consumed in an FO operation is by means of the circulation pumps (Mazlan *et al.*, 2016; Phuntsho *et al.*, 2011). However, since FO occurs spontaneously, the purpose of the pumps is to circulate FS and DS to ensure a steady osmotic gradient across the membrane and the pumps do not contribute directly to mass transport (Phuntsho *et al.*, 2011). In membrane processes, system energy is determined by the amount of energy consumed per unit of product output (Altaee *et al.*, 2014). With FO

reliant on an osmotic gradient for mass transport, any decrease in the osmotic gradient or resistance to mass transport (Membrane fouling) will subsequently increase system energy consumption due to a decrease in product output (Altaee *et al.*, 2014).

2.6.1 Pump load

Energy consumption in electrical equipment is directly proportional to operational load. As a result, electrical energy consumption will increase with the load as more energy is required to overcome generated resistance. The purpose of pumps in an FO operation is to circulate the FS and DS on either side of the membrane. This is to guarantee the system act upon the principles of natural osmosis, the FS and DS are maintained at equal flow rates in order to ensure no pressure gradient across the membrane. Thus, water flux is exclusively formed by the osmotic gradient between the FS and DS.

Electrical energy consumed by a pump motor (P_{Motor}) is affected by various factors as can be observed from Equation 2.1, 2.2 and 2.3. However, the main factors affecting electrical energy consumption is by factors from pump hydraulic power (Equation 2.1). Pump hydraulic power ($P_{Hydraulic}$) is a function of volumetric flow rate (Q), the specific weight of the transported solutions ($\rho.g$) as well as the total pump head (H) (Phuntsho *et al.*, 2013).

$$P_{Hydraulic} = Q \cdot \rho \cdot g \cdot H \qquad \textbf{Equation 2.1}$$

$$P_{Shaft} = \frac{P_{Hydraulic}}{\eta_{Pump}} \qquad \textbf{Equation 2.2}$$

$$P_{Motor} = \frac{P_{Shaft}}{\eta_{Motor}} \qquad \textbf{Equation 2.3}$$

By expanding Equation 2.1, it can be estimated which parameters affect energy consumption in an FO operation.

Expanding the volumetric flow rate (Q) from Equation 2.1, it can be observed that the pipe cross-sectional area (A) and fluid velocity (ν) contributes to pump power consumption.

$$Q = A \cdot v \qquad \textbf{Equation 2.4}$$

Expanding the total pump head (H) from Equation 2.1 is more complex as it comprises of various other heads containing their own determining factors. The total pump head is defined

as the total loss of pressure within a system due to fluid physicochemical properties, equipment and system configurations (Sinnott, 2005). The total pump head (Equation 2.5) is the sum of the static head (H_{Static}) and dynamic head ($H_{Dynamic}$) of a pumping system (Sinnott, 2005).

$$Total\ pump\ head\ (H) = Static\ head\ (H_{Static}) + Dynamic\ head\ (H_{Dynamic}) \quad \textbf{Equation 2.5}$$

The static head (H_{Static}) (Equation 2.6) is the sum of the elevation head (Equation 2.7) and pressure head (Equation 2.8) of a system. The elevation head is the pressure drop due to a difference in elevation between the pump suction and discharge with respect to a reference plane. Similarly, the pressure head is the difference in pressure between the pump suction and discharge (Sinnott, 2005).

$$Static\ head\ (H_{Static}) = Elevation\ had\ (H_{Elevation}) + Pressure\ head\ (H_{Pressure}) \quad \textbf{Equation 2.6}$$

$$Elevation\ head\ (H_{Elevation}) = \left(h_{Discharge} - h_{Suction}\right) = \Delta h \quad \textbf{Equation 2.7}$$

$$Pressure\ head\ (H_{Pressure}) = \frac{\left(P_{Discharge} - P_{Suction}\right)}{\rho \cdot g} = \frac{\Delta P}{\rho \cdot g} \quad \textbf{Equation 2.8}$$

The dynamic head ($H_{Dynamic}$) (Equation 2.9) is more complex than the static head (H_{Static}) as more factors determine this head. The dynamic head is a sum of the velocity head ($H_{Velocity}$) and friction head ($H_{Friction}$) (Sinnott, 2005).

$$Dynamic\ head\ (H_{Dynamic}) = Velocity\ head\ (H_{Velocity}) + Friction\ head\ (H_{Friction}) \quad \textbf{Equation 2.9}$$

The velocity head ($H_{Velocity}$) (Equation 2.10) is a pressure drop generated by equipment and fittings within a hydrodynamic system (i.e. bends, reducing or enlarging sections, tee junctions etc.) which restricts fluid flow. This head is a function of the sum of the velocity heads of all pressure drop equipment (K), fluid velocity (ν) and gravitational acceleration (g) (Sinnott, 2005).

$$Velocity\ head\ (H_{Velocity}) = \sum K \cdot \frac{v^2}{2.g} \quad \textbf{Equation 2.10}$$

The friction head ($H_{Friction}$) (Equation 2.11) is a pressure drop within a system pipelines due to friction between the pipe wall and the fluid being transported. This head is a function of a friction factor (f_D), pipe length (L), pipe internal diameter ($D_{Intenal}$), fluid density (ρ) and transport velocity (ν) (Sinnott, 2005).

$$Friction\,head\,(H_{Friction}) = f_D \cdot \left(\frac{L}{D_{Internal}}\right) \cdot \left(\frac{v^2}{2g}\right) \qquad \textbf{Equation 2.11}$$

The observations from the above equations, indicate fluid velocity (ν) to be a major contributor to the increase in system power consumption as it corresponds to the pump operational speed. Moreover, fluid velocity is a determining factor in the volumetric flow rate (Equation 2.4) as well as the system dynamic head (Equation 2.10 + Equation 2.11). However, the physicochemical properties of the FS and DS will likewise be influencing factors towards an increase in pump power consumption as it affects both the system dynamic head and the specific weight of the solutions ($\rho.g$) (Equation 2.1). The specific weight of the solution is influenced by the increase in solution concentration as it corresponds to solution density. Solutions viscosity is also affected by concentration which subsequently affects the total pump head (H), fluid velocity (ν) (Phuntsho *et al.*, 2013) as well as shaft and pump efficiency (Equation 2.2 and 2.3). A study by Zou & He (2016) reported the power consumption by the circulation pumps to be one of the major contributors to system power consumption in an FO operation.

2.7 FO system energy consumption

Since FO is considered a low energy process with the potential of extracting high quality water from impaired waters (Xiang *et al.*, 2017; Pardeshi *et al.*, 2016; Akther *et al.*, 2015; Phuntsho *et al.*, 2011; Tiraferri *et al.*, 2011), the application of FO for the desalination of saline water has attracted widespread attention.

2.7.1 FO energy consumption for water desalination

The desired application for FO would be part of a process where no draw regeneration is required and the diluted DS can directly be used as a product (Shaffer *et al.*, 2015; Phuntsho *et al.*, 2012a). The advantage of this type of FO application is a low energy requirement given that FO operates as a standalone process. The only energy consumed is by circulation pumps that will need to overcome the channel pressure drop (Mazlan *et al.*, 2016) in order to transport the FS and DS tangentially along the membrane. Although standalone FO is considered energy efficient, reports on specific energy consumption remain relatively elusive (Xiang *et al.*, 2017; Zou & He, 2016).

A recent study by Xiang (2017) evaluated the energy consumption of a submerged FDFO system by the use of a commercial liquid fertiliser. The study assessed three DS dilution ratios (25, 50 and 100%), three flow rates (25, 50 and 100 mL/min) with DI water and wastewater as an FS and operated in FO mode.

Table 2.4: SEC, water flux and RSF obtained for different FS's, DS concentrations and system flow rates for a liquid FDFO system (Data adapted from Xiang *et al*., 2017)

FS	DS concentration (%)	Flow rate (mL/min)	Energy consumption (kWh/m^3)	J_W (L/m^2.h)	Total nitrogen J_S (m mole/m^2.h)
DI	25	25	0.09 ±0.02[a]	3.2±0.6[a]	VNI
DI	25	50	0.37±0.08[a]	3.1±0.7[a]	96.9±4.0[a]
DI	25	50	0.53±0.14[b]	VNI	VNI
DI	25	100	1.30±0.28[a]	3.6±0.1[a]	VNI
DI	50	50	0.34±0.11[b]	VNI	VNI
DI	100	50	0.25±0.08[b]	VNI	304.5±7.5[b]
PWW	25	25	0.17±0.04[a]	VNI	VNI
SWW	25	25	0.10±0.05[a]	3.1±0.2[a]	VNI

a = 24 h, b = 72 h

The study concluded that FS type, DS concentration and recirculation flow rate had significant effects on system energy consumption due to the fluctuation in water flux or recirculation pump energy consumption (Xiang *et al.*, 2017). Xiang (2017) further recommended lower circulation flow rates to be considered for the reason that high flow rates did not improve the system performance significantly (Table 2.4). Previous work by Zou & He (2016) also evaluated the energy consumption of a submerged FDFO system, however, solid fertiliser was used as DS. In this investigation treated wastewater was used as an FS and operated in FO mode. Xiang (2017) reported that the increase in system flow rate did not improve system performance significantly. However, the increase in system flow rate did increase the system energy consumption as can be seen from Table 2.5.

Table 2.5: SEC obtained for different system flow rates for a solid FDFO system (Data adapted from Zou & He, 2016)

Flow rate (mL/min)	Energy consumption (kWh/m^3)
10	0.02±0.01
50	0.47±0.13
100	1.86±0.47

2.7.2 Hybrid FO energy consumption for water desalination

FO is sufficient for extracting high-quality water from saline waters. However, one detriment transpires as soon as extracted water is for potable use. The end product from the FO process is in the form of a diluted DS which is a mixture of extracted water and draw solute (Chung *et al.*, 2015). Therefore, an additional post-treatment process is required to the existing FO process which results in a hybrid FO system. This treatment is solely for the separation of water from the DS in a process known as draw regeneration (Figure 2.5) in which the regenerated DS is reused and the pure water is extracted as a product (Altaee *et al.*, 2014; Shaffer *et al.*, 2012). The draw regeneration process is considered the most expensive stage in hybrid FO systems regardless of the type DS used (Altaee *et al.*, 2014). Various draw regeneration processes have been implemented in hybrid FO systems and are mainly membrane separation processes, e.g. NF, UF and RO (Shaffer *et al.*, 2015). However, other processes such as membrane distillation (MD) and electrodialysis (ED) has also been applied (Bitaw *et al.*, 2016; Zou & He, 2016; Altaee *et al.*, 2014).

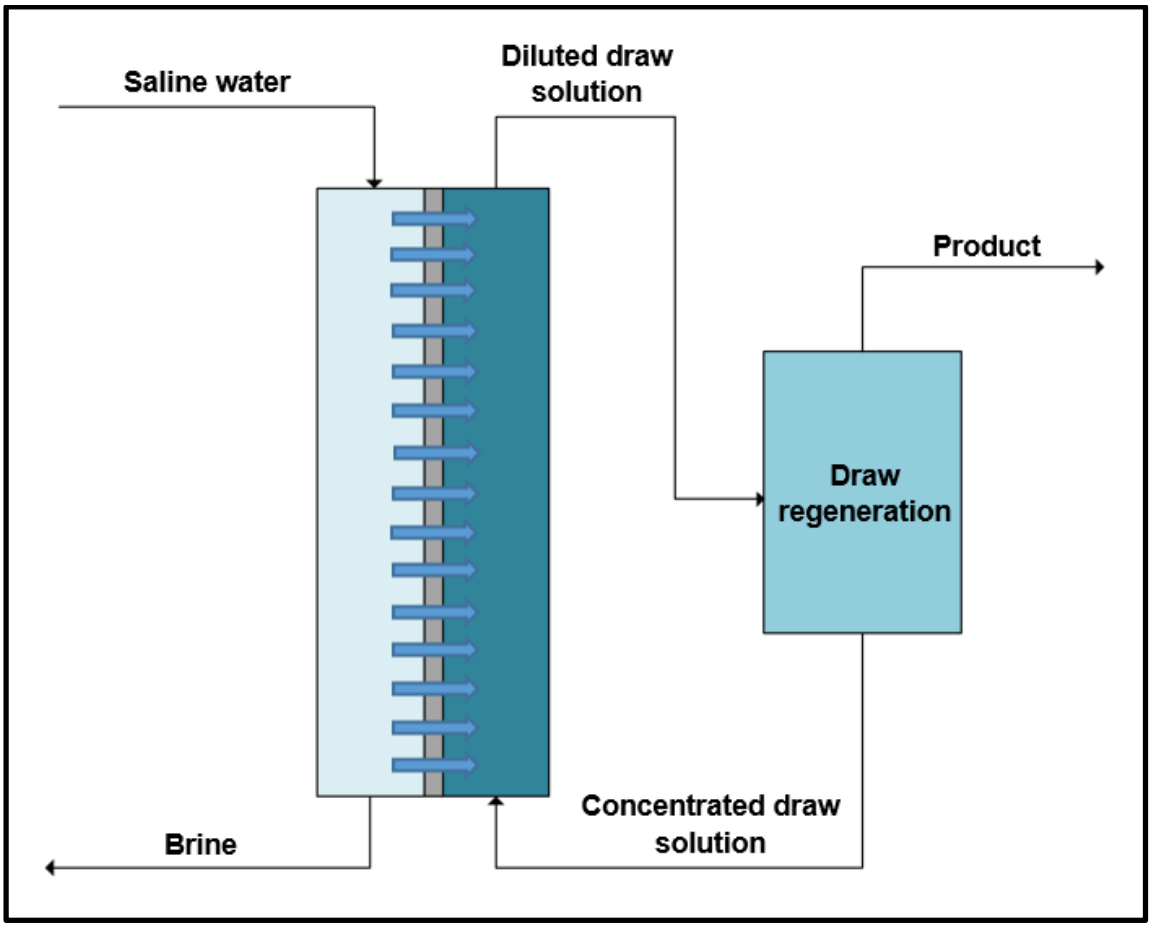

Figure 2.5: Basic depiction of a hybrid FO system

A comparative study by Mazlan (2016) investigated the energy consumption of hybrid FO systems by simulating FO with a single and two-stage NF DS recovery for the desalination of seawater. Additionally, FO was measured to single and two-stage RO systems. The study included an FO-UF recovery featuring nanoparticles as a DS and an FO-Distillation applying NH_4HCO_3 as a DS. The study findings concluded no significant difference in energy consumption between FO-NF with $MgSO_4$ as DS and standalone RO systems (Mazlan *et al.*, 2016) (Table 2.6). However, the capital cost of FO-NF systems was significantly greater compared to single and two-stage RO systems due to an increase in the required membrane area (Mazlan *et al.*, 2016). Additionally, the study also evaluated an FO-Distillation system by incorporating a thermolytic draw solute in the form of ammonium bicarbonate NH_4HCO_3 as a DS. This ammonium salt has excellent draw solute properties as it is highly soluble in water and requires moderate thermal energy (60 ^{0}C) to decompose into ammonia (NH_3) and carbon dioxide (CO_2) gasses (Korenak *et al.*, 2017; McCutcheon *et al.*, 2006), and therefore simplifying the regeneration process.

Results from the study indicated this type hybrid FO system consumed the least amount of energy in comparison with FO-NF and RO systems. However, trace amounts of ammonia remained in the product water that exceeded the allowable limit according to the World Health Organisation (Mazlan *et al.*, 2016). These trace amounts of ammonia bring about taste and odour challenges and have the potential to decrease disinfectant efficiency since ammonia reacts with chlorine (Mazlan *et al.*, 2016). Subsequently, system energy will escalate, as additional treatment processes are required for the removal of ammonia.

Table 2.6: SEC and % water recovery comparison for different hybrid FO systems (Data adapted from Mazlan *et al*., 2016)

System configuration	SEC (kWh/m^3)	Water recovery (%)	Specific area (m^2.h/m^3)
FO-NF recovery	2.4	50	204
FO-two stage NF recovery	2.4	50	204
RO	2.3	50	44
Two-stage RO	2.3	50	54
FO-NF recovery	33	75	628
FO-UF (NP)	3.2	75	N/A
FO-two stage NF recovery	2.4	75	641
Two-stage RO	2.3	75	54
FO-Distil (NH_4HCO_3)	1.2	75	N/A

A study conducted by McGovern and Lienhard (2014) compared the energy consumption of an FO-RO DS recovery system with an RO operation. The study concluded that a single pass RO system should operate at a 47% efficiency in order to achieve an SEC of 2.34 kWh/m^3 (McGovern & Lienhard, 2014). Whereas, the regeneration part of a hybrid FO system should operate at a 70% efficiency in order to utilize the same amount of energy (McGovern & Lienhard, 2014). Therefore, the osmotic dilution or regeneration process in a hybrid FO system should be 23% more efficient, if the overall FO-RO system energy consumption is to be comparable with standalone RO systems.

An RO and FO-RO hybrid systems simulation study were performed and compared by Altaee *et al.* (2014) in which a variety of saline water as an FS, ranging from 32,000 to 45,000 mg/L, was evaluated. The DS applied in the FO-RO process consisted of a 1 or 1.2 M NaCl or 0.65 M $MgCl_2$. Results from the study concluded that the FO-RO system utilising 1.2 M NaCl achieved the highest recovery rate for all FS salinities, though at a cost of higher energy consumption compared to the other processes. This is due to the high DS concentration. RO with 35,000 mg/L saline water produced 20% more water flux than the FO-RO. However, owing to membrane scaling, the RO process could not achieve a recovery rate greater than 50%. Furthermore, the FO part of the FO-RO system contributed to merely 2 to 4% of the total specific energy consumption of the process. Therefore, the regeneration process is considered the energy-intensive part in the FO-RO process. However, the specific energy consumption of the FO-RO process was still greater than the RO process.

Another study by Shaffer *et al.* (2012) examined seawater desalination for agricultural use by simulating an integrated FO and RO system and compared this to a conventional two-stage RO system. This system was recommended due to the rigid set of standards on boron and chlorine for agricultural irrigation water (Shaffer *et al.*, 2012). The advantages of this system are the fouling and solute rejection properties of FO as well as the double barrier for boron and chloride removal. The World Health Organisation standard for irrigation water is more stringent than for potable water (Table 2.7). Therefore, seawater desalination for agricultural irrigation will be more energy intensive compared to that of potable water (Shaffer *et al.*, 2012).

Table 2.7: Regulatory standards for Boron, TDS and chloride for potable and irrigation water (Data adapted from Shaffer *et al.*, 2012)

Species	Potable water species concentration (mg/L)	Agricultural irrigation water species concentration (mg/L)
Boron	2.4	Less than 0.5
Total Dissolved Solids (TDS)	250	Less than 450
Chloride	1000	Less than 105

The study simulated FO as a pre-treatment process for RO as the energy consumption in RO processes is approaching its thermodynamic minimum of approximately 1.5 kWh/m^3 (Shaffer *et al.*, 2012). Therefore, only a small reduction in RO energy consumption is expected by system modification. Thus, to further reduce the SEC of seawater RO (SWRO) desalination processes will be by reducing the energy consumption of the pre- and post-treatment processes (Shaffer *et al.*, 2012).

The study concluded that FO does serve as a possible candidate for a pre-treatment process for RO. This FO-RO hybrid process is less energy intensive than a two-stage RO system. However, there is a trade-off between energy consumption and membrane area which will affect capital and operational cost with a similar conclusion made by Mazlan *et al*, 2016 (refer to Table 2.6).

Nevertheless, hybrid FO does have the potential to be more economical when compared to standalone thermal desalination technologies such as MED, MSF and MVC (Table 2.8) (Akther *et al.*, 2015; Shaffer *et al.*, 2015; McGovern & Lienhard, 2014). These desalination technologies are currently utilised for the treatment of high salinity waters of which the OP extends the operational limit of RO (Akther *et al.*, 2015; Shaffer *et al.*, 2015; McGovern & Lienhard, 2014).

Table 2.8: SEC comparison for different desalination technologies (Data adapted from Phuntsho *et al*., 2012a; Bitaw *et al*., 2016; Zou & He *et al.,* 2016)

Desalination technologies	SEC (kWh/m^3)	References
MSF	10 – 58	(Phuntsho *et al.*, 2012a)
MED	6 – 58	(Phuntsho *et al.*, 2012a)
MVC	20	(Zou & He, 2016)
MED low temp/electrical	5 - 6.5	(Phuntsho *et al.*, 2012a)
RO	4 – 7	(Bitaw *et al.*, 2016; Phuntsho *et al.*, 2012a)
RO with energy recovery	3 – 4	(Phuntsho *et al.*, 2012a)
FO-Electrodialysis-RO	2.48	(Bitaw *et al.*, 2016)
FO-RO	2.40	(Bitaw *et al.*, 2016)
FO-Crystallisation-RO	2.35	(Bitaw *et al.*, 2016)
FO-Distillation (NH_4HCO_3)	0.84	(Phuntsho *et al.*, 2012a)

In conclusion, it seems evident that with current FO technologies, hybrid FO energy consumption and product quality remains incomparable with an RO process. Therefore, the only solution for hybrid FO to be more economical than RO is to use an advanced draw solute. This solute should require a regeneration process that has an (i) low capital cost, (ii) low energy consumption and with (iii) nominal operating cost (Korenak *et al.*, 2017; Zou & He, 2016; Phuntsho *et al.*, 2012a). Nonetheless, the general agreement appears to be for RO to continue as the prominent and most efficient membrane desalination technology in use (Mazlan *et al.*, 2016; Dabaghian & Rahimpour, 2015; Lotfi *et al.*, 2015; McGovern & Lienhard, 2014).

CHAPTER 3
MATERIALS AND METHODS

In this chapter, all operating procedures for experiments and instrument recordings are described in detail. The chapter includes the design of the experiments as well as the analytical methods used. Additionally, the section will describe the bench scale setup, the operating conditions, the experimental design as well as the estimated timeframe for the study.

3.1 Experiment bench scale set-up

For this study, a bench scale forward osmosis (FO) setup (Figures 3.1 and 3.2) was utilised and comprised of an:

i) FO membrane cell (Sterlitech™ Co., CF042D, Sterlitech, United States of America (USA)) with outer dimensions of 0.127 x 0.1 x 0.083 m, a flow channel of 0.092 x 0.046 x 0.0023 m and a membrane area of 0.0042 m^2;
ii) a double head variable speed peristaltic pump (Watson-Marlow, 323E/D, Dune Engineering, South Africa (SA)), for transporting the feed solution (FS) and draw solution (DS), respectively;
iii) a digital scale (WIS, WA606, Weighing Instrument Services (Pty) Ltd, SA) to determine the DS mass variation over time;
iv) a magnetic stirrer (BANTE, MS400, Labotec, SA), to agitate the FS;
v) two reservoirs for the FS and DS, respectively;
vi) a digital multiparameter meter (Lovibond, SD150, Selectech (Pty) Ltd, SA), to determine the EC of the FS; and
vii) a digital electrical multimeter (Toptronic, TBM251, Yebo Electronics, SA), to determine the power consumption of the peristaltic pump. (see Appendix D, Figure D1 for custom build electrical multimeter)

The system was operated in a batch mode with the FS and DS flowing in a counter-current direction with respect to the membrane. A counter-current flow configuration was selected due to its process efficiency (Cath *et al.*, 2006) and the provision of a slightly higher water flux (Phuntsho *et al.*, 2013) in comparison to the co-current flow configuration. As the membrane cell was positioned horizontally, the FS flowed in the top channel of the cell whilst the DS flowed in the bottom channel. This orientation was selected in order for the

water flux to flow with gravity and not against it. All experiments were conducted at ambient temperature.

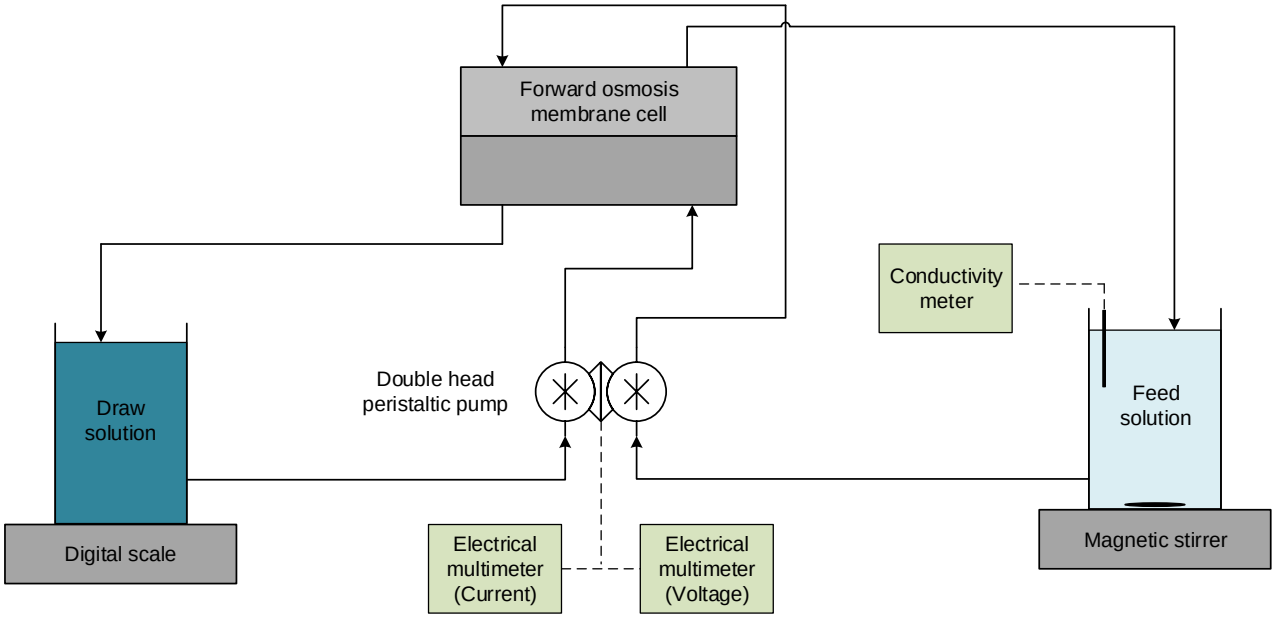

Figure 3.1: P&ID demonstration of the bench-scale FO setup

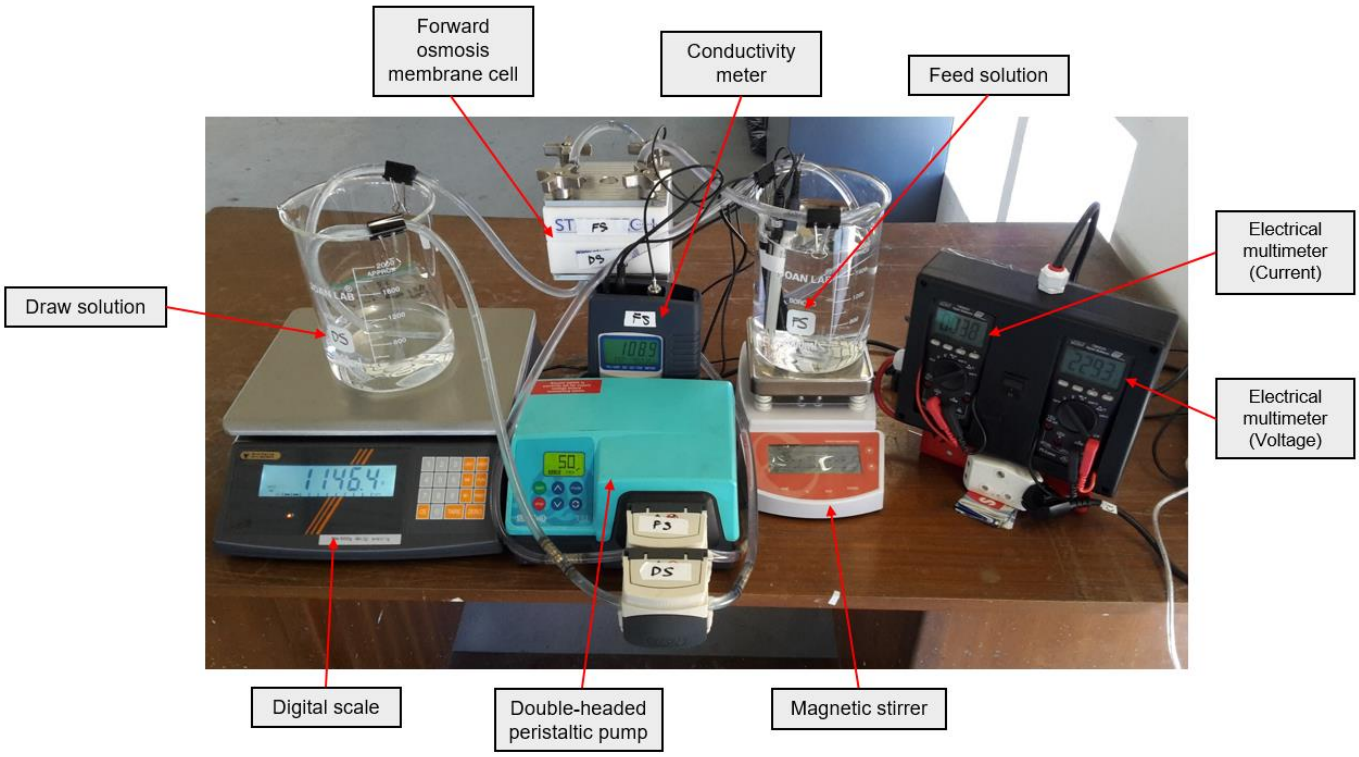

Figure 3.2: Picture of the actual FO bench-scale setup (Picture captured by the custom build portable camera)

The membrane used was a flat-sheet CTA membrane supplied by Fluid Technology Solutions Inc. (Albany, Oregon, USA). The membrane is constructed from cellulose triacetate embedded in a polyester woven mesh and was selected based on its availability and the utilisation as previously reported in other studies (Augustine, 2017; Majeed *et al.*, 2015; Phuntsho *et al.*, 2014; Zhao & Zou, 2011; Achilli *et al.*, 2010). See Appendix C for membrane preparation procedure.

The FS utilised during the pre- and post-FDFO membrane control experiments was deionised (DI) water (A Milli-Q Academic A10 water filter was used to produce DI water and was supplied by, Merck, Gauteng, South Africa). The FS used in the FDFO experiments comprised of a synthetic brackish water (SBW5) solution with a NaCl content of 5 g/L and was selected as it represents an abundant global water source. NaCl used was of analytical grade (purity 98.2%) and was supplied by Merck, Gauteng, South Africa. See Appendix A, section A2 for FS preparation procedure.

The DS used in the pre- and post-FDFO membrane control experiments was a 1 M NaCl solution as previously described in other studies (Lotfi *et al.*, 2015; Phuntsho *et al.*, 2014). The DS utilised for FDFO experiments comprised of a potassium chloride (KCl) fertiliser solution and was selected based on its production of the highest pure water flux in comparison to other inorganic fertilisers evaluated (Augustine, 2017; Phuntsho *et al.*, 2012a; Phuntsho *et al.*, 2011; Achilli *et al.*, 2010). KCl is also one of the most common potassium-based fertilisers used in the agricultural industry (Ren *et al.*, 2015). The KCl used was of analytical grade (purity of ≥99%) and was supplied by Merck, Gauteng, South Africa. See Appendix A, section A3 for DS preparation procedure.

Additionally, a custom build portable camera (Volkano Adrenaline, Outdoor Warehouse, Cape Town, South Africa) was used to monitor the FO setup and to record instrument readings throughout an experiment. See Appendix D, Figure D2 for the custom build portable camera.

3.2 Experiment operating conditions

During the study the following process parameters were adjusted:

- The FO membrane orientation (FO mode vs. PRO mode)
- The FS and DS volumetric flow rates (100, 200 and 400 mL/min)
- The DS concentration (0.5, 1 and 2 M KCl)

Table 3.1: FDFO experimental operating conditions with SBW5 as the FS

Run	Membrane orientation	Flow rate (ml/min)	DS concentration (M)
1	FO mode	100	0.5
2	PRO mode	100	0.5
3	FO mode	200	0.5
4	PRO mode	200	0.5
5	FO mode	400	0.5
6	PRO mode	400	0.5
7	FO mode	100	1
8	PRO mode	100	1
9	FO mode	200	1
10	PRO mode	200	1
11	FO mode	400	1
12	PRO mode	400	1
13	FO mode	100	2
14	PRO mode	100	2
15	FO mode	200	2
16	PRO mode	200	2
17	FO mode	400	2
18	PRO mode	400	2

Experiments were designed with the aid of an experimental design software program (Design Expert, Version 7 (Trail version)) that produced a data set of 18 experiments (Table 3.1). Each experiment was performed in duplicate to validate the result.

3.3 Experiment design and timeframe

Table 3.2 illustrates the individual steps and operating times for the experiment. The operating time selected for the pre- and post-FDFO membrane control experiments (steps a & d) was to ensure 5 data points to compare experimental results. The runtime for the cleaning procedure (steps b, e & g) was selected based on previously reported runtimes (Phuntsho *et al.*, 2014). For the FDFO experiment (step c), a runtime of 24 h was selected as it represents one daytime. The runtime for the membrane damage dye identification procedure (step f) was experimentally determined.

Table 3.2: Individual steps for each experiment

	Experiment	FS	DS	Operating time
a	Pre-FDFO membrane control experiment	DI	1 M NaCl	5 h
b	Membrane cleaning procedure	DI	DI	30 min
c	FDFO experiment	SBW5	0.5; 1; 2 M KCl	24 h
d	Post-FDFO membrane control experiment	DI	1 M NaCl	5 h
e	Membrane cleaning procedure	DI	DI	30 min
f	Membrane damage dye identification procedure	Methyl violet dye solution	2 M NaCl	40 min
g	Membrane cleaning procedure	DI	DI	30 min

Instrument readings were recorded every hour except for the membrane cleaning and membrane damage dye identification procedures where readings were recorded every 10 min.

One experiment required approximately 4 days to complete. Therefore, 144 days were required to complete all 18 experiments including the duplicate experiments. A 30%-day error (approximately 44 days) was added to the existing 144 days to cover for unforeseen incidents or where an experiment required another repeat. Thus, a total of 188 days were reserved to complete all the experiments for this study.

3.4 Experiment operating procedures

This section presents a comprehensive description of the FO bench scale experiment assembly as well as a detailed procedure for each step performed during the experiment.

3.4.1 Determining the relationship between pump revolutions per minute to system flow rate

Prior to commencing of an experiment, the relationship between pump revolutions per minute (RPM) contributed by the pump and system flow rate required to be established, since pumping speed could only be adjusted in RPM and not in mL/min. The cross-flow velocity was determined by dividing the obtained flow rate with the FO membrane cell channel area of 0.00105 m^2. The relationship between pump RPM, flow rate and crossflow velocity is given in Table 3.3.

Table 3.3: Pump RPM corresponding to the volumetric flow rate and membrane cell cross flow velocity

RPM	Flow rate (mL/min)	Solution cross flow velocity in membrane cell (cm/s)
25	100	1.6
50	200	3.2
100	400	6.3
150	600	9.5

Note: These flow rates were determined using a Watson-Marlow 323E/D pump with 6.4 mm Tygon tubing (Dune Engineering, SA)

3.4.2 Bench-scale forward osmosis cell assembly

Assembling the bench scale setup required the positioning of the FO membrane cell, circulation pump, magnetic stirrer, laboratory scale and electric multimeter onto a cleaned working surface. The electrical multimeter was connected to the power mains followed by connecting the pump to the multimeter. Next, the DS digital scale and magnetic stirrer were connected to the power mains. All electrical equipment was turned on to verify functionality. Afterwards, rubber tubing was positioned into each individual pump head of the peristaltic pump. Thereafter, the tubing was connected to the membrane cell. The membrane cell was prepared by untightening the four butterfly nuts and removing the top part of the cell to present the designated compartment for the FO membrane. The prepared membrane (see Appendix C for membrane preparation procedure) was removed gently from the packaging by wearing laboratory latex gloves and positioning it into the designated membrane compartment ensuring the correct orientation being tested (see Table 3.1). Thereafter, the membrane cell was closed by replacing the top part of the cell and fastening the four butterfly nuts firmly. Next, the membrane was acclimatised. For this procedure, a beaker containing 0.5 L DI water was positioned onto the workbench after which the pump tubing was submerged in the water. The tubing was then attached to the walls of the beaker with binding clips to prevent tubes emerging from the water. The pump was prepared by setting the pumping speed to 100 RPM corresponding to 400 mL/min and then started. Membrane acclimatisation continued for 10 min after which the pump was temporally stopped to remove the suction tubing from the beaker followed by resuming pumping. The pump continued to operate until all DI water was displaced from the system and then stopped.

3.4.3 Pre- and post- fertiliser-drawn forward osmosis membrane control experiment

For the pre- and post- FDFO membrane control experiments (Table 3.2 a & d), a beaker containing 0.5 L of a 1 M NaCl DS (see Appendix A, section A1 for DS preparation procedure) were positioned onto the digital scale followed by recording the mass (the mass of the beaker was accounted for). A second beaker containing 2 L of DI water FS was then placed onto the magnetic stirrer followed by the addition of a 2 cm stirring bar to the beaker. Thereafter, the EC and temperature probes of the multiparameter were suspended into the FS. The tubing was placed into the respective beakers followed by fastening the tubing to the beakers using binder clips. The mass of the DS was recorded a second time to account for the mass addition of the tubing. The pump was prepared by setting the pumping speed to 100 RPM corresponding to 400 mL/min followed by turning on the pump to prime the system (higher

flow rates were used for priming as low flow rates are ineffective for eliminating air from the system). The pump was operated until all air was displaced and then stopped. The mass of the DS was recorded for a third time to account for the mass loss during the priming step. Thereafter, the magnetic stirrer was set to a medium agitating speed (agitation speed was adjusted to prevent vortex formation) and then turned on. The pump RPM was re-adjusted to 50 RPM corresponding to 200 mL/min and then initiated. The system operated for 10 min before initial DS mass, FS EC, the voltage supplied and the current drawn by the pump was recorded. The experiment operated for 5 h with DS mass, FS EC, voltage and current readings recorded for every hour. After the completion of the experiment, the pump was temporarily paused followed by removing the pump suction tubing from the FS and DS beakers, respectively, and submerging it into a beaker containing 200 mL DI water. The pump was restarted, allowing to operate until all solutions in the system were replaced with DI water. The pump continued to operate until the system was clear of DI water and then bring to an end. The pre- and post- FDFO membrane control experiments were performed before and after the FDFO experiment to investigate the occurrence of membrane fouling during the FDFO process by comparing pre- and post- FDFO membrane control water recoveries.

3.4.4 Membrane cleaning procedure

The membrane cleaning procedure (Table 3.2 b, e & g) used DI water in the FS and DS compartments of the FO membrane cell to physically clean the membrane of any possible fouling. First, 0.5 L DI water was added to the FS and DS beakers, respectively. The pump tubing was positioned into the respective beakers and fastened with binder clips to the beaker. The pump speed was set to 150 RPM corresponding to 600 mL/min and then started. The system operated for 10 min after which the initial voltage and current readings were recorded. The cleaning procedure continued for 30 min with voltage and current readings recorded for every 10 min. At the end of the procedure, the pump was stopped after which the pump suction tubing was removed from the FS and DS beakers, respectively, and submerged in a beaker containing 200 mL fresh DI water. Once again the pump was started and allowed to operate until the beaker containing the fresh DI water was empty. The pump continued to operate until the system was clear of water and then stopped. The membrane cleaning steps were performed after the pre- and post- FDFO membrane control experiments as well as after the membrane damage dye identification procedure (Table 3.2 b, e & g). The cleaning was performed at these intervals to ensure a clean membrane for each individual experiment steps.

3.4.5 Fertiliser-drawn forward osmosis experiment

For the FDFO experiment (Table 3.2 c), a beaker containing 0.5 L of 0.5, 1 or 2 M KCl DS (depending on the concentration being tested) (see Table 3.1) (see Appendix A, section A3 for DS preparation procedure) were positioned onto the digital scale followed by the recording of the beaker mass (the mass of the beaker was accounted for). An additional beaker containing 2 L SBW5 (see Appendix A, section A2 for FS preparation procedure) was positioned onto the magnetic stirrer followed by adding a 2 cm stirring bar to the beaker. Next, the EC and temperature probes of the multiparameter meter were submerged into the FS. Then, the pump tubing was placed into the respective beakers and fasten with binding clips to prevent tubes emerging from the solutions. The mass of the DS beaker was recorded a second time to account for the mass gained by the tubing. The pump was prepared by setting the pumping speed to 100 RPM corresponding to 400 mL/min followed by turning on the pump to prime the system (higher flow rates were used for priming as low flow rates are ineffective for removing air from the system). The pump operated until all air displaced from the system after which the pump was stopped. The mass of the DS was recorded for a third time to account for the mass loss during the priming step. Thereafter, the magnetic stirrer was set to a medium agitating speed (agitation speed was adjusted to prevent vortex formation) and then started. The pump speed was also re-adjusted to 25, 50 or 100 RPM corresponding to 100, 200 and 400 mL/min depending on the flow rate being tested (see Table 3.1). The system operated for 10 minutes before the initial FS and DS OP as well as the DS mass, FS EC, voltage and current readings, were recorded. The experiment continued for 24 h with DS mass, FS EC, voltage and current reading recorded for every hour. After the experiment was completed, final FS and DS OP was measured after which the pump was stopped, the suction tubing was removed from the respective beakers and submerged into a beaker containing 200 mL DI water. Pumping was resumed and continued until all solutions within the system were replace with DI water. The pump continued to operate until the system was clear of water after which the pump was stopped.

3.4.6 Membrane damage dye identification procedure

For the membrane damage dye identification procedure (Table 3.2 f), the membrane active layer should always face the FS (FO mode). Therefore, the membrane should be re-orientated after it was tested in the PRO mode. This is an important step and if the membrane orientation was not correct the procedure will produce misleading results. The procedure was performed after every 2nd experiment due to the CTA membrane durability. For this procedure, 0.5 L of a 2 M NaCl (see Appendix B, section B2 for DS preparation procedure) was positioned onto the digital scale followed by recording the mass (the mass of the beaker was accounted for). A second beaker containing 0.5 L methyl violet dye solution (see Appendix B, section B1 for FS preparation procedure) was positioned close to the pump. Thereafter, pump tubing was added to the respective beakers and fasten to the beaker with binding clips. The mass of the DS was recorded for a second time to account for the mass gained by the tubing. The pump was prepared by setting the pumping speed to 100 RPM corresponding to 400 mL/min followed by starting the pump in order to prime the system (higher flow rates were used for priming as low flow rates are ineffective for removing air from the system). The pump continued to operate until all air was displaced after which the pump was stopped. The mass of the DS was recorded a third time to account for the mass loss during the priming step. The pump was re-adjusted to 50 PRM corresponding to 200 mL/min and then started. The system operated for 10 min after which the initial DS mass was recorded. The experiment continued until a minimum of 10 mL (± 10 g) was gained by the DS. After the experiment was completed, the pump was stopped followed by removing the suction tubing from the respective beakers. The pump was restarted and operated until the system was clear of solutions and then stopped. Next, the membrane was removed from the membrane cell (wearing latex laboratory gloves) and was inspected for damage. Any surface damage on the membrane-displayed purple whilst an undamaged membrane remained unstained (see Appendix E, Figure E1 for example images). If any damage was noted, the membrane was discarded whilst an undamaged membrane was re-used after a physical membrane cleaning procedure.

3.5 Experimental analysis and calculations

The change in DS mass was recorded to determine the pure water flux and water recovery. The FS EC was recorded to estimate the RSF. Pump voltage and the current were recorded to calculate pump power consumption which was combined with the water recovery to determine the SEC of the FO system.

3.5.1 Osmotic pressure measurement & calculations

3.5.1.1 Osmotic pressure measurement

To measure the OP of the FS and DS, the osmometer was turned on and was allowed to prepare for the measuring conditions by producing ice. Thereafter, the measure button was pushed on the digital touchscreen. Next, 50 µL of the FS and DS was collected, respectively, using a pipette and transferred to their respective polymerase chain reaction (PCR) test tubes. To prevent cross-contamination new pipette tips were used when collecting samples from the FS and DS. The test solution tube was positioned onto the measuring point of the osmometer followed by sliding the measuring point downwards using the allocated handle. After closing the measuring point, the sample analysis was initiated automatically. The reading on the digital screen was allowed to reach a constant value before it was recorded.

3.5.1.2 Calculating osmotic pressure

OP of the FS and DS was determined with the aid of a cryoscopic osmometer (OSMOMAT 3000, Gonotec, Germany). OP results obtained from the osmometer was recorded in milliosmole per kg (mOsmol/kg) which was converted to kPa using the relationship from Equations 3.1, 3.2 and 3.3 (Larcher, 2003; Alexander, 1981) (see Appendix F, section F1 for a sample calculation).

$$\frac{1\,Osmole}{kg}H_2O = 2.48\,MPa \qquad \textbf{Equation 3.1}$$

$$\frac{1\,mOsmole}{1\,kg}H_2O = \frac{0.001\,Osmole}{kg}H_2O \qquad \textbf{Equation 3.2}$$

$$\frac{1\,mOsmole}{kg}H_2O = 2.48\,kPa \qquad \textbf{Equation 3.3}$$

3.5.2 Calculating experimental water flux

Water flux was determined based on the mass variation of the DS with time and was calculated from Equations 3.4 and 3.5 (Dabaghian & Rahimpour, 2015) (see Appendix F, section F2 for a sample calculation)

$$J_W = \frac{V_{DSt_2} - V_{DSt_1}}{A_m \cdot (t_2 - t_1)} \qquad \textbf{Equation 3.4}$$

$$J_W = \frac{m_{DSt_2} - m_{DSt_1}}{\rho \cdot A_m \cdot (t_2 - t_1)} \qquad \textbf{Equation 3.5}$$

Where J_w (L/m^2.h) is the water flux, V_{DSt_1} (L) is the volume of the DS at recording time interval t_1 (h), V_{DSt_2} (L) is the volume of the DS at recording time interval t_2 (h), m_{DSt_1} (g) is the mass of the DS at recording time interval t_1 (h), m_{DSt_2} (g) is the mass of the DS at recording time interval t_2 (h), A_m (m^2) is the effective membrane area, and t_1 and t_2 (h) is the recording time intervals, ρ (g/L) is the density of the solution. It is assumed that the change in mass of the DS is mainly attributed to the permeation of pure water. Therefore, the density of water (ρ = 1000 g/L) was used for the mass to volume conversions.

3.5.3 Feed solution electrical conductivity measurements and reverse solute flux calculations

3.5.3.1 Feed solution electrical conductivity measurements

To measure the EC, the digital multiparameter meter was prepared by connecting the EC and temperature probe to their respective connection points located at the top of the meter. The meter mode was changed by pressing the mode button until the meter indicated the EC auto temperature setting. The EC and temperature probes were submerged into the FS and swirled around manually to remove any trapped air bubbles around the probes. The meter reading was allowed to reach a constant value before it was recorded. The meter automatically alters the EC units from µS/cm to mS/cm depending on the solutions EC. EC was measured throughout an experiment and compared with the accumulative water recoveries obtained to estimate RSF.

3.5.3.2 Calculating reverse solute flux

RSF was determined based on the EC variation of the FS with time and was calculated from Equation 3.6 (Dabaghian & Rahimpour, 2015) (see Appendix F, section F3 for a sample calculation)

$$J_S = \frac{V_{FS_{t_2}} \cdot C_{FS_{t_2}} - V_{FS_{t_1}} \cdot C_{FS_{t_1}}}{A_m \cdot (t_2 - t_1)} \qquad \textbf{Equation 3.6}$$

Where J_s (g/m^2.h) is the RSF, $V_{FS_{t_1}}$ (L) is the volume of the FS at recording time interval t_1 (h), $V_{FS_{t_2}}$ (L) is the volume of the FS at recording time interval t_2, $C_{FS_{t_1}}$ (g solute/L water) is the mass concentration of the FS at recording time interval t_1 (h), $C_{FS_{t_2}}$ (g solute/L water) is the mass concentration of the FS at recording time interval t_2, A_m (m^2) is the effective membrane area, and t_1 and t_2 (h) is the recording time intervals. Note RSF was only calculated for the pre- and post- FDFO membrane control experiments. RSF's for the FDFO experiments was estimated as mentioned in section 3.5.3.1.

3.5.4 Calculating volume water recovery

Volume water recovery was determined by the amount of water that fluxed from the FS to the DS during an experiment. Water recovery was determined from Equation 3.7 and 3.8. (see Appendix F, section F4 for a sample calculation):

$$Volume\,water\ \ recovery = V_{FS_{t_1}} - V_{FS_{t_2}} \qquad \textbf{Equation 3.7}$$

$$Volume\,water\ \ recovery = V_{FS_{t_1}} - \left(V_{FS_{t_1}} - \left(\frac{m_{DS_{t_2}} - m_{DS_{t_1}}}{\rho} \right) \right) \qquad \textbf{Equation 3.8}$$

Where $V_{FS_{t_1}}$ (L) is the volume of the FS at recording time interval t_1, $V_{FS_{t_2}}$ (L) is the volume of the FS at recording time interval t_2, $m_{DS_{t_1}}$ (g) is the mass of the DS at recording time interval t_1 (h), $m_{DS_{t_2}}$ (g) is the mass of the DS at recording time interval t_2 (h), ρ (g/L) is the density of the solution. It is assumed that the change in mass of the DS is mainly attributed to the permeation of pure water. Therefore, the density of water (ρ = 1000 g/L) was used for the mass to volume conversions.

3.5.5 Pump power measurement and specific energy consumption calculations

3.5.5.1 Pump power measurement

To measure pump power consumption, the custom build multimeter containing two identical electrical meters were switched on. Meter 1 was set to the AC current setting and meter 2 was set to the AC voltage setting. Thereafter, the electrical circuit was exchanged from meter bypass mode to the point where current flow through the meters by pushing the exchange switch located between the meters (see Appendix D, Figure D1). The readings on the two meters were allowed to reach a constant value before it was recorded.

3.5.5.2 Calculating specific energy consumption for a fertiliser-drawn forward osmosis system

The SEC of the system were determined based on the electrical power consumed of the circulation pump and the recovered water volume. SEC was calculated from Equations 3.9 and 3.10) (see Appendix F, section F5 for a sample calculation):

$$SEC = \frac{Total\ energy\ consumed\ by\ pump\ (kWh)}{Total\ volume\ recovered\ (m^3)} \qquad \textbf{Equation 3.9}$$

$$= \frac{(PF \cdot V_{Volt} \cdot I_{Amp}) \cdot (Total\ hours\ of\ operation)}{(1000) \cdot (Total\ volume\ recovered\ for\ hours\ of\ operation)} \qquad \textbf{Equation 3.10}$$

Where *SEC* (kWh/m^3) is the specific energy consumption, *PF* is the power factor (Dimensionless), V_{Volt} (W/A) is the electrical potential (Voltage) applied to the pump, I_{Amp} (A) is the electrical current (Ampere) drawn by the pump. The pump used was a single phase, however, the power factor (*PF*) was assumed to be 1. Note the SEC was calculated in terms of the electrical duty and not the work performed by the pump.

CHAPTER 4
RESULTS AND DISCUSSIONS

4.1 Evaluating the performance recovery of the pre-fertiliser-drawn forward osmosis membrane control experiment

In this section, results of the membrane performance recovery of the pre-FDFO membrane control experiment are presented. Performance recovery was measured in terms of water flux, RSF and water recovery.

4.1.1 Performance recovery for the pre-fertiliser-drawn forward osmosis membrane control experiment: Water flux

In this study, a pre-FDFO membrane control experiment (Table 3.2 a) were performed and compared with post-FDFO membrane control experiments (Table 3.2 d) to investigate if membrane fouling did occur during the FDFO experiment (Table 3.2 c). Figure 4.1 illustrates the water fluxes obtained during a 5 h operation for 6 pre-fertiliser membrane control experiments using the same membrane whilst operating in a) FO and b) PRO mode with a DS concentration of 1 M NaCl and DI water as the FS both at a flow rate of 200 mL/min, respectively. The initial difference in osmotic pressure (ΔOP) obtained using 1 M NaCl and DI water was $\pm$4184 kPa. The membrane used in this study was subjected to a membrane damage dye identification procedure (Table 3.2 f) to determine the re-usability of the membrane. Throughout the study, membrane damage tests did not indicate any membrane impairment and subsequently, the same membrane was used repetitively followed by a physical cleaning technique. From Figure 4.1 (a), an average initial water flux obtained between the 6 pre-FDFO membrane control experiments was 3.9$\pm$0.09 L/m^2.h after which it steadily declined due to osmotic dilution to result in an average final water flux of 3.3$\pm$0.22 L/m^2.h. Whilst on the other hand, from Figure 4.1 (b) an average initial water flux of 3.5$\pm$0.13 L/m^2.h was obtained between the 6 pre-fertiliser membrane control experiments after which the fluxes steadily decreased to a final average water flux of 3.1$\pm$0.09 L/m^2.h. It can be seen from Figure 4.1 that the FO mode resulted in a slightly greater water flux compared to the PRO mode. It was hypothesised that the cause for FO mode obtaining a greater water flux compared to the PRO mode was due to CP as the same membrane was used for FO and PRO mode experiments. Section 4.4 will elaborate in more detail regarding this phenomenon.

Nonetheless, it can be seen that the initial water flux performance recovery after the membrane cleaning resulted in similar water fluxes to that obtained from the 1st pre-FDFO membrane control experiment. This indicates that the membrane cleaning was effective in recovering water fluxes. As the membrane water fluxes remained consistent with a minimal deviation between experiments, the pre-FDFO membrane control and membrane cleaning step (steps (a) and (b) from Table 3.2) was discontinued after the 6th experiment. Results obtained from these 6 pre-FDFO membrane control experiments were used to compare post-FDOF membrane control experiments to investigate membrane fouling.

a)

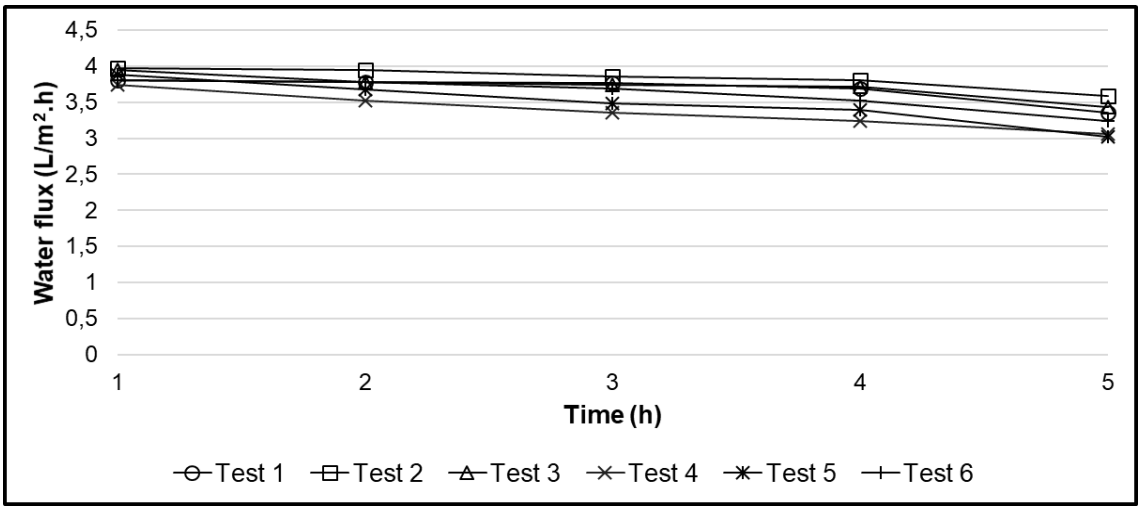

b)

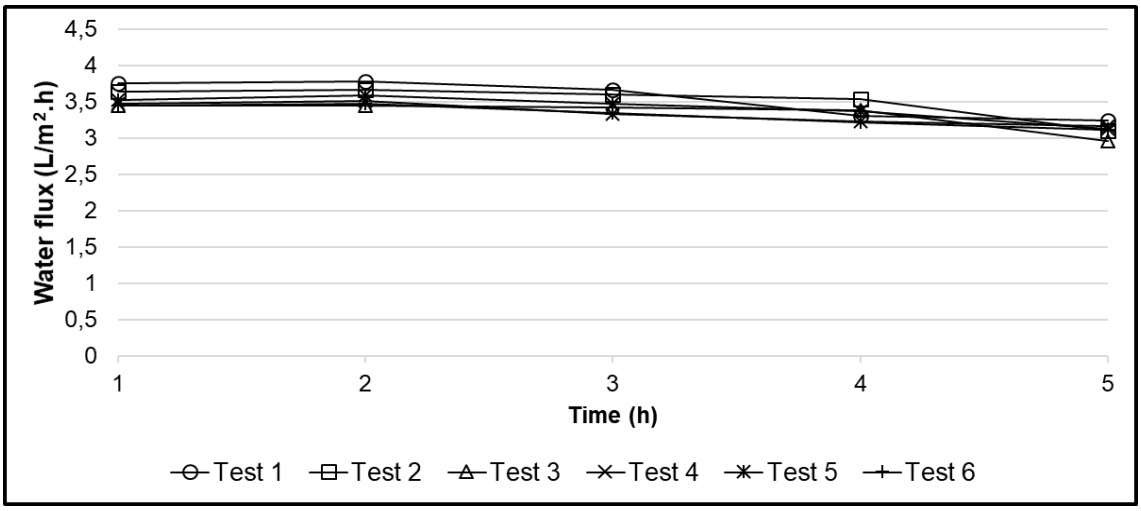

Figure 4.1: Water fluxes obtained during a 5 h operation for 6 pre-FDFO membrane control experiments using the same membrane whilst operating in a) FO and b) PRO modes at a DS concentration of 1 M NaCl with DI water as the FS both at a flow rate of 200 mL/min, respectively.

4.1.2 Performance recovery for the pre-fertiliser-drawn forward osmosis membrane control experiment: Reverse solute flux

Figure 4.2 illustrates the RSF's obtained during a 5 h operation for 6 pre-fertiliser membrane control experiments using the same membrane whilst operating in a) FO and b) PRO modes with a DS concentration of 1 M NaCl and DI water as the FS both at a flow rate of 200 mL/min, respectively. From Figure 4.2 (a), an average initial RSF of 0.66±0.07 g/m^2.h was obtained between the 6 pre-fertiliser membrane control experiments after which the RSF's decreased to an average final RSF of 0.46±0.06 g/m^2.h. Additionally, from Figure 4.2 (b), an average initial RSF of 0.60±0.07 g/m^2.h was achieved between the 6 pre-fertiliser membrane control experiments which decreased to an average final RSF of 0.38±0.05 g/m^2.h. The RSF obtained whilst operating in FO mode for the 1st pre-FDFO membrane control experiment was less than that obtained for the PRO mode. This observation is in agreement with other reports in literature (Phuntsho *et al.*, 2013). This anticipated higher solute concentration at the membrane active layer in the PRO mode compared to the FO mode produces a slight increase in osmotic driving force which sequentially results in a greater water flux but also increases RSF. It should be noted that RSF's deviated slightly from the 1st pre-FDFO membrane control experiment as the membrane was subjected to different FDFO experiments at altered DS concentrations. Thus, the remaining solutes from these experiments might have remained within the membrane support layer after the membrane cleaning. Therefore, these solutes might contribute to an increase in DI water conductivity which will produce different RSF results compared to the 1st pre-FDFO membrane control experiment.

a)

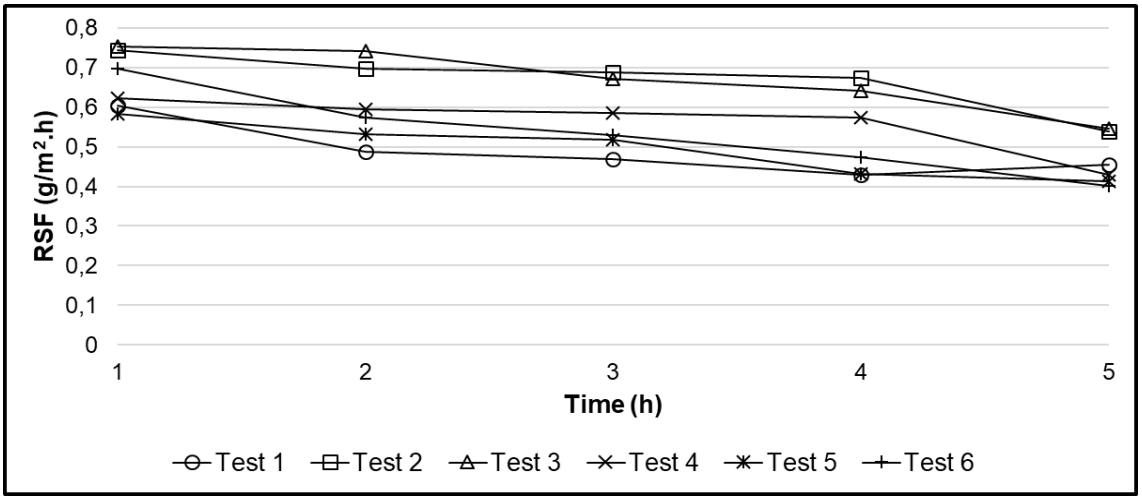

b)

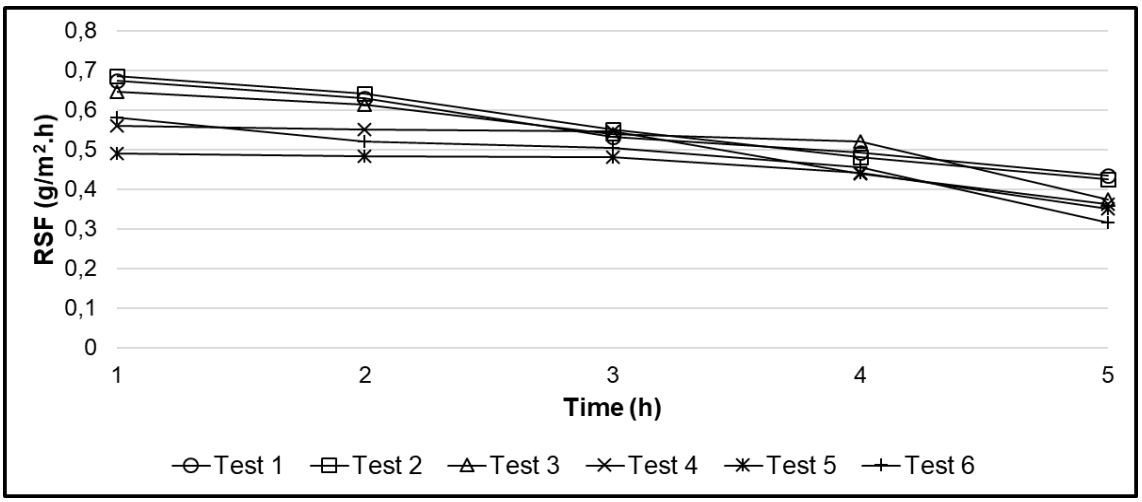

Figure 4.2: RSF's obtained during a 5 h operation for 6 pre-fertiliser membrane control experiments using the same membrane whilst operating in a) FO and b) PRO modes at a DS concentration of 1 M NaCl with DI water as the FS both at a flow rate of 200 mL/min, respectively.

4.1.3 Performance recovery for the pre-fertiliser-drawn forward osmosis membrane control experiment: Water recovery

Figure 4.3 illustrates the accumulative water recoveries obtained during a 5 h operation for 6 pre-FDFO membrane control experiments using the same membrane whilst operating in a) FO and b) PRO modes with a DS concentration of 1 M NaCl and DI water as a FS both at a flow rate of 200 mL/min, respectively. From Figure 4.3 (a), an average accumulative water recovery of 76±3.4 mL was achieved whilst on the other hand from Figure 4.3 (b) an accumulative water recovery of 71±2.1 mL was obtained. As water recovery is directly related to water flux it can be observed the FO mode resulted in a slightly greater water recovery compared to the PRO mode which was assumed to be owing to the effects of CP as previously mentioned.

a)

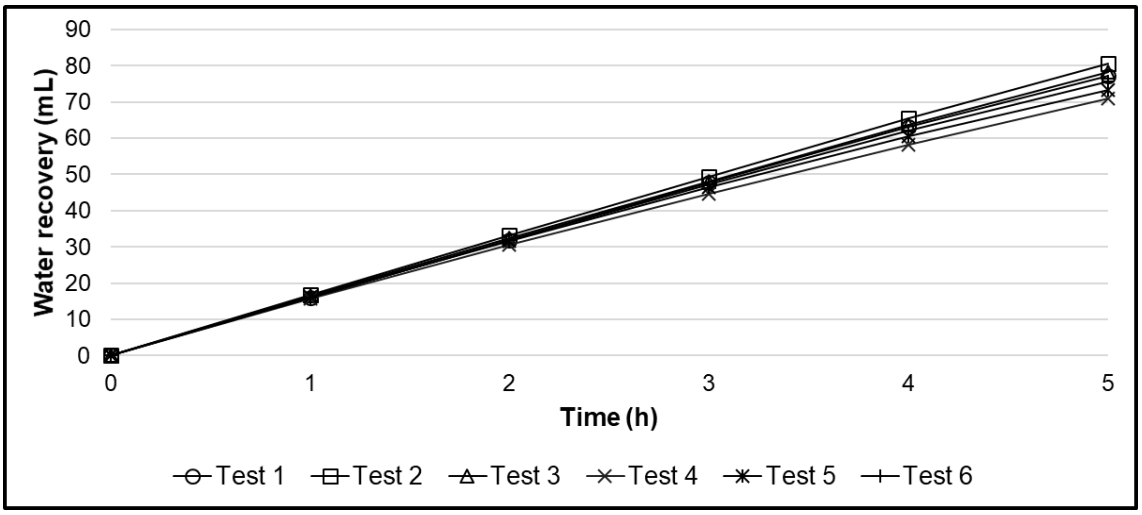

b)

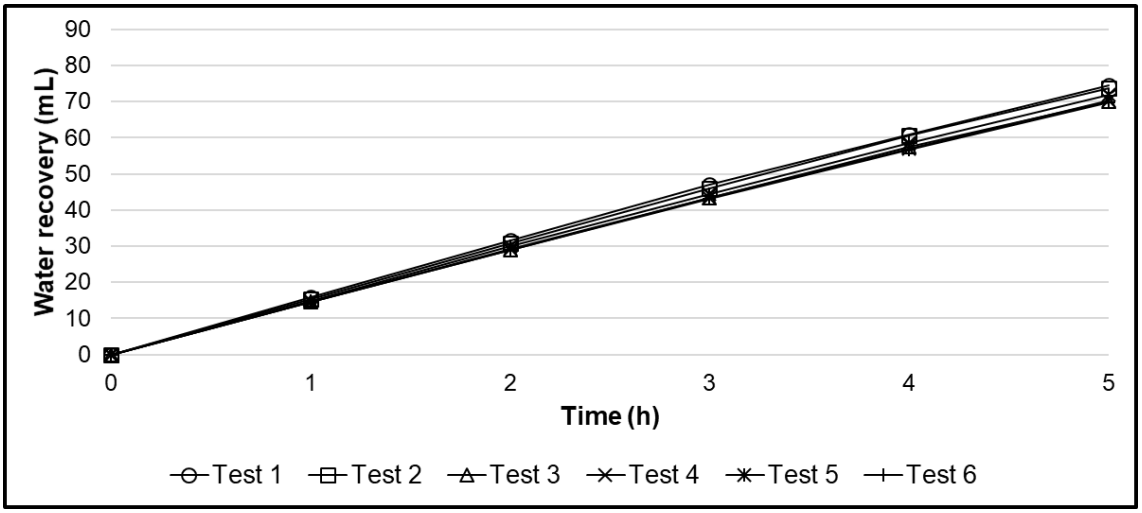

Figure 4.3: Accumulative water recoveries obtained during a 5 h operation for 6 pre-fertiliser membrane control experiments using the same membrane whilst operating in a) FO and b) PRO modes at a DS concentration of 1 M NaCl with DI water as the FS both at a flow rate of 200 mL/min, respectively.

4.2 Water flux trends obtained during fertiliser-drawn forward osmosis experiments

In this section, the water flux trends obtained during FDFO experiments (Table 3.2 c) is discussed.

4.2.1 Discussing fertiliser-drawn forward osmosis water flux trends

In the majority of experiments conducted, the initial water fluxes started low then peaked between hourly points 2 or 3, after which water fluxes steadily declined once more (see Figure 4.5). This increase followed by a decrease in water flux during the initial stages of the experiment and contradicts the FO driving mechanism. At the commencement of an experiment, the osmotic driving force is greatest and ought to result in the highest water flux followed by a decrease. This decline in flux is the result of a decline in osmotic driving force attributed to osmotic dilution of the DS, effects of CP and membrane fouling. As previously mentioned the membrane used was subjected to a membrane damage dye identification procedure to determine if the membrane is re-usable. Membrane damage tests did not indicate any membrane damage and subsequently, the same membrane was used repetitively after a thorough cleaning. The trends of the initial increase in water flux followed by a decrease observed in this study were similar to, Zou & He (2016) that reported water flux data with a similar trend. However, Zou & He (2016) did not discuss the trend development. Zou & He (2016) further described the experiment operated in FO mode whilst using wastewater and a multipurpose fertiliser as an FS and DS, respectively. The results from their study indicated a new membrane to produce the greatest initial water flux followed by a flux decline. In addition, they continue to describe the effects when the same membrane was chemically cleaned and re-used. The results produced a graph trend similar to the results obtained in this study.

An independent experiment was performed using a new membrane and the water fluxes were compared to the repetitively used membranes water flux to investigate the unfamiliar trend. Figure 4.4 illustrates water fluxes obtained for a) FO and b) PRO modes with a DS concentration of 2 M KCl with SBW5 as the FS at a flow rate of 400 mL/min. The initial ΔOP achieved at a DS concentration of 2 M KCl and SBW5 as the FS was $\pm$8613 kPa. Figure 4.4 (a) indicates that initial water fluxes increased by 3.2 L/m^2.h from a water flux of 4.3 to 7.5 L/m^2.h for a used and new membrane, respectively. Whilst from Figure 4.4 (b), initial water fluxes increased by 5.8 L/m^2.h from a water flux of 3.2 to 9.0 L/m^2.h for a used and a new membrane, respectively. Additionally, it can be seen from Figure 4.4, that the tests whilst using

a new membrane, resulted in the PRO mode obtaining a higher initial flux compared to that of the FO mode, which is in agreement with other reports in literature.

Notwithstanding a significant increase in water flux can be observed between a new and used membrane. Additionally, the irregular trend of an initial water flux increase followed by a decrease, only occurred when the membrane was re-used. These results are in agreement with reports by Zou & He (2016) which imply the unfamiliar trend observed was due to membrane re-use. Whilst this observation was previously reported but never fully examined, it was hypothesised that the low initial water fluxes obtained when the membrane was re-used was the result of the effect of internal concentration polarisation (ICP). As the physical membrane cleaning procedure used in this study would be more effective in cleaning the outer surfaces of the membrane it would be less effective to clean within the membrane support layer. Therefore, when a membrane was re-used, solutions from a previous experiment which caused ICP remained captured within the membrane support layer as the membrane cleaning was unable to penetrate the support layer. Thus, dilutive internal concentration polarisation (DICP) would remain within the membrane if it was tested in an FO mode orientation whilst concentrative internal concentration polarisation (CICP) would remain if a PRO mode orientation was tested. Consequently, these polarised layers create an additional resistance through which the new bulk solutions must diffuse in order to produce an effective osmotic driving force essential for generating water flux. The low initial water fluxes observed during the study may be attributable to a low effective osmotic driving force because of the ICP. However, as the bulk solutions started to diffuse through the ICP layers a greater driving force is generated due to the difference in osmotic pressure between the bulk FS and DS which in turn produce an increased water flux as observed.

The effects of DS concentrations on water fluxes, RSF's and water recoveries as well as its effects on FDFO system energy consumption is discussed in section 4.3.

a)

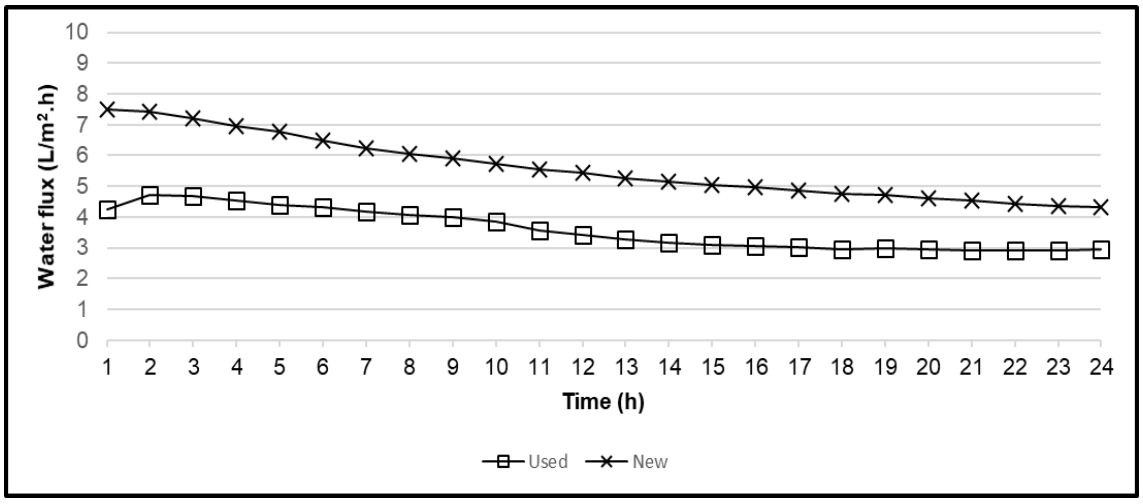

b)

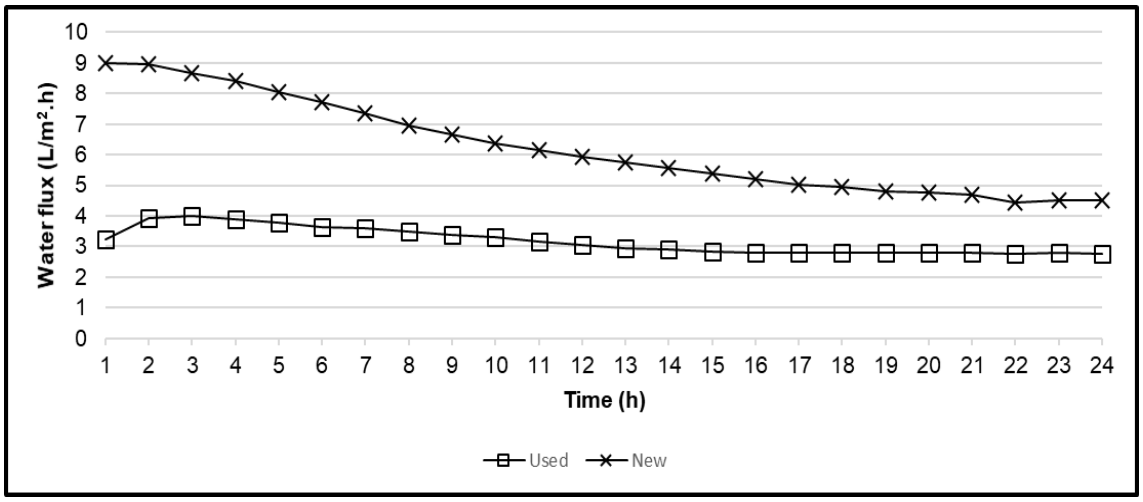

Figure 4.4: Water fluxes obtained during a 24 h operation between a used and new membrane for a) FO and b) PRO modes at a DS concentration of 2 M KCl and SBW5 as the FS both flowing at a rate of 400 mL/min, respectively.

4.3 The effect of draw solution concentration on the fertiliser-drawn forward osmosis system performance and energy consumption

In this section, the effects of DS concentration on the FDFO system performance and energy consumption is described. The observed effects on system performance in terms of water flux, RFS and water recovery is deliberated. Subsequently, the changes in SEC is discussed.

4.3.1 The effects of draw solution concentration on the fertiliser-drawn forward osmosis system performance: Water flux

In this study, DS concentrations varied from 0.5, 1 and 2 M KCl which corresponded to an initial OP of ±2017, ±4067 and ±9045 kPa, respectively. Thus, resulting in an initial ΔOP of ±1611, ±3661 and ±8639 with SBW5 as the FS. Figure 4.5 illustrates a comparison of water fluxes obtained during a 24 h operation at DS concentrations of 0.5, 1 and 2 M KCl with SBW5 as the FS whilst operating in a) FO and b) PRO modes at flow rates of i) 100, ii) 200 and iii) 400 mL/min, respectively. From Figure 4.5 (a) (i) at a DS concentration of 0.5 M, an initial water flux of 0.3±0.2 L/m^2.h was obtained followed by a flux increased to 0.9±0.2 L/m^2.h which remained consistent throughout the 24 h operation. However, at a DS concentration of 1 M, an initial water flux of 2.7±0.4 L/m^2.h was achieved that increased to a flux of 2.9±0.3 L/m^2.h followed by a steady flux decline resulting in a final water flux of 1.9±0.1 L/m^2.h. Additionally, at a DS concentration of 2 M, an initial water flux of 4.2±0.1 L/m^2.h resulted which increased to a flux of 4.8±0.5 L/m^2.h after which the water flux declined steadily to a final water flux of 3.1±0.3 L/m^2.h. Figure 4.5 (a) (ii) indicate at a DS concentration of 0.5 M, an initial water flux of 1.1±0.4 L/m^2.h was achieved which decreased slightly to result in a final water flux of 0.8 ±0.2 L/m^2.h. On the other hand, at a DS concentration of 1 M, an initial water flux of 2.9±0.4 L/m^2.h was obtained which declined to a final water flux of 1.9 L/m^2.h. Additionally, at a DS concentration of 2 M, an initial water flux of 3.9±0.1 L/m^2.h occurred followed by a flux increase to 4.2±0.5 L/m^2.h afterwards the flux decreased to result in a final water flux 2.9±0.1 L/m^2.h. Figure 4.5 (a) (iii) illustrates a DS concentration of 0.5 M, an initial water flux of 0.5±0.3 L/m^2.h was obtained followed by a flux increase to 0.9±0.2 L/m^2.h which remained consistent throughout the 24 h experiment. At a DS concentration of 1 M, an initial water flux of 3.0±0.3 L/m^2.h was achieved after which the water flux steadily decreased to a final water flux of 1.9± 0.0 L/m^2.h. Additionally, at a DS concentration of 2 M an initial water flux of 3.8±0.4 L/m^2.h was obtained followed by a flux increase to 4.5±0.4 L/m^2.h which declined steadily to result in

a final water flux of 2.9±0.2 L/m^2.h. Figure 4.5 (b) (i) indicate at some point at a DS concentration of 0.5 M, an initial water flux of 0.6±0.2 L/m^2.h was achieved followed by a slight increase to a flux of 1.0±0.1 L/m^2.h which remained consistent throughout the 24 h experiment. At a DS concentration of 1 M, an initial water flux of 2.6±0.3 L/m^2.h was achieved followed by a slight increase to a flux of 2.9±0.1 L/m^2.h after which the water flux decreased to a final water flux of 1.9±0.1 L/m^2.h. Furthermore, at a DS concentration of 2 M, an initial water flux of 5.1±0.3 L/m^2.h was attained after which fluxes declined to a final water flux of 3.0±0.3 L/m^2.h. Figure 4.5 (b) (ii) illustrates a DS concentration of 0.5 M, an initial water flux of 0.9±0.1 L/m2.h was obtained which increased slightly to a flux of 1.2±0.0 L/m^2.h at hour 3 followed by a decrease result in a concluding water flux of 0.9 L/m^2.h. Subsequently, at a DS concentration of 1 M, an initial water flux of 2.6±0.3 L/m^2.h was achieved followed by a slight increase to a flux of 2.8±0.2 L/m^2.h after which the water flux steadily decreased to a final water flux of 1.8±0.2 L/m^2.h. Additionally, at a DS concentration of 2 M, an initial water flux of 5.0±0.5 L/m^2.h was obtained which steadily declined to a final water flux of 3.0±0.2 L/m^2.h. Figure 4.5 (b) (iii) indicate at a DS concentration of 0.5 M, an initial water flux of 1.0±0.2 L/m^2.h was achieved which increased slightly to a flux of 1.2±0.2 L/m^2.h which followed a decrease to result in a final water flux of 0.8±0.1 L/m^2.h. Moreover, at a DS concentration of 1 M, an initial water flux of 2.7±0.3 L/m^2.h was obtained which increased to a flux 3.0±0.6 L/m^2.h followed by a flux decline to result in a final water flux of 1.9 L/m^2.h. Lastly, at DS concentration of 2 M, an initial water flux of 3.2±0.3 L/m^2.h was obtained which increased to a flux of 4.0±0.1 L/m^2.h at hour 3 after which water fluxes decreased to a final water flux of 2.8±0.3 L/m^2.h.

It can be seen from Figure 4.5 (a) and (b) (i) – (iii) water fluxes increased by approximately threefold from a DS concentration increase of 0.5 to 1 M which subsequently increased once more by an additional 30 to 50 % with a DS concentration increase from 1 to 2 M. These findings are in agreement with previous reports on producing a greater water flux as a result of increased DS concentration. However, water fluxes obtained during this study was significantly lower compared to earlier reports. A study by Phuntsho *et al.* (2013) described water fluxes up to ±9 L/m^2.h at a DS concentration of 1 M whilst operating in an FO mode and ±10 L/m^2.h in a PRO mode at a flow rate of 400mL/min using SBW5 as the FS. From the independent experiment conducted in section 4.2, Figure 4.4 (a) and (b) illustrates that water fluxes of up to 7.5 and 9 L/m^2.h was achieved for FO and PRO modes, respectively at a DS concentration of 2 M KCl with SBW5 as the FS at a flow rate of 400 mL/min using a new membrane. These fluxes were slightly lower than reported by Phuntsho *et al.* (2013), however,

there remained some similar observations. Nonetheless, the highest water fluxes obtained whilst re-using the membrane at a DS concentration of 0.5, 1 and 2 M KCl was 1.4, 3.3 and 5.4 L/m^2.h, respectively. Assumingly, the significant decrease in water flux observed was the result of ICP. Given that the membrane was re-used throughout the study, ICP might have been transferred from one experiment to the next by means of insignificant membrane cleaning in the PRO mode orientation as previously mentioned. It was previously reported that water fluxes could be impaired by up to 80% attributable to the effects of ICP (Gray *et al.*, 2006). An additional parameter which might support this assumption is the difference in final OP at the end of the FDFO experiment. It was established that the average final ΔOP obtained after a 24 h experiment with a DS concentration of 0.5, 1 and 2 M was ±1243, ±2299 and ±4326 kPa, respectively. At these OP's, much higher water fluxes were expected and the membrane and membrane cleaning is proposed to be the limitation in this study. The severity of ICP on water flux observed is apparent and should be considered a major factor when considering the reuse of FO membranes.

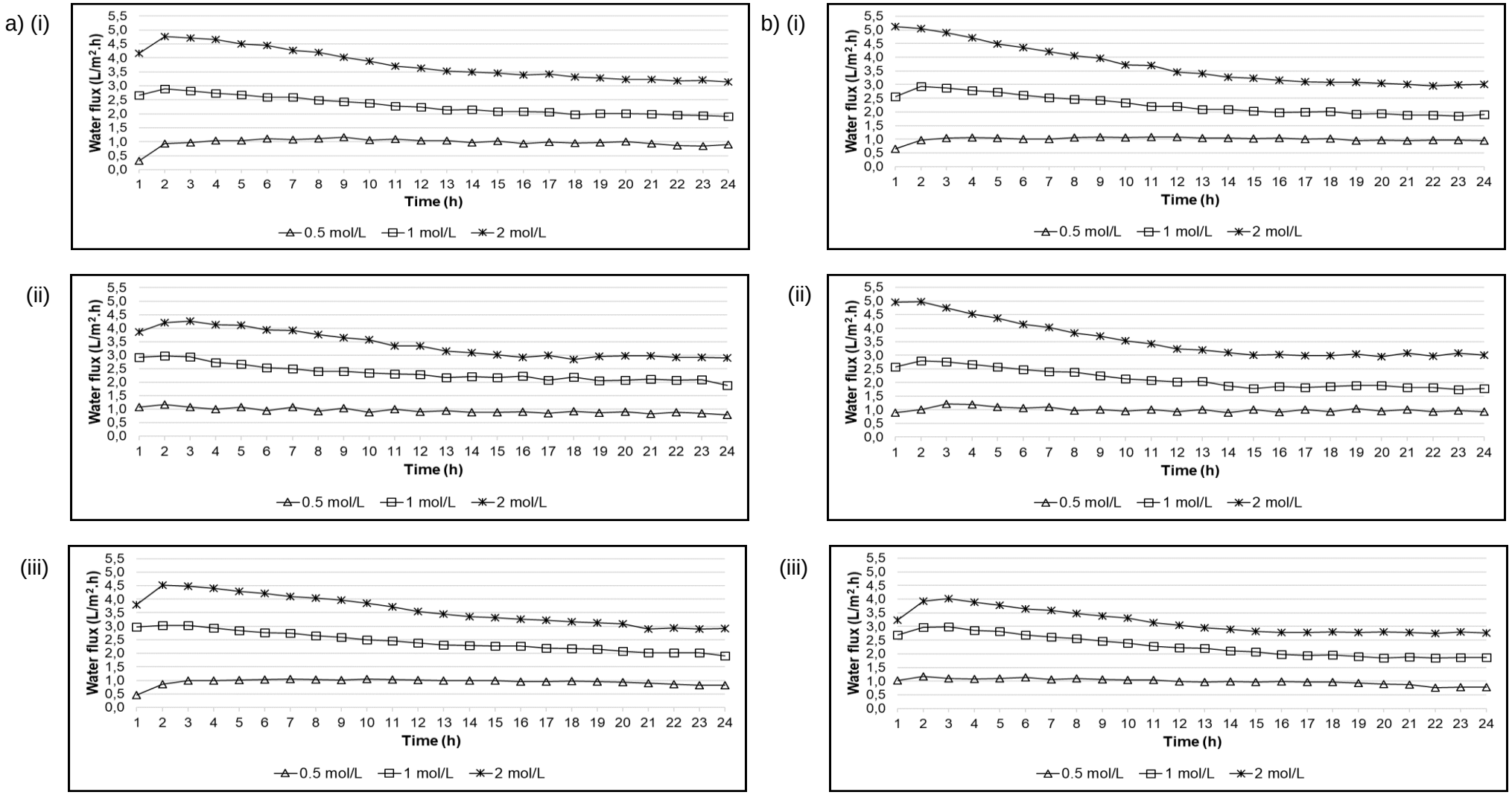

Figure 4.5: Water fluxes obtained during a 24 h operation for DS concentrations of 0.5, 1 and 2 M KCl with SBW5 as the FS whilst operating in a) FO and b) PRO modes at flow rates of i) 100, ii) 200 and iii) 400 mL/min, respectively.

4.3.2 The effects of draw solution concentration on the fertiliser-drawn forward osmosis system performance: Reverse solute flux

RSF in any membrane separation process is inevitable as no membrane is perfect (Phuntsho *et al.*, 2011). This phenomenon is a key factor responsible for limiting system performance which in turn increase operational cost. In this study, RSF was estimated by comparing the EC's and water recoveries of the FS in FO and PRO modes during a 24 h operation. As the FDFO system operated in batch mode the FS EC will increase over time. This increase in FS EC is determined by two factors, viz. (i) the concentrating effect of the FS due to the water permeation to the DS and (ii) as a result of RSF form the DS.

Figure 4.6 illustrates the accumulative water recoveries and FS EC's obtained during a 24 h operation for DS concentrations of 0.5, 1 and 2 M KCl with SBW5 as the FS whilst operating in a) FO and b) PRO modes at flow rates of i) 100, ii) 200 and iii) 400 mL/min, respectively. Figure 4.6 (a) (i) indicate that the FS EC's increased from an initial conductivity of 9.4 mS/cm to a final conductivity of 10.2±0.2, 11.2±0.1 and 12.0±0.3 mS/cm whilst an accumulative water recovery of 97.3±7.7, 232.1±12.6 and 382.3±17.4 mL was obtained for DS concentrations of 0.5, 1 and 2 M, respectively. Whilst from Figure 4.6 (a) (ii), a final FS EC of 10.3±0.0, 11.3±1.0 and 11.9±0.2 mS/cm was obtained with an accumulative water recovery of 95.6±16.1, 238.6±18.1 and 347.0±16.3 mL for DS concentration of 0.5, 1 and 2 M, respectively. Additionally, Figure 4.6 (a) (iii) illustrates that the FS EC increased to a final EC of 10.3±0.2, 11.6±0.0 and 12.0±0.0 mS/cm whilst achieving an accumulative water recovery of 95.7±13.2, 246.9±12.6 and 365.4±12.9 mL for DS concentration of 0.5, 1 and 2 M, respectively. Notwithstanding, from Figure 4.6 (b) (i) a final FS EC of 10.3±0.2, 11.3±0.1 and 12.1±0.2 mS/cm was obtained while achieving an accumulative water recovery of 101.4±5.6, 228.5±3.5 and 375.2±19.2 mL for DS concentration of 0.5, 1 and 2 M, respectively. Whereas, from Figure 4.6 (b) (ii) a final FS EC of 10.2±0.1, 11.0±0.2 and 12.1±0.2 mS/cm was achieved whilst obtaining an accumulative water recovery of 103.4±5.4, 218.3±3.9, and 361.5±23.7 mL for DS concentration of 0.5, 1 and 2 M, respectively. Lastly, Figure 4.6 (b) (iii) indicate that a final FS EC of 10.4±0.3, 11.1±0.2 and 11.6±0.1 mS/cm was achieved whilst obtaining an accumulative water recovery of 100.1±3.5, 231.6±18.2 and 320.8±5.7 mL for DS concentration of 0.5, 1 and 2 M, respectively.

Nevertheless, based on the method used by comparing accumulative water recoveries and FS EC's to estimate RSF, no definitive evidence indicated that RSF has occurred along with an increase in DS concentration. For the mere reason that both accumulative water recoveries and FS EC's increase simultaneously with the rise in DS concentration, as a result, it is particularly difficult to reach a final conclusion. Nevertheless, according to the literature, RSF is dependent on the concentration gradient between the FS and DS (Phuntsho *et al.*, 2012b). Thus, increasing the DS concentration will produce an increased concentration gradient and so RSF as the FO system tend to a thermodynamic equilibrium. It is therefore important to consider that even though a higher fertiliser DS concentration will produce an increase water recovery, the implications of a DS concentration upsurge would result in the loss of solutes to the FS which can cause additional complications (Phuntsho *et al.*, 2013).

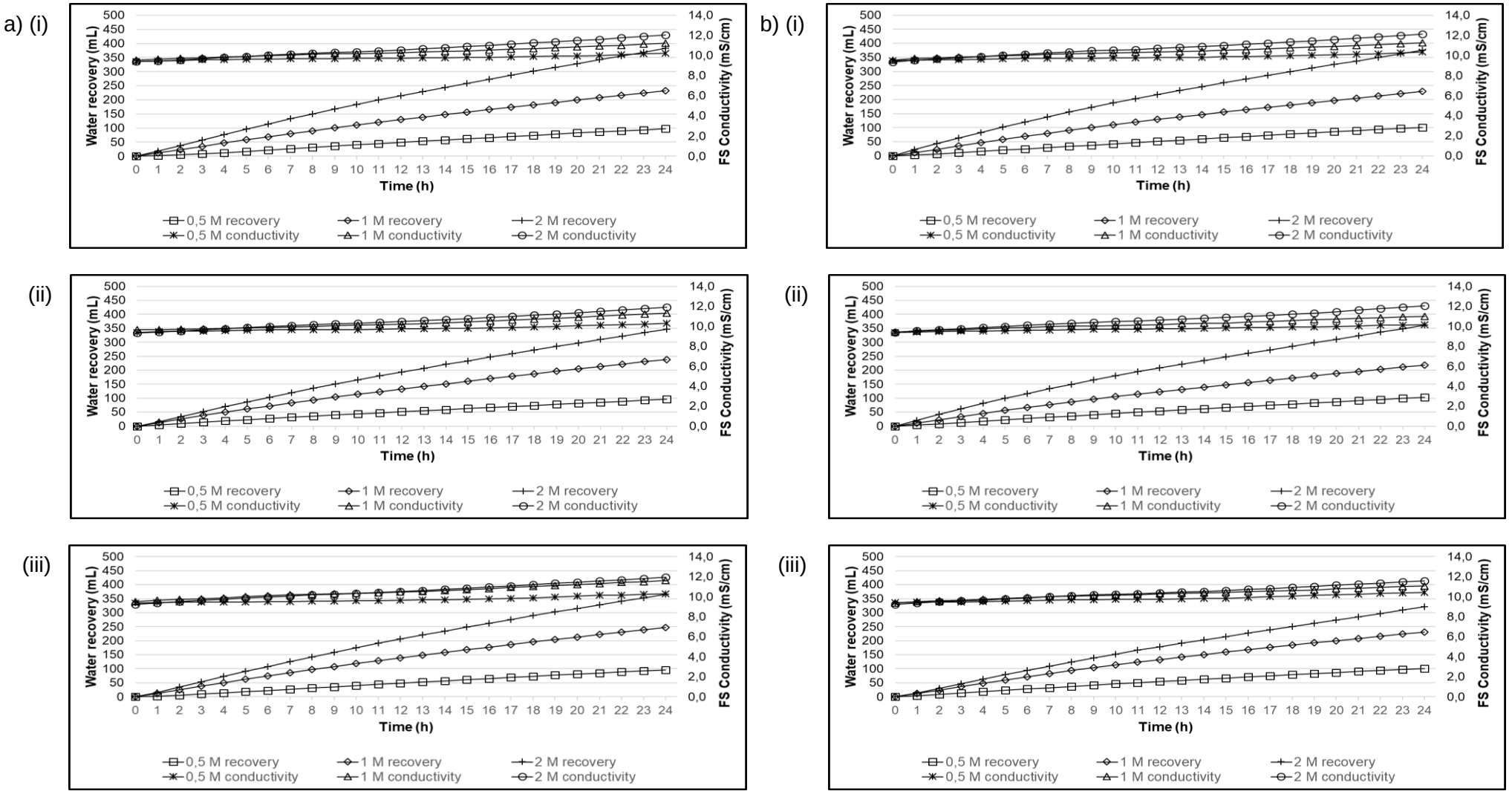

Figure 4.6: Accumulative water recoveries and FS EC's obtained during a 24 h operation for DS concentrations of 0.5, 1 and 2 M KCl with SBW5 as the FS whilst operating in a) FO and b) PRO modes at flow rates of i) 100, ii) 200 and iii) 400 mL/min, respectively.

4.3.3 The effects of draw solution concentration on the fertiliser-drawn forward osmosis system performance: Water recovery

Figure 4.7 illustrates the accumulative water recoveries obtained during a 24 h operation for DS concentrations of 0.5, 1 and 2 M KCl with SBW5 as the FS whilst operating in a) FO and b) PRO modes at flow rates of i) 100, ii) 200 and iii) 400 mL/min, respectively. The initial ΔOP of ±1611, ±3661 and ±8639 kPa was achieved for DS concentrations of 0.5, 1 and 2 M, respectively. From Figure 4.7 (a) (i) an accumulative water recovery of 97.3±7.7, 232.1±12.6 and 382.3±17.4 mL was achieved for DS concentrations of 0.5, 1 and 2 M, respectively. While from Figure 4.7 (a) (ii) an accumulative water recovery of 95.6±16.1, 238.6±18.1 and 347.0 ±16.3 mL was obtained for DS concentration of 0.5, 1 and 2 M, respectively. Additionally, Figure 4.7 (a) (iii) indicates that an accumulative water recovery of 95.7±13.2, 246.9±12.6 and 365.4±12.9 mL resulted for DS concentrations of 0.5, 1 and 2 M, respectively. Notwithstanding, the accumulative water recovery achieved in Figure 4.7 (b) (i) for DS concentration of 0.5, 1 and 2 M was 101.4±5.6, 228.5±3.5 and 375.2±19.2 mL, respectively. Whilst from Figure 4.7 (b) (ii), an accumulative water recovery of 103.4±5.4, 218.3±3.9, and 361.5±23.7 mL was achieved for DS concentrations of 0.5, 1 and 2 M, respectively. Lastly, from Figure 4.7 (b) (iii), an accumulative water recovery of 100.1±3.5, 231.6±18.2 and 320.8 ±5.7 mL was achieved for DS concentrations of 0.5, 1 and 2 M, respectively.

From Figure 4.7, observations to the increase in water recovery are directly related to DS concentration. Therefore, a DS concentration of 2 M obtained the greatest accumulative water recovery followed by a DS concentration of 1 and 0.5 M. This upsurge in reclaimed water was anticipated due to the greater ΔOP's. As OP is a colligative property (Phuntsho *et al.*, 2012b), a solution containing a greater concentration irrespective of the species will produce a greater OP. Thus, the effective osmotic driving force between the FS and DS increase due to the upsurge in DS concentration which in turn produce an elevated water flux and so water recovery. However, it was noted that after 24 h that the average final ΔOP obtained whilst operating in FO mode at DS concentrations of 0.5, 1 and 2 M was 1248±38, 2331±44 and 4248±67 kPa, respectively. Whilst an average final ΔOP of 1238±24, 2267±34 and 4403± 59 kPa was obtained whilst operating in PRO mode at DS concentrations of 0.5, 1 and 2 M, respectively. As previously mentioned in section 4.3.1, at these ΔOP's much greater water recoveries was anticipated, however, due to the severity of ICP significantly lower water fluxes and so water recoveries were obtained.

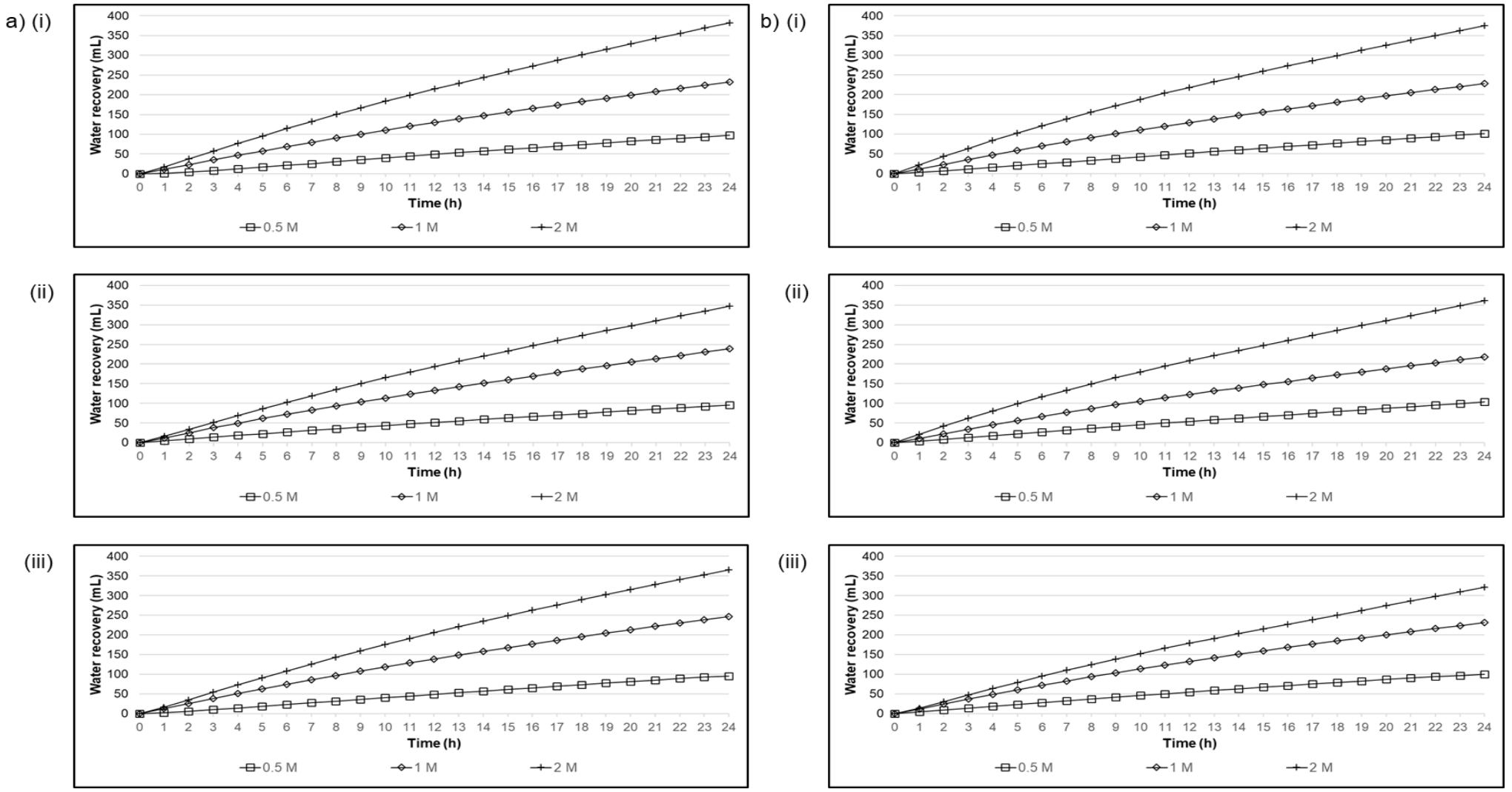

Figure 4.7: Accumulative water recoveries obtained during a 24 h operation for DS concentrations of 0.5, 1 and 2 M KCl with SBW5 as the FS whilst operating in a) FO and b) PRO mode at flow rates of i) 100, ii) 200 and iii) 400 mL/min, respectively.

4.3.4 The effects of draw solution concentration on the fertiliser-drawn forward osmosis system energy consumption

Figure 4.8 illustrates the accumulative pump power consumption, water recovery as well as the SEC obtained during a 24 h operation whilst operating in a) FO and b) PRO modes at DS concentrations of 0.5, 1 and 2 M KCl with SBW5 as the FS at flow rates of i) 100, ii) 200 and iii) 400 mL/min, respectively. Figure 4.8 (a) (i) indicates that a total pump power consumption of 0.22±0.01, 0.23±0.01 and 0.24±0.02 kWh was achieved while obtaining an accumulative water recovery of 97.3±7.7, 232.1±12.6 and 382.3±17.4 mL which in turn produced a SEC of ±2295.3, ±995.2 and ±631.5 kWh/m^3 for DS concentrations of 0.5, 1 and 2 M, respectively. Figure 4.8 (a) (ii) illustrates a pump power consumption of 0.20±0.01, 0.20±0.02 and 0.22±0.0 kWh whilst an accumulative water recovery of 95.6±16.1, 238.6±18.1 and 347.0±16.3 mL was achieved which resulted in an SEC of ±2056.0, ±835.9 and ±619.7 kWh/m^3 for DS concentration of 0.5, 1 and 2 M, respectively. Additionally, Figure 4.8 (a) (iii) indicates a total pump power consumption of 0.30±0.02, 0.32±0.01 and 0.26±0.0 kWh whilst an accumulative water recovery of 95.7±13.2, 246.9±12.6 and 365.4±12.9 mL was achieved which resulted in an SEC of ±3098.2, ±1278.7 and ±720.8 kWh/m^3 for DS concentration of 0.5, 1 and 2 M, respectively. Whilst on the other hand, from Figure 4.8 (b) (i) a total pump power consumption of 0.22±0.0, 0.23±0.01 and 0.24±0.0 kWh was obtained whilst achieving a total water recovery of 101.4±5.6, 228.5±3.5 and 375.2±19.2 mL, therefore, resulting in an SEC of ±2184.6, ±1024.5 and ±637.6 for DS concentration of 0.5, 1 and 2 M, respectively. Subsequently, Figure 4.8 (b) (ii) indicates that a total pump power consumption of 0.20±0.01, 0.22±0.0 and 0.23±0.0 kWh was achieved whilst obtaining an accumulative water recovery of 103.4±5.4, 218.3±3.9, and 361.5±23.7 mL which in turn produced a SEC of ±1924.3, ±991.5 and ±624.1 kWh/m^3 for DS concentration of 0.5, 1 and 2 M, respectively. Lastly, Figure 4.8 (b) (iii) illustrates a total pump power consumption of 0.32 ±0.01, 0.32±0.01 and 0.28±0.0 kWh whilst an accumulative water recovery of 100.1±3.5, 231.6±18.2 and 320.8±5.7 mL was achieved which resulted in an SEC of ±3187.5, ±1385.0 and ±870.0 kWh/m^3 for DS concentration of 0.5, 1 and 2 M, respectively.

It can be seen from Figure 4.8 (a) an increase in DS concentration from 0.5 to 1 M decreased the system's SEC with an average of 58 %, followed by an additional 35 % reduction from a DS concentration alteration of 1 to 2 M. Figure 4.5 (b) indicate similar results with an increase in DS concentration. Here, the SEC was reduced by 53 % at a DS concentration increase of 0.5 to 1 M, with a subsequent reduction of 37 % at a DS concentration increase of 1 to 2 M.

Seeing that a system's SEC is determined by two factors, i) the power consumed by the system and ii) the product recovered from the energy consumed. The increase of DS concentration, in theory, will affect pump power consumption by reason of the additional headloss created by the solutions physical properties such as its density, viscosity etc. However, the additional head created by the increase in DS concentration in this study was insignificant as very diluted solutions were used. However, a decrease in SEC was anticipated with an increase in DS concentration as supplementary water is recovered at similar pump power consumptions. Therefore, higher DS concentrations are recommended to decrease the SEC of the FDFO system and to improve economic viability. However, additional capital will be required to dilute fertilisers as the fertiliser concentration will be insufficient for direct applications. Subsequently, additional cost might be essential to treat feed waters due to the occurrence of RSF. It should be noted that the SEC's obtained was extremely high. This is due to the electrical power consumption of the pump used in SEC calculations and not the work performed by the pump as theoretically calculated in literature. It should be noted that since this is a bench scale setup, the pump used was greatly oversized hence a larger power consumption was noted for the scale of the system. Therefore, if the correct pump size was used for this system, SEC results would have been similar to that reported in the literature.

The effects of membrane orientation on water fluxes, RSF's and water recoveries as well as its effects on FDFO system energy consumption is discussed in section 4.4.

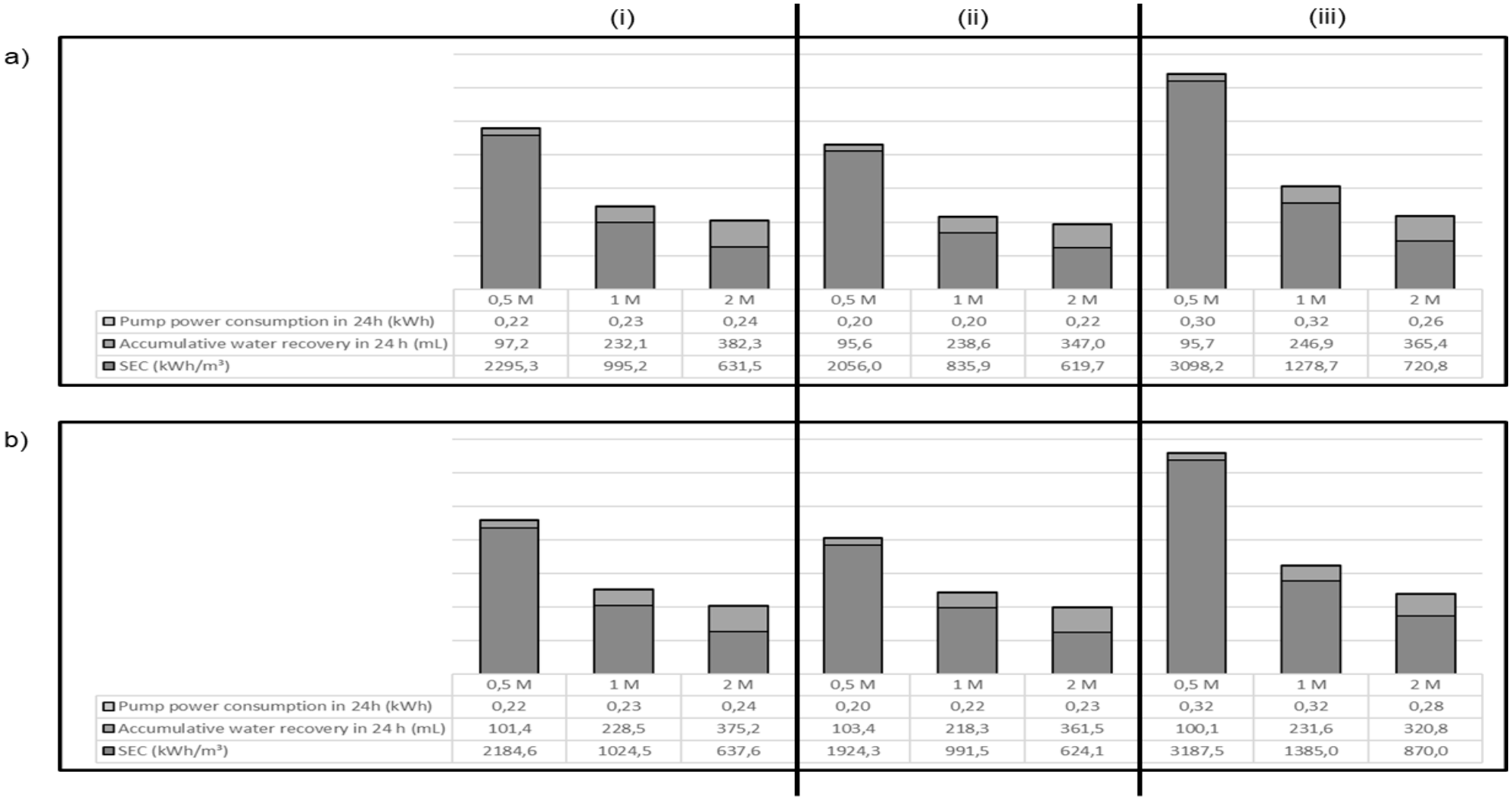

Figure 4.8: Accumulative pump power consumption, water recovery and SEC consumption obtained during a 24 h operation for a) FO and b) PRO modes at DS concentrations of 0.5, 1 and 2 M KCl with SBW5 as the FS at flow rates of i) 100, ii) 200 and iii) 400 mL/min, respectively.

4.4 Evaluating the effects of membrane orientation on the fertiliser-drawn forward osmosis system performance and energy consumption

In this section, the effects of membrane orientation on FDFO system performance and energy consumption is presented. The system performance measured in terms of water flux, RSF and water recovery is deliberated. Subsequently, the changes in the SEC is discussed.

4.4.1 The effects of membrane orientation on the fertiliser-drawn forward osmosis system performance: Water flux

Figure 4.9 illustrates the water fluxes obtained during a 24 h operation for FO and PRO mode orientations at DS concentrations of a) 0.5, b) 1 and c) 2 M KCl with SBW5 as the FS at flow rates of i) 100, ii) 200 and iii) 400 mL/min, respectively. Figure 4.9 (a) (i) indicate that in the FO mode, an initial water flux of 0.3±0.2 L/m^2.h was obtained after which it increased to a flux of 0.9±0.2 L/m^2.h where it remained consistent throughout the 24 h operation. Whilst, for the PRO mode an initial water flux of 0.6±0.2 L/m^2.h was achieved after which it increased to a flux of 1.0±0.1 L/m^2.h where it also remained consistent throughout the 24 h experiment. Figure 4.9 (a) (ii) illustrates that in the FO mode an initial water flux of 1.1±0.4 L/m^2.h was achieved which slightly decreased to a final water flux of 0.8±0.2 L/m^2.h. Whilst, for the PRO mode an initial water flux of 0.9±0.1 L/m2.h was obtained which increased to a flux of 1.2±0.0 L/m^2.h followed by a flux decline to a final water flux of 0.9 L/m^2.h. Figure 4.9 (a) (iii) indicates that during the FO mode an initial water flux of 0.5 L/m^2.h was obtained which increased to 0.9±0.2 L/m^2.h which remained consistent throughout the 24 h experiment. For the PRO mode, an initial water flux of 1.0±0.2 L/m^2.h was achieved which slightly increased to a flux of 1.2±0.2 L/m^2.h after which the water flux decreased to a final water flux of 0.8±0.1 L/m^2.h. Additionally, Figure 4.9 (b) (i) illustrates that during the FO mode an initial water flux of 2.7±0.4 L/m^2.h was achieved which increased to a flux of 2.9±0.3 L/m^2.h followed by a steady flux reduction to a final water flux of 1.9±0.1 L/m^2.h. During the PRO mode an initial water flux of 2.6±0.3 L/m^2.h was obtained which increased slightly to a flux of 2.9±0.1 L/m^2.h followed by a steadily decrease to a result in a final water flux of 1.9±0.1 L/m^2.h. Figure 4.9 (b) (ii) indicates that during the FO mode an initial flux of 2.9±0.4 L/m^2.h was obtained which steadily declined to a final water flux of 1.9 L/m^2.h. For the PRO mode, an initial water flux of 2.6±0.3 L/m^2.h was achieved which increased to a flux of 2.8±0.2 L/m^2.h after which the flux decreased to a final water flux of 1.8±0.2 L/m^2.h. Figure 4.9 (b) (iii) indicates that during the FO mode an initial water flux of 3.0±0.3 L/m^2.h was achieved followed by a decrease in flux to a final water flux of 1.9±0.0 L/m^2.h. Whilst for the PRO mode an initial water flux of

2.7±0.3 L/m^2.h was obtained which increased to a flux of 3.0±0.6 L/m^2.h followed by a steady decline to result in a final water flux of 1.9 L/m^2.h. Additionally, Figure 4.9 (c) (i) illustrates that the FO mode produced an initial water flux of 4.2±0.1 L/m^2.h which increased to a flux of 4.8 ±0.5 L/m^2.h followed by a steady decline to result in a final water flux of 3.1±0.3 L/m^2.h. During the PRO mode, an initial water flux of 5.1±0.3 L/m^2.h developed after which the water flux steadily decreased to a final water flux of 3.0±0.3 L/m^2.h. Figure 4.9 (c) (ii) indicates that during the FO mode an initial water flux of 3.9±0.1 L/m^2.h was achieved after which it increased to the flux of 4.2±0.5 L/m^2.h followed by a decrease to a final water flux 2.9±0.1 L/m^2.h. The PRO mode resulted in an initial water flux of 5.0±0.5 L/m^2.h after which the water flux decreased to a final flux of 3.0±0.2 L/m^2.h. Lastly, Figure 4.9 (c) (iii) illustrates that the FO mode produced an initial water flux of 3.8±0.4 L/m^2.h which increased to a flux of 4.5±0.4 L/m^2.h followed by a steady flux decline to a final water flux of 2.9±0.2 L/m^2.h. The PRO mode resulted in an initial water flux of 3.2±0.3 L/m^2.h which increased to a flux of 4.0±0.1 L/m^2.h which decreased to a final water flux of 2.8±0.3 L/m^2.h.

It can be seen from Figure 4.9 (a) (i) – (iii) that water fluxes for FO and PRO modes were nearly identical. A similar observation can be made from Figure 4.9 (b) (i) - (iii), however, greater water fluxes was achieved for both orientations due to a greater osmotic driving force as a result of an increase in DS concentration. Additionally, from Figure 4.9 (c) (i) and (ii), water fluxes for FO and PRO modes was also similar for the majority of the experiments. However, the PRO mode obtained a slightly greater initial water flux compared to the FO mode. This can be explained as a higher solute concentration is attained at the membrane surface during a PRO mode compared to the FO mode which in turn produces an increase water flux as a result of a greater osmotic driving force (Phuntsho *et al.*, 2013). The condition where FO and PRO mode water fluxes deviated the greatest is illustrated in Figure 4.1 (c) (iii). At this point, the FO mode produced a water flux ±0.5 L/m^2.h greater compared to the PRO mode. However, water fluxes started merging after the 21st hour where it remained consistent until the completion of the experiment. It was previously hypothesised that this deviation between FO and PRO modes was due to ICP. In theory, altering the membrane orientation from FO to PRO mode should produce an improved water flux (McCutcheon & Elimelech, 2006). However, the results obtained from this study indicated that the PRO mode did not contribute to a significant beneficial water recovery compared to the FO mode.

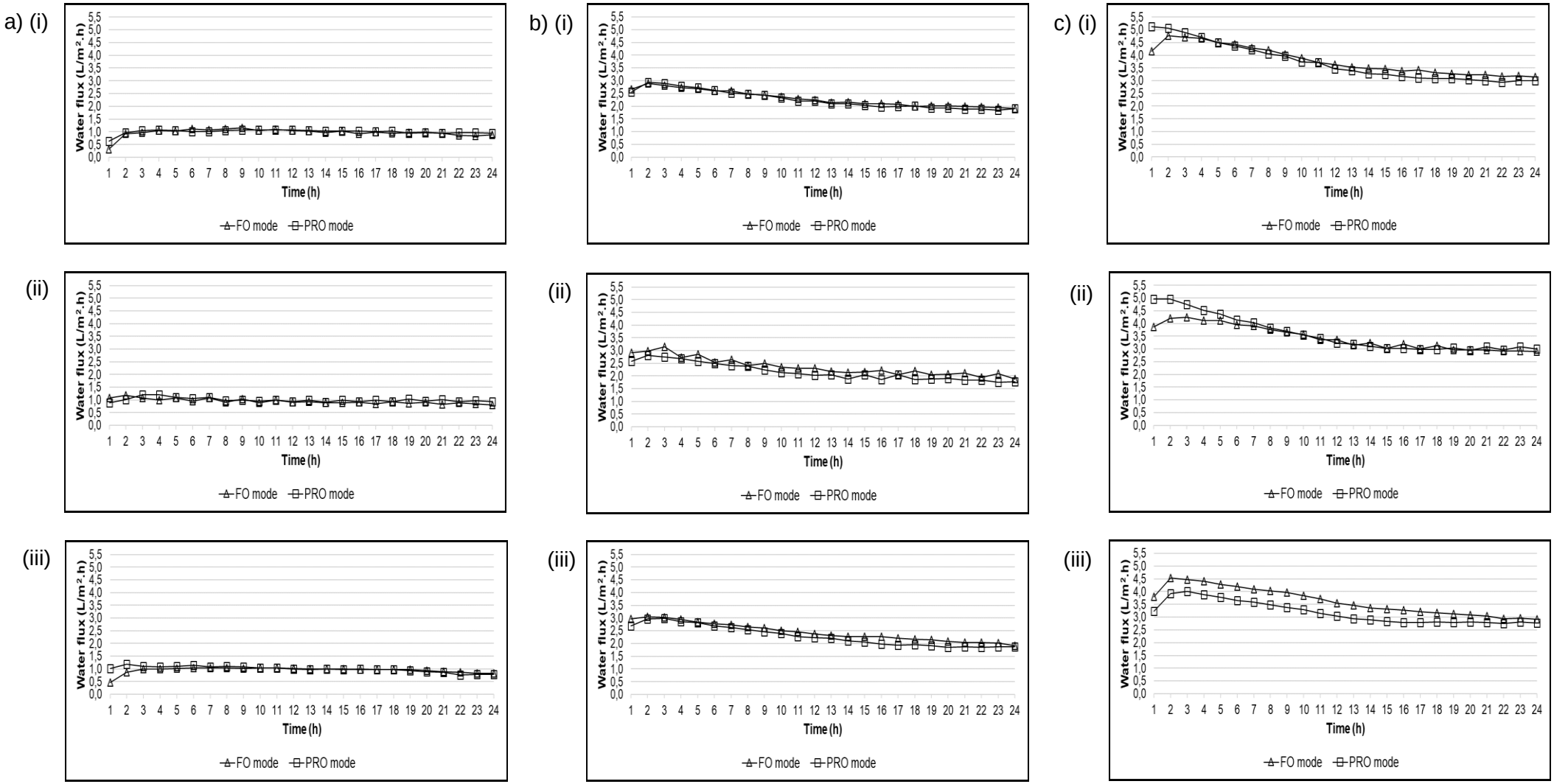

Figure 4.9: Water fluxes obtained during a 24 h operation for FO and PRO modes at DS concentrations of a) 0.5, b) 1 and c) 2 M KCl with SBW5 as the FS at flow rates of i) 100, ii) 200 and iii) 400 mL/min, respectively.

The motive for the FO and PRO modes to result in the similar water fluxes was hypothesised to the cleaning procedure used. Observations from the independent experiment, whilst using a new membrane (section 4.2, Figure 4.4), the PRO mode should produce significantly greater water fluxes compared to the FO mode. As previously mentioned the membrane was repetitively used throughout the study after a thorough cleaning. The membrane cleaning procedure used was adopted from Phuntsho *et al.* (2014), which reported effective recovering water fluxes to its original condition which was confirmed in section 4.1. Contrasting in this study, the cleaning procedure was applied to both FO and PRO mode orientations. It was therefore postulated that the procedure is ineffective for the PRO mode orientation. Considering that experiments were performed in a certain order (see Table 3.2), insufficient membrane cleaning in the PRO mode could have affected subsequent experiments. Therefore, the resembling water fluxes produced by the FO and PRO mode orientations may be the result of membrane re-use.

In this study, it is further theorised that PRO water fluxes were impaired as a consequence of ICP specifically to concentrative internal concentration polarisation (CICP). Unlike the FO mode where rejected solutes accumulate on the active layer open to system hydrodynamics, in the PRO mode, rejected solutes accumulate within the membrane support layer causing CICP. Previous reports recounted ICP to be a key contributor to flux decline and allegedly the leading factor responsible for restricting system performance (Hawari *et al.*, 2016; Wang *et al.*, 2016; Dabaghian & Rahimpour, 2015; McGovern & Lienhard, 2014; Phuntsho *et al.*, 2011; Zhao & Zou, 2011; Achilli *et al.*, 2010). Taking into consideration ICP occurs within the membrane support layer, a reduction it is especially difficult as it occurs out of the reach of system hydrodynamics. For that reason, the physical cleaning method used in this study is recommended for application in the FO mode orientations only and not in the PRO mode orientations given that it may possibly generate conflicting results as observed in this study.

4.4.2 The effects of membrane orientation on the fertiliser-drawn forward osmosis system performance: Reverse solute flux

Figure 4.10 illustrates the accumulative water recoveries and FS EC's obtained during a 24 h operation for FO and PRO modes at a DS concentration of a) 0.5, b) 1 and c) 2 M KCl with SBW5 as the FS at flow rates of i) 100, ii) 200 and iii) 400 mL/min, respectively. It can be seen from Figure 4.10 (a) (i) that the FS EC increased from an initial EC of 9.4 mS/cm to a final EC of 10.2±0.2 and 10.3±0.2 mS/cm while obtaining an accumulative water recovery of 97.3± 7.7 and 101.4±5.6 mL for FO and PRO modes, respectively. However, Figure 4.10 (a) (ii) illustrates that a final FS EC of 10.3±0.0 and 10.2±0.1 mS/cm was achieved whilst obtaining a total water recovery of 95.6±16.1 and 103.4±5.4 mL for FO and PRO modes, respectively. Figure 4.10 (a) (iii) indicates that a final FS EC of 10.3±0.2 and 10.4±0.3 mS/cm was obtained whilst a total water recovery of 95.7±13.2 and 100.1±3.5 mL was achieved for FO and PRO modes, respectively. Figure 4.10 (b) (i) illustrates a final FS EC of 11.2±0.1 and 11.3±0.1 mS/cm was obtained whilst obtaining an accumulative water recovery of 238.6± 18.1 and 218.3±3.9 mL for FO and PRO modes, respectively. Notwithstanding, Figure 4.10 (b) (ii) indicate that a final FS EC of 11.3±1.0 and 11.0±0.2 mS/cm was achieved whilst an accumulative water recovery of 238.6±18.1 and 218.3±3.9 mL was obtained for FO and PRO modes, respectively. Additionally, Figure 4.10 (b) (iii) illustrates that a final FS EC of 11.6±0.0 and 11.1±0.2 mS/cm was obtained whilst achieving an accumulative water recovery of 246.9 ±12.6 and 231.6±18.2 mL for FO and PRO modes, respectively. Figure 4.10 (c) (i) illustrates that a final FS EC of 12.0±0.3 and 12.1±0.2 mS/cm was obtained whilst an accumulative water recovery of 382.3±17.4 and 361.5±23.7 mL was achieved for FO and PRO modes, respectively. Figure 4.10 (c) (ii) indicate a final FS EC of 11.9±0.2 and 12.1±0.2 mS/cm whilst obtaining an accumulative water recovery of 347.0±16.3 and 361.5±23.7 mL for FO and PRO modes, respectively. Lastly, Figure 4.10 (c) (iii) illustrates that a final FS EC of 12.0±0.0 and 11.6±0.1 mS/cm was achieved whilst a total water recovery of 365.4±12.9 and 320.8±5.7 mL was obtained for FO and PRO modes, respectively.

It can be observed that the FS EC and water recoveries between FO and PRO modes were fairly comparable. It was therefore estimated that the RSF between membrane orientations had to have been similar. The only experiment where RSF might have been significant was at a DS concentration of 2 M at a flow rate of 400 mL/min. Further observations from Figure 4.10 (c) (iii) indicate that the final FS EC for FO (12.0±0.0 mS/cm) and PRO (11.6±0.1 mS/cm) modes were similar, however, the water recoveries between these orientations deviated slightly (FO mode = 365.4±12.9 mL; PRO mode = 320.8±5.7 mL). It was therefore estimated that an increase RSF might have occurred during the PRO mode compared to the FO mode at a DS concentration of 2 M at a flow rate of 400 mL/min.

In theory, PRO mode should produce a higher RSF compared to the FO mode. As the membrane active layer is facing the DS in a PRO mode operation, solute concentration is significantly higher at the membrane surface compared to the FO mode which in turn produce a higher effective osmotic driving force and so water flux (Phuntsho *et al.*, 2013) but also increase RSF. Some studies revealed the PRO mode orientation not be recommended for water desalination as this orientation is more susceptible to pore clogging as the support layer is open to the concentrating FS (Phuntsho *et al.*, 2013). Hence, there is advantages and disadvantages to both orientations. For instance, FO mode is recommended for troubled feed waters and for lower RSF, yet it produces lower water fluxes. In contrast, PRO mode orientation produces higher water flux but is more susceptible to RSF and membrane clogging.

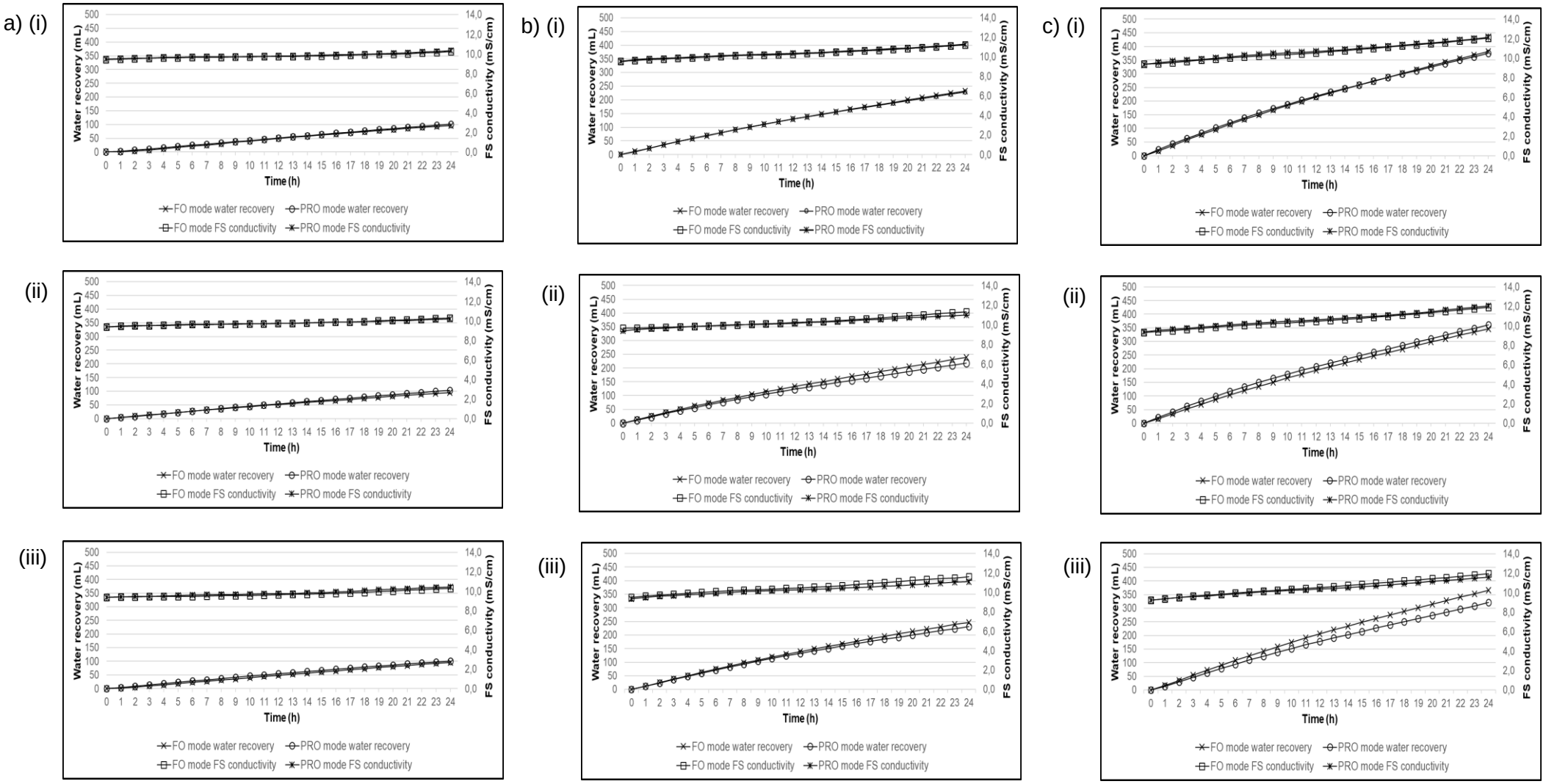

Figure 4.10: Accumulative water recoveries and FS EC's obtained during a 24 h operation for FO and PRO modes operating at DS concentrations of a) 0.5, b) 1 and c) 2 M KCl with SBW5 as the FS at flow rates of i) 100, ii) 200 and iii) 400 mL/min, respectively.

4.4.3 The effects of membrane orientation on the fertiliser-drawn forward osmosis system performance: Water recovery

Figure 4.11 illustrates the accumulative water recoveries obtained during a 24 h operation for FO and PRO modes at DS concentrations of a) 0.5, b) 1 and c) 2 M KCl with SBW5 as the FS at flow rates of i) 100, ii) 200 and iii) 400 mL/min, respectively. Figure 4.11 (a) (i) illustrates that an accumulative water recovery of 97.3±7.7 and 101.4±5.6 mL was achieved for FO and PRO modes, respectively. Whilst Figure 4.11 (a) (ii) indicates that an accumulative water recovery of 95.6±16.1 and 103.4±5.4 mL was obtained for FO and PRO modes, respectively. Additionally, Figure 4.11 (a) (iii) illustrates an accumulative water recovery of 95.7±13.2 and 100.1±3.5 mL was achieved for FO and PRO modes, respectively. Figure 4.11 (b) (i) indicate an accumulative water recovery of 232.1±12.6 and 228.5±3.5 mL was obtained for FO and PRO modes, respectively. Whilst Figure 4.11 (b) (ii) illustrates that an accumulative water recovery of 238.6±18.1 and 218.3±3.9 mL was achieved for FO and PRO modes, respectively. Figure 4.11 (b) (iii) indicate that an accumulative water recovery of 246.9±12.6 and 231.6±18.2 mL was obtained for FO and PRO modes, respectively. Figure 4.11 (c) (i) illustrates that an accumulative water recovery of 382.3±17.4 and 375.2±19.2 mL was obtained for FO and PRO modes, respectively. Whilst Figure 4.11 (c) (ii) indicate a total water recovery of 347.0±16.3 and 361.5±23.7 mL was obtained for FO and PRO modes, respectively. Lastly, Figure 4.11 (c) (iii) illustrates that an accumulative water recovery of 365.4 ±12.9 and 320.8±5.7 mL was achieved for FO and PRO modes, respectively.

Whilst water recovery is dependent on water flux, comparable accumulative water recoveries between FO and PRO mode experiments was observed. However, it was noted that at DS concentration of 0.5 M, the PRO mode recovered approximately 5.3 % more water than the FO mode. On the other hand, at DS concentrations of 1 and 2 M, the FO mode achieved 5.4 and 7.0 % greater accumulative water recoveries, respectively. However, at a DS concentration of 2 M and flow rate of 200 mL/min the FO mode recovered 4 % less water compared to the PRO mode.

It is believed that similar or slightly higher water recoveries achieved by the FO mode, in comparison to the PRO mode, in this study, are mainly the result of ICP. When the membrane is orientated in the PRO mode the porous support layer is facing the FS. Thus, solutes from the FS and DS (i.e. RSF) will accumulate within the support layer, not only because it is a static zone but also due to the high solute rejection of the CTA membrane. This accumulation of solutes creates CICP which in turn lower the effective osmotic driving force and thus water recovery (Zou & He, 2016). However, in the FO mode, DICP occur within the membrane support layer which also decrease the effective osmotic driving force and so water recovery (Zou & He, 2016). Since Zou & He (2016) reported CICP to be more prominent, the results from this study revealed that CICP and DICP were nearly identical as water recoveries between FO and PRO modes were similar.

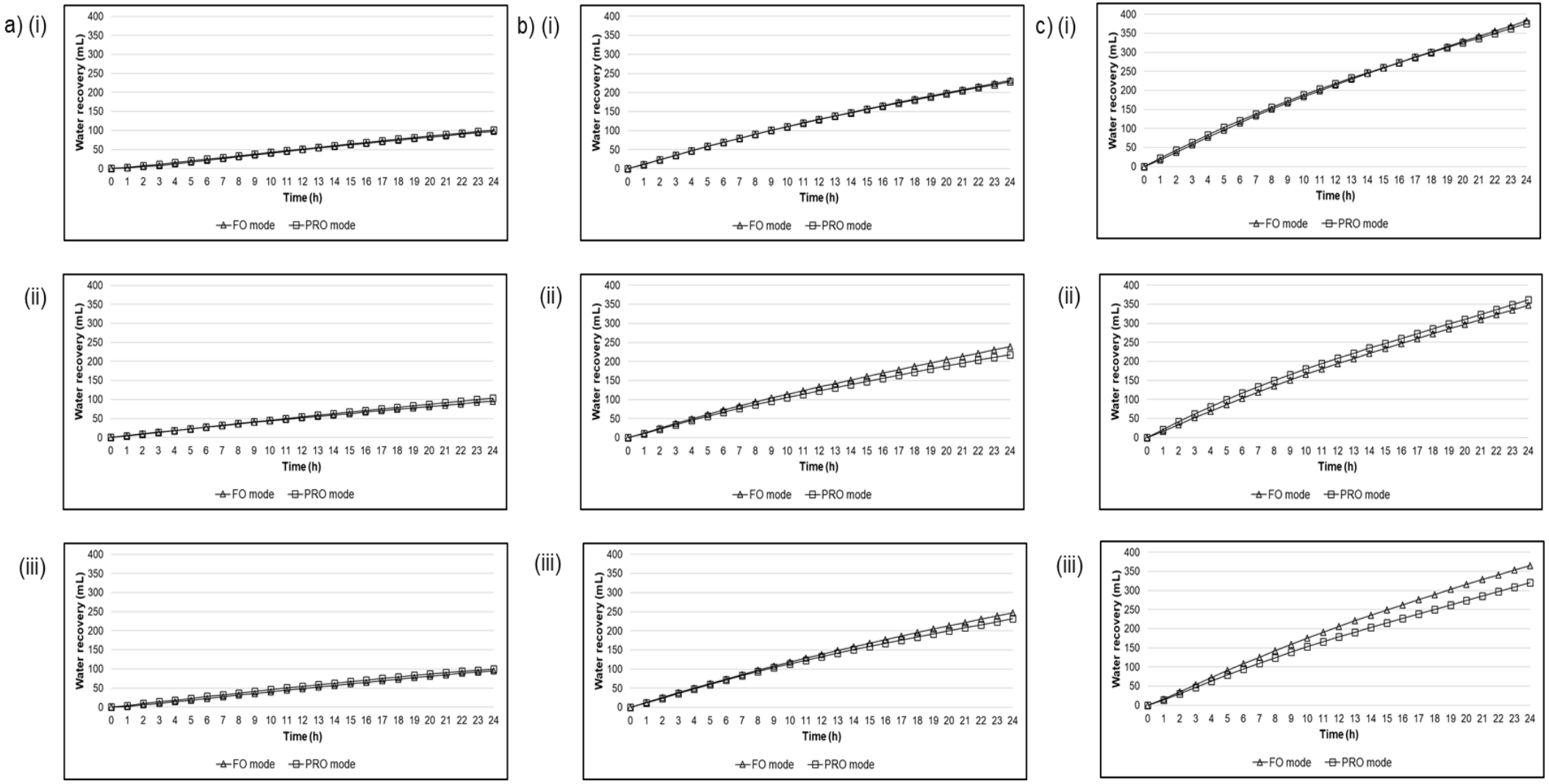

Figure 4.11: Accumulative water recoveries obtained during a 24 h operation for FO and PRO modes at DS concentrations of 0.5, 1 and 2 M KCl with SBW5 as the FS at flow rates of i) 100, ii) 200 and iii) 400 mL/min, respectively.

4.4.4 The effects of membrane orientation on the fertiliser-drawn forward osmosis system energy consumption

SEC of a system is determined by two factors, viz. (i) system power consumption (electrical power consumption by the pump) and (ii) the amount of product produced from the power consumed. Figure 4.8 illustrates the accumulative pump power consumption, water recovery as well as the SEC obtained during a 24 h operation whilst operating in a) FO and b) PRO modes at DS concentrations of 0.5, 1 and 2 M KCl with SBW5 as the FS and at flow rates of i) 100, ii) 200 and iii) 400 mL/min, respectively. Considering that the only power consumed by FDFO system is by the circulation pump, power consumption is unaffected by the membrane orientation. Nonetheless, product recovery is the factor that might be affected by membrane orientation. As a result of intermittent pump power consumption during the study, SEC fluctuated from one experiment to the next. Therefore, the only definitive SEC comparison between FO and PRO modes is from Figure 4.8 (a) (i) and (b) (i) for the reason that these experiments obtained the same pump power consumption. Figure 4.8 (a) (i) indicates that a total pump power consumption of 0.22±0.01, 0.23±0.01 and 0.24±0.02 kWh was achieved while obtaining an accumulative water recovery of 97.3±7.7, 232.1±12.6 and 382.3±17.4 mL which in turn produced a SEC of ±2295.3, ±995.2 and ±631.5 kWh/m^3 for DS concentrations of 0.5, 1 and 2 M, respectively. Whilst Figure 4.8 (b) (i) indicate that a total pump power consumption of 0.22±0.0, 0.23±0.01 and 0.24±0.0 kWh was obtained whilst achieving a total water recovery of 101.4±5.6, 228.5±3.5 and 375.2±19.2 mL which resulted in a SEC of ±2184.6, ±1024.5 and ±637.6 for DS concentration of 0.5, 1 and 2 M, respectively.

As previously mentioned at a DS concentration of 0.5 M KCl the PRO mode resulted in a greater water recovery whilst DS concentrations of 1 and 2 M KCl the FO mode resulted in greater water recovery. Nonetheless, water recovery influences SEC and therefore the mode which produces the greatest water recovery will be more economically viable.

The effects of flow rate on water fluxes, RSF's and water recoveries as well as its effects on FDFO system energy consumption is discussed in section 4.5.

4.5 The effects of flow rate on the fertiliser-drawn forward osmosis system performance and energy consumption

In this section, the effects of flow rate on FDFO system performance and energy consumption is described. The observed outcomes on system performance in terms of water flux, reverse solute flux and water recovery is deliberated. Subsequently, the changes in SEC is discussed.

4.5.1 The effects of flow rate on the fertiliser-drawn forward osmosis system performance: Water flux

Figure 4.12 illustrates water fluxes obtained during a 24 h operation for flow rates of 100, 200 and 400 mL/min whilst operating in a) FO and b) PRO modes with SBW5 as the FS at DS concentrations i) 0.5, ii) 1 and iii) 2 M KCl, respectively. It can be seen from Figure 4.12 (a) (i) although operating at a flow rate of 100 ml/min, an initial water flux of 0.3±0.2 L/m^2.h was obtained that increased to a flux of 0.9±0.2 L/m^2.h and remained consistent throughout the 24 h operation. Whilst at a flow rate of 200 mL/min, an initial water flux of 1.1±0.4 L/m^2.h was obtained that decreased slightly to a final water flux of 0.8±0.2 L/m^2.h. On the other hand, at a flow rate of 400 mL/min, an initial water flux of 0.5 L/m^2.h was achieved which increase to 0.9±0.2 L/m2.h and remained consistent throughout the 24 h experiment. Figure 4.12 (a) (ii) indicates that at a flow rate of 100 mL/min, an initial water flux 2.7±0.4 L/m^2.h was achieved which increased to a flux of 2.9±0.3 L/m^2.h followed by a flux reduction to result in a final water flux of 1.9±0.1 L/m^2.h. At a flow rate of 200 mL/min, an initial flux of 2.9±0.4 L/m^2.h was achieved which decreased to a final water flux of 1.9 L/m^2.h. Whilst at a flow rate of 400 mL/min, an initial water flux of 3.0±0.3 L/m^2.h was obtained after which the flux steadily decreased to a final water flux of 1.9±0.0 L/m^2.h. Figure 4.12 (a) (iii) illustrates at a flow rate of 100 mL/min, an initial water flux of 4.2±0.1 L/m^2.h was obtained which increased to 4.8±0.5 L/m^2.h followed by a steady decline to a final water flux of 3.1±0.3 L/m^2.h. Whilst at a flow rate of 200 mL/min, an initial water flux of 3.9±0.1 L/m^2.h was achieved after which it increased to the flux of 4.2±0.5 L/m^2.h followed by a steady decrease to a final water flux 2.9±0.1 L/m^2.h. On the other hand, at a flow rate of 400 mL/min, an initial water flux of 3.8±0.4 L/m^2.h resulted which increased to a flux of 4.5±0.4 L/m^2.h after which the flux declined to a final water flux of 2.9±0.2 L/m^2.h. It can be seen from Figure 4.12 (b) (i) at a flow rate of 100 mL/min an initial water flux of 0.6±0.2 L/m^2.h was achieved which increased to 1.0±0.1 L/m^2.h and remained consistent throughout the 24 h experiment. Whilst at a flow rate of 200 mL/min an initial water flux of 0.9±0.1 L/m2.h was obtained which slightly escalated to a flux of 1.2±0.0 L/m^2.h which again declined to a final water flux of 0.9 L/m^2.h. At a flow rate of 400 mL/min, an initial water

flux of 1.0±0.2 L/m^2.h was obtained followed by a slight flux increase to 1.2±0.2 L/m^2.h after which the flux decreased to a final water flux of 0.8±0.1 L/m^2.h. Figure 4.12 (b) (ii) illustrates that at a flow rate of 100 mL/min an initial water flux of 2.6±0.3 L/m^2.h was obtained followed by a slight increase to a flux of 2.9±0.1 L/m^2.h after which water fluxes steadily decreased to a final water flux of 1.9±0.1 L/m^2.h. Whilst at a flow rate of 200 mL/min an initial water flux of 2.6±0.3 L/m^2.h was achieved which increased to a flux of 2.8±0.2 L/m^2.h after which fluxes decreased steadily to a final water flux of 1.8±0.2 L/m^2.h. And at a flow rate of 400 mL/min, an initial water flux of 2.7±0.3 L/m^2.h was obtained which increased to 3.0±0.6 L/m^2.h followed by a steady decline to a final water flux of 1.9 L/m^2.h. Figure 4.12 (b) (iii) indicates that at a flow rate of 100 mL/min an initial water flux of 5.1±0.3 L/m^2.h was achieved followed by a steady flux reduction to result in a final water flux of 3.0±0.3 L/m^2.h. Whilst at a flow rate of 200 mL/min an initial water flux of 5.0±0.5 L/m^2.h was obtained which decreased to a final water flux of 3.0±0.2 L/m^2.h. Lastly, at a flow rate of 400 mL/min an initial water flux of 3.2±0.3 L/m^2.h was obtained which increased to a flux of 4.0±0.1 L/m^2.h after which the flux decreased to a final water flux of 2.8±0.3 L/m^2.h.

It can be seen from Figure 4.12 (a) (i) and (b) (i) water fluxes were almost identical for flow rates of 100, 200 and 400 mL/min with a similar observation from Figure 4.12 (a) (ii) and (b) (ii). However, from Figure 4.12 (a) (iii) water fluxes deviated slightly between the different flow rates. At this point, a flow rate of 100 mL/min achieved the highest water flux followed by 400 and 200 mL/min. On the other hand, from Figure 4.12 (b) (iii) water fluxes deviated slightly greater between flow rates. The flow rate which obtained the highest water flux was a flow rate of 100 mL/min followed by 200 mL/min and 400 mL/min. It is believed that the water flux obtained at a flow rate of 400 mL/min in Figure 4.12 (b) (iii) might be as a result of ICP as previously mentioned.

According to literature, the increase in system flow rate in an FO operation should improve system performance. Concurring to the film theory, an increase in system flow rate will alter a systems flow regime which in turn will reduce the formation of external concentration polarisation (ECP) (Wang *et al.*, 2016; Phuntsho *et al.*, 2013). As similar water flux trends were obtained during this study between 100, 200 and 400 mL/min at a constant DS concentration and membrane orientations, it may be as a consequence of low ECP formation. Considering that ECP is related to water flux (Wang *et al.*, 2016; Hawari *et al.*, 2016) and with relatively low water fluxes obtained during this study, the formation of ECP (CECP and DECP) ought to be identical. Therefore, an increase in system flow rate did not contribute to a beneficial water flux as each flow rate mitigated ECP with similar effects.

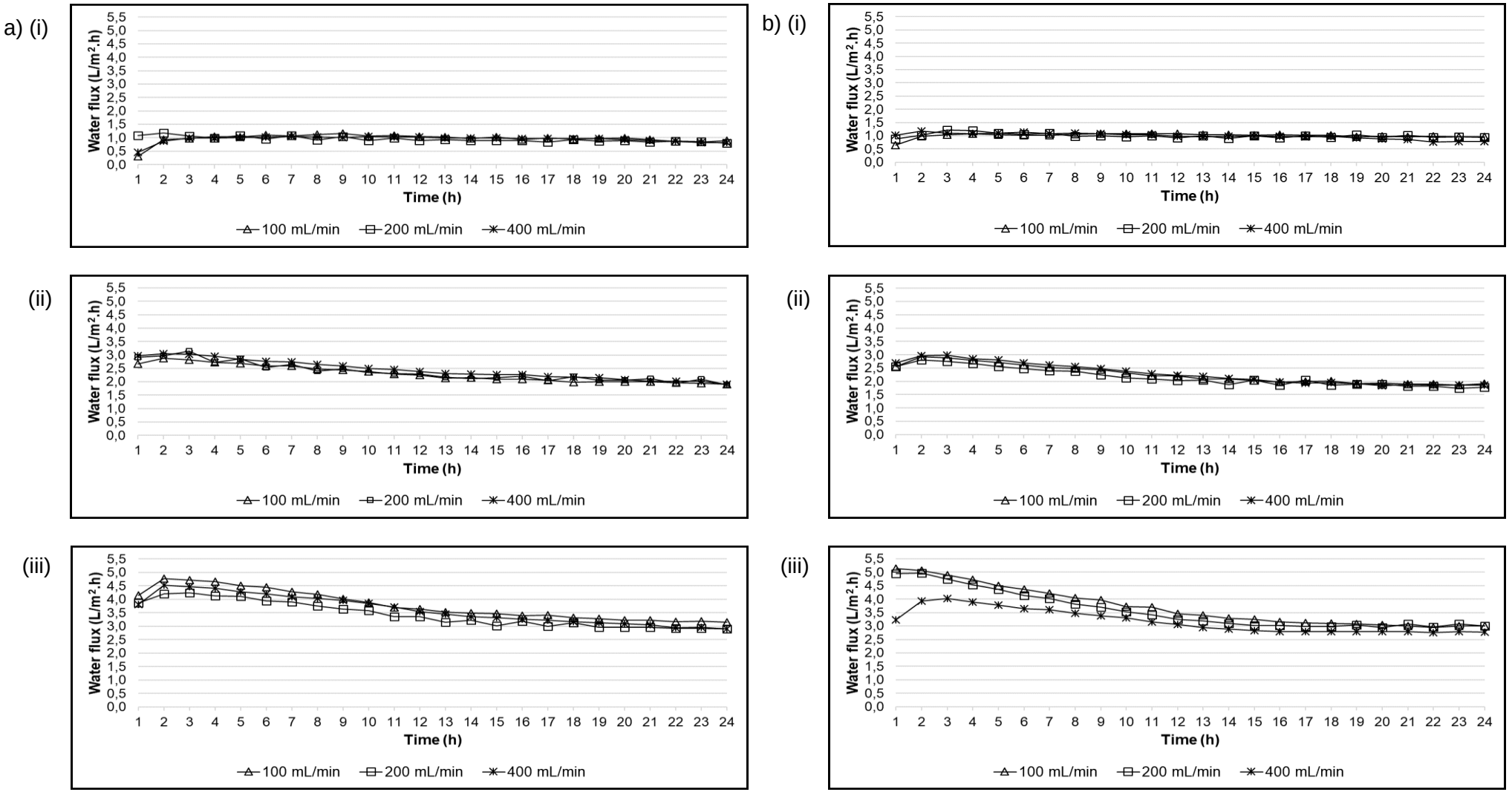

Figure 4.12: Water fluxes obtained during a 24 h operation for flow rates of 100, 200 and 400 mL/min whilst operating in a) FO and b) PRO mode with SBW5 as the FS at DS concentrations of i) 0.5, ii) 1 and iii) 2 M KCl, respectively.

4.5.2 The effects of flow rate on the fertiliser-drawn forward osmosis system performance: Reverse solute flux

Figure 4.13 illustrates the accumulative water recoveries and FS EC's obtained during a 24 h operation for flow rates of 100, 200 and 400 mL/min whilst operating in a) FO and b) PRO modes with SBW5 as the FS at DS concentrations of i) 0.5, ii) 1 and iii) 2 M, respectively. Figure 4.13 (a) (i) illustrate the FS EC increase from an initial EC of 9.4 mS/cm to a final EC 10.2±0.2, 10.3±0.0 and 10.3±0.2 mS/cm whilst obtaining an accumulative water recovery of 97.3±7.7, 95.6±16.1 and 95.7±13.2 mL for flow rates of 100, 200 and 400 mL/min, respectively. Figure 4.13 (a) (ii) indicates that a final FS EC of 11.2±0.1, 11.3±1.0 and 11.6 ±0.0 mS/cm was obtained whilst achieving an accumulative water recovery of 232.1±12.6, 238.6±18 and 246.9±12.6 mL for flow rates of 100, 200 and 400 mL/min, respectively. Additionally, from Figure 4.13 (a) (iii) a final FS EC of 12.0±0.3, 11.9±0.2 and 12.0±0.0 mS/cm was achieved whilst an accumulative water recovery of 382.3±17.4, 347.0±16.3 and 365.4±12.9 mL was obtained for flow rates of 100, 200 and 400 mL/min, respectively. Figure 4.13 (b) (i) illustrate that a final FS EC of 10.3±0.2, 10.2±0.1 and 10.4±0.3 mS/cm was obtained whilst a total water recovery of 101.4±5.6, 103.4±5.4 and 100.1±3.5 mL was achieved for flow rates of 100, 200 and 400 mL/min, respectively. Figure 4.13 (b) (ii) indicate that a final FS EC of 11.3±0.1, 11.0±0.2 and 11.1±0.2 mS/cm was obtained whilst obtaining an accumulative water recovery of 228.5±3.5, 218.3±3.9 and 231.6±18.2 mL for flow rates of 100, 200 and 400 mL/min, respectively. Lastly, from Figure 4.13 (b) (iii) a final FS EC of 12.1 ±0.2, 12.1±0.2 and 11.6±0.1 mS/cm was achieved whilst obtaining an accumulative water recovery of 375.2±19.2, 361.5±23.7 and 320.8±5.7 mL for flow rates of 100, 200 and 400 mL/min, respectively.

Observations from Figure 4.13 (a) (i) and (b) (i) indicates the final FS EC's and accumulative water recoveries for flow rates of 100, 200 and 400 mL/min was nearly identical, which suggest that RSF had to have been similar. A similar observation can be made from Figure 4.13 (a) (ii) and (b) (ii). However, from Figure 4.13 (a) (iii) by comparing FS EC and accumulative water recoveries RSF had to have occurred. By comparing FS EC and water recoveries, a flow rate of 200 mL/min obtained the highest RSF followed by a flow rate of 400 and 100 mL/min. In contrast, from Figure 4.13 (b) (iii) the highest RSF obtained was at a flow rate of 400 mL/min followed by a flow rate of 200 and 100 mL/min. From these findings, no clear relationship between flow rate and RSF could be identified for FO nor PRO mode orientations. Nonetheless, a study conducted by Hawari *et al.* (2016) reported RSF to be lower at increased

DS flow rates at FO mode whilst a higher RSF was observed at an increase FS flow rate during a PRO mode.

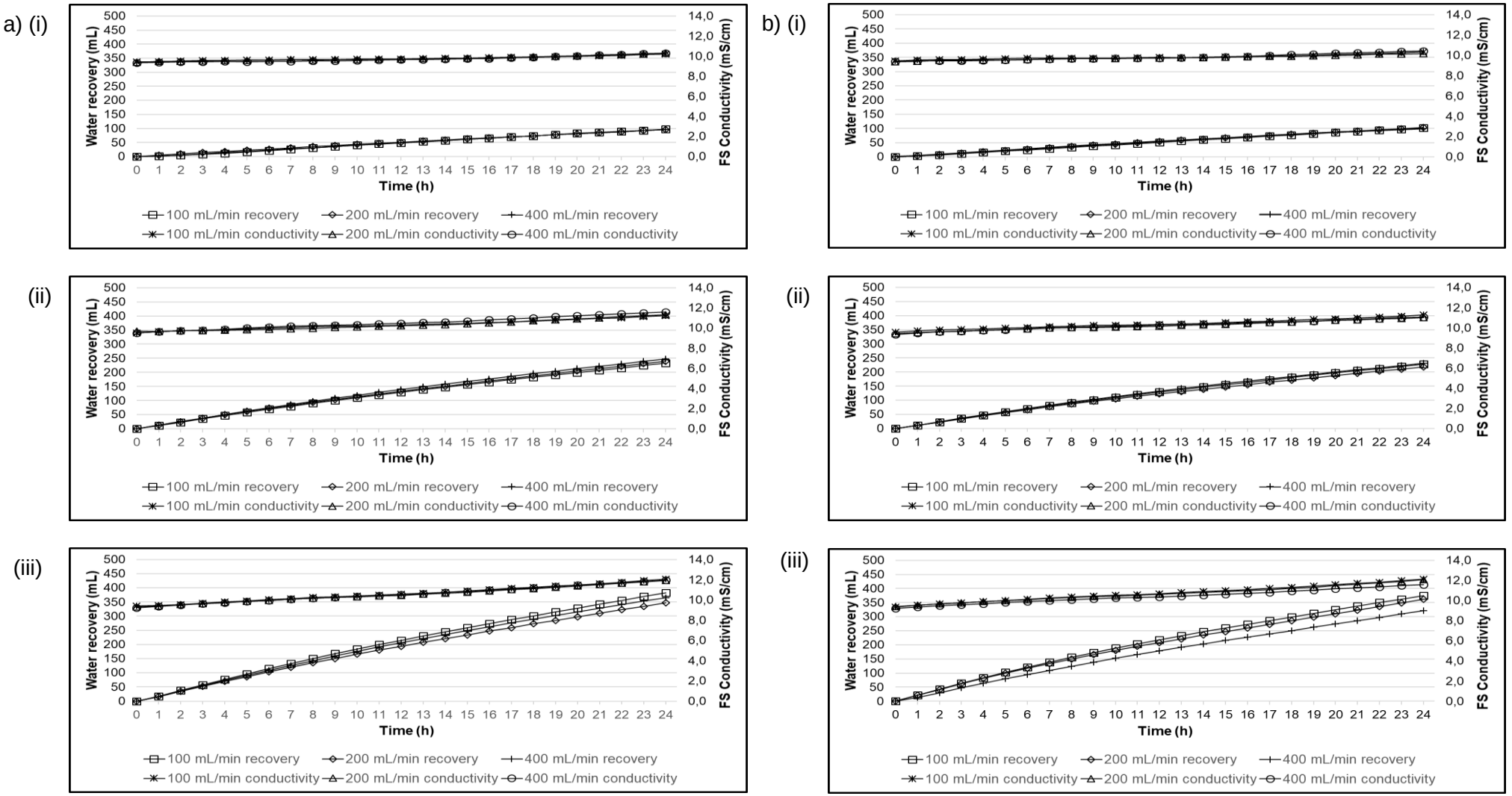

Figure 4.13: Accumulative water recoveries and FS EC's obtained during a 24 h operation for flow rates of 100, 200 and 400 mL/min whilst operating in a) FO and b) PRO mode with SBW5 as the FS at DS concentrations of i) 0.5, ii) 1 and iii) 2 M KCl, respectively.

4.5.3 The effects of flow rate on the fertiliser-drawn forward osmosis system performance: Water recovery

Figure 4.14 illustrates the accumulative water recovery obtained during a 24 h operation for flow rates of 100, 200 and 400 mL/min whilst operating in a) FO and b) PRO modes with SBW5 as the FS at different DS concentrations of 0.5, 1 and 2 M KCl, respectively. Figure 4.14 (a) (i) indicate that an accumulative water recovery of 97.3±7.7, 95.6±16.1 and 95.7±13.2 mL was achieved for flow rates of 100, 200 and 400 mL/min, respectively. Whilst from Figure 4.14 (a) (ii) an accumulative water recovery of 232.1±12.6, 238.6±18 and 246.9±12.6 mL was obtained for flow rates of 100, 200 and 400 mL/min, respectively. Additionally, Figure 4.14 (a) (iii) indicate that an accumulative water recovery of 382.3±17.4, 347.0±16.3 and 365.4±12.9 mL was achieved for flow rates of 100, 200 and 400 mL/min, respectively. Figure 4.14 (b) (i) illustrates that an accumulative water recovery of 101.4±5.6, 103.4±5.4 and 100.1±3.5 mL was obtained for flow rates of 100, 200 and 400 mL/min, respectively. Whilst, from Figure 4.14 (b) (ii) an accumulative water recovery of 228.5±3.5, 218.3±3.9 and 231.6±18.2 mL was obtained for flow rates of 100, 200 and 400 mL/min, respectively. Lastly, Figure 4.14 (b) (iii) illustrates that an accumulative water recovery of 375.2±19.2, 361.5±23.7 and 320.8±5.7 mL was achieved for flow rates of 100, 200 and 400 mL/min, respectively.

Observations from Figure 4.14 (a) (i) and (b) (i) indicate that the accumulative water recoveries for a flow rate of 100, 200 and 400 mL/min were nearly identical. However, from Figure 4.14 (a) (ii) however, recoveries deviate slightly greater. Here, a flow rate of 400 mL/min generated the greatest accumulative water recovery followed by 200 and 100 mL/min. From Figure 4.14 (b) (ii) the greatest water recovery obtained was from a flow rate of 400 mL/min followed by 100 and 200 mL/min. However, from Figure 4.14 (a) (iii) for a flow rate of 100 mL/min achieved the greatest accumulative water recovery followed by 400 and 200 mL/min. Whilst from Figure 4.14 (b) (iii) the flow rate which obtained the greatest water recovery was 100 mL/min followed by 200 and 400 mL/min.

As previously mentioned, an increase in flow rate ought to improve system performance due to the deduction of ECP layers which in turn produce a greater effective osmotic driving force and so water recovery. However, observations suggest at lower DS concentrations an increase in flow rate did not contribute to a beneficial water recovery however at higher DS concentrations flow rate alterations affected water recoveries. Here, the alterations in flow rate might have reduced ECP which in turn contributed to beneficial water recoveries.

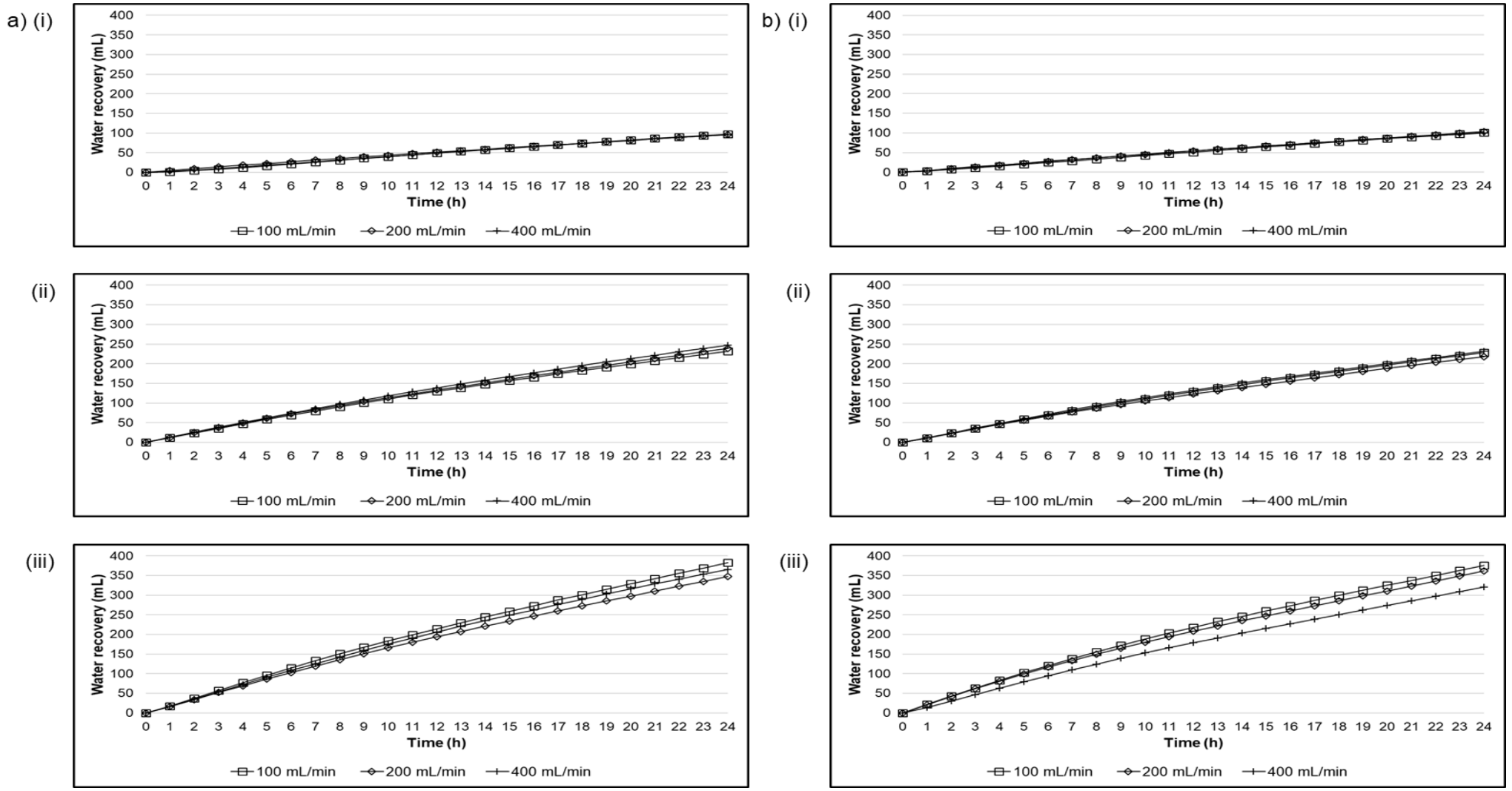

Figure 4.14: Accumulative water recoveries obtained during a 24 h operation for rates of 100, 200 and 400 mL/min whilst operating in a) FO and b) PRO mode with SBW5 as the FS at different DS concentrations of i) 0.5, ii) 1 and iii) 2 M KCl, respectively.

4.5.4 The effects of flow rate on the fertiliser-drawn forward osmosis system energy consumption

Figure 4.15 illustrates the accumulative pump power consumption, water recovery as well as the SEC obtained during a 24 h operation whilst operating in a) FO and b) PRO modes for flow rates of 100, 200 and 400 mL/min at DS concentrations of 0.5, 1 and 2 M KCl respectively with SBW5 as the FS. Figure 4.15 (a) (i) indicates that a total pump power consumption of 0.22±0.01, 0.20±0.01 and 0.30±0.02 kWh was achieved whilst obtaining an accumulative water recovery of 97.3±7.7, 95.6±16.1 and 95.7±13.2 mL which in turn produced an SEC of ±2295.3, ±2056.0 and ±3098.2 kWh/m^3 for flow rates of 100, 200 and 400 mL/min, respectively. Whilst, from Figure 4.15 (a) (ii) a total pump power consumption of 0.23±0.01, 0.20±0.02 and 0.32±0.01 kWh was obtained whereas an accumulative water recovery of 232.1±12.6, 238.6±18.1 and 246.9±12.6 mL was achieved which resulted in an SEC of ±995.2, ±835.9 and ±1278.7 kWh/m^3 for flow rates of 100, 200 and 400 mL/min, respectively. Additionally, Figure 4.15 (a) (iii) illustrates that a total pump power consumption of 0.24±0.02, 0.22±0.0 and 0.26±0.0 kWh was obtained whilst obtaining a total water recovery of 382.3±17.4, 347.0±16.3 and 365.4±12.9 mL which resulted in an SEC of ±631.5, ±619.7 and ±720.8 kWh/m^3 for flow rates of 100, 200 and 400 mL/min, respectively. Figure 4.15 (b) (i) illustrates a total pump power consumption of 0.22±0.0, 0.20±0.01 and 0.32±0.01 kWh was obtained whilst an accumulative water recovery of 101.4±5.6, 103.4±5.4 and 100.1±3.5 mL was achieved which produced an SEC of ±2184.6, ±1924.3 and ±3187.5 kWh/m^3 for flow rates of 100, 200 and 400 mL/min, respectively. Figure 4.15 (b) (ii) indicate that a total pump power consumption of 0.23±0.01, 0.22±0.0 and 0.32±0.01 kWh was obtained whilst an accumulative water recovery of 228.5±3.5, 218.3±3.9 and 231.6±18.2 mL was obtained which resulted in an SEC of ±1024.5, ±991.5 and ±1385.0 kWh/m^3 for flow rates of 100, 200 and 400 mL/min, respectively. Lastly, Figure 4.15 (b) (iii) illustrates that total pump power consumption of 0.24±0.0, 0.23±0.0 and 0.28±0.0 kWh was achieved whilst an accumulative water recovery of 375.2±19.2, 361.5±23.7 and 320.8±5.7 mL was obtained which in turn produced an SEC of ±637.6, ±624.1 and ±870.0 kWh/m^3 for flow rates of 100, 200 and 400 mL/min, respectively.

Observations from Figure 4.15 (a) and (b) illustrate that SEC decreased with a flow rate increase of 100 to 200 mL/min followed by an incline in SEC at a flow rate alteration of 200 to 400 mL/min. It was expected that SEC would increase with the increase in flow rate as the pump would require more power to pump faster. However, this irregular SEC trend was mainly due to the fluctuation of pump power consumption and not so much as the water recovery. A possible explanation for the unfamiliar trend in pump power consumption could be the result of the replacement of tubing within the pump head. Taking into consideration that the pump used was a peristaltic pump, tubing within the head was replaced regularly due to wear, an increase in power consumption was observed as soon as a replacement tubing was used. It is proposed that this action is a result of the inflexibility of the tubing that consequently instigates a resistance to the rotation of the pump head. Subsequently, pump power consumption will be affected as more power is required to overcome the surplus resistance. Nonetheless, as the tubing degrades, a reduction in power consumption was observed. At this point, the more flexible tubing reduces resistance to the rotation of the pump head which in turn lessened pump power consumption.

The effects of membrane fouling on FDFO system performance and energy consumption is discussed in section 4.6.

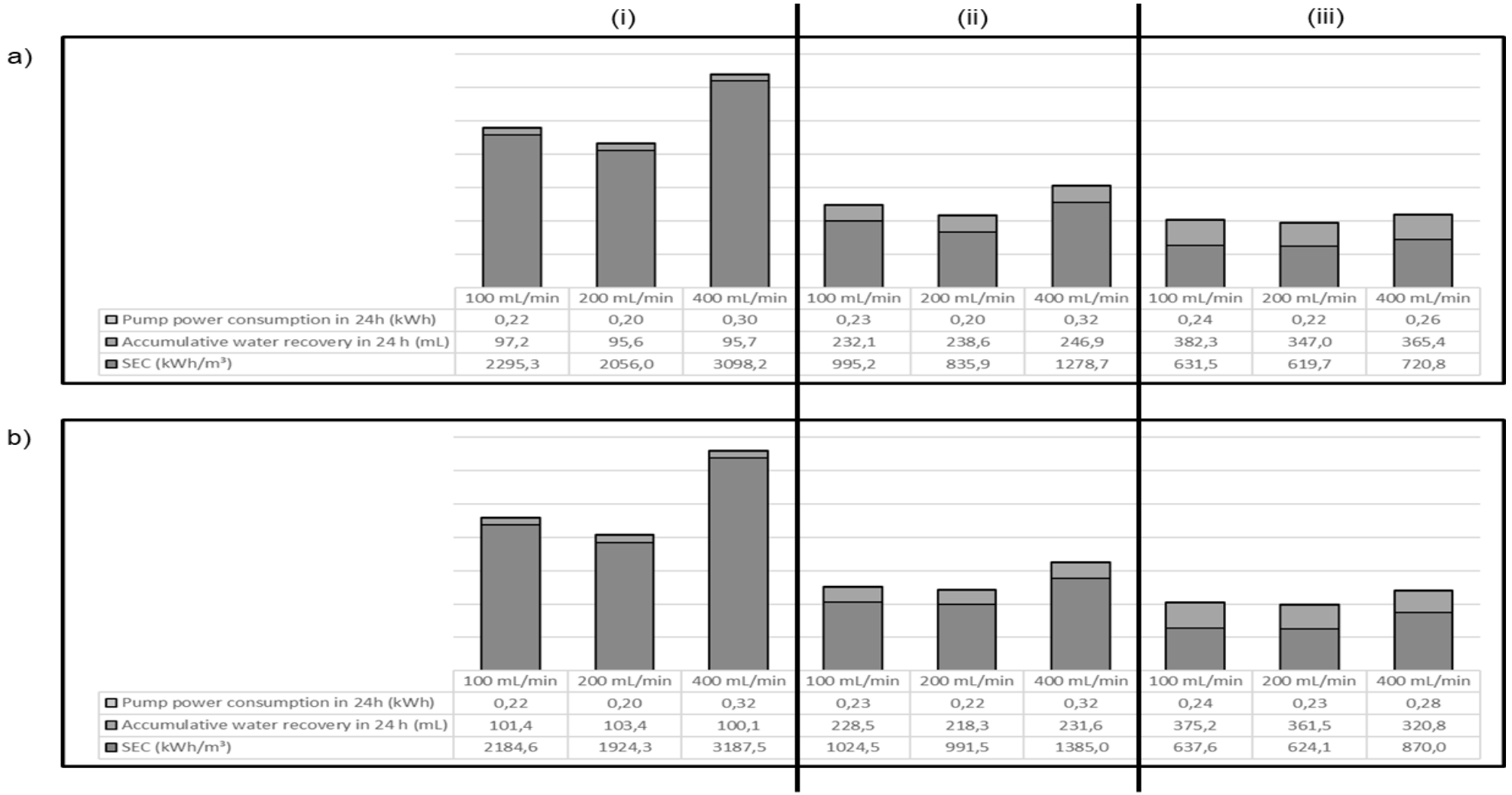

Figure 4.15: Accumulative pump power consumption, water recovery and SEC consumption obtained during a 24 h operation for a) FO and b) PRO modes for flow rates of 100, 200 and 400 mL/min at DS concentrations of i) 0.5, ii) 1 and iii) 2 M KCl, respectively with SBW5 as the FS.

4.6 The effect of fouling on the fertiliser-drawn forward osmosis system performance and energy consumption

In this section, the effects of membrane fouling on system performance and energy consumption are described. Moreover, the observed effects on FDFO system performance were measured in terms of water recovery and are deliberated whilst the subsequent effects on SEC are discussed.

4.6.1 The effects of membrane fouling on the fertiliser-drawn forward osmosis system performance

Figure 4.16 illustrates the accumulative water recovery obtained during a 5 h operation whilst operating in a) FO and b) PRO modes at a DS concentration of 1 M NaCl with DI water as the FS at a flow rate of 200 mL/min, respectively. The accumulative water recoveries obtained from the post-FDFO membrane control experiments were compared to that of the pre-FDFO membrane control experiments to identify if any membrane fouling had occurred during the FDFO process. Figure 4.16 (a) (control) indicates that the pre-FDFO membrane control experiment obtained an accumulative water recovery of 77.3±3.7 mL. Whilst Figure 4.16 (a) (i) illustrate that the post-FDFO membrane control experiments obtained an accumulative water recovery of 76.6±0.8, 64.7±1.7 and 66.9±0.8 mL for an FDFO experiment operating at a DS concentration of 0.5, 1 and 2 M KCl, respectively. Figure 4.16 (a) (ii) illustrates that the post-FDFO membrane control experiments obtained an accumulative water recovery of 61.0 ±4.7, 72.9±3.0 and 54.5±1.9 mL for FDFO experiments which operated at a DS concentration of 0.5,1 and 2 M KCl, respectively. Additionally, Figure 4.16 (a) (iii) indicate that the post-FDFO membrane control experiments achieved an accumulative water recovery of 54.1±3.5, 66.1±1.3 and 50.2±1.5 mL for FDFO experiments which operated at DS concentration of 0.5, 1 and 2 M KCl, respectively. On the other hand, Figure 4.16 (b) (control) indicates that the pre-FDFO membrane control experiment obtained an accumulative water recovery of 73.4±1.4 mL. Figure 4.16 (b) (i) illustrates that the post-FDFO membrane control experiment obtained an accumulative water recovery of 60.5±8.8, 65.3±0.1 and 65.3±0.6 mL for FDFO experiments operating at DS concentrations of 0.5, 1 and 2 M, respectively. Figure 4.16 (b) (ii) illustrates post-FDFO membrane control experiment achieved an accumulative water recovery of 59.4±1.3, 57.8±0.3 and 60.0±0.8 mL for FDFO experiments which operated at a DS concentration of 0.5, 1 and 2 M KCl, respectively. Lastly, Figure 4.16 (b) (iii) indicates that the post-FDFO membrane control experiment obtained some accumulative water recoveries of 62.8±4.5, 59.5±1.5 and 42.9±1.6 mL for FDFO experiments which operated a DS concentration of 0.5, 1 and 2 M KCl, respectively.

Figure 4.16 (a) and (b) indicates that a reduction in post-FDFO membrane control accumulative water recoveries were obtained. This would imply that membrane fouling might have occurred during the FDFO experiments. However, no identifiable trend in post-FDFO membrane control accumulative water recoveries were observed which in turn indicate different degrees of membrane fouling was produced by the FDFO experiments. Additionally, the extent of membrane fouling on FDFO experiment performance was also unknown as no correlation between post-FDFO membrane control results could be linked to inconsistent FDFO performances.

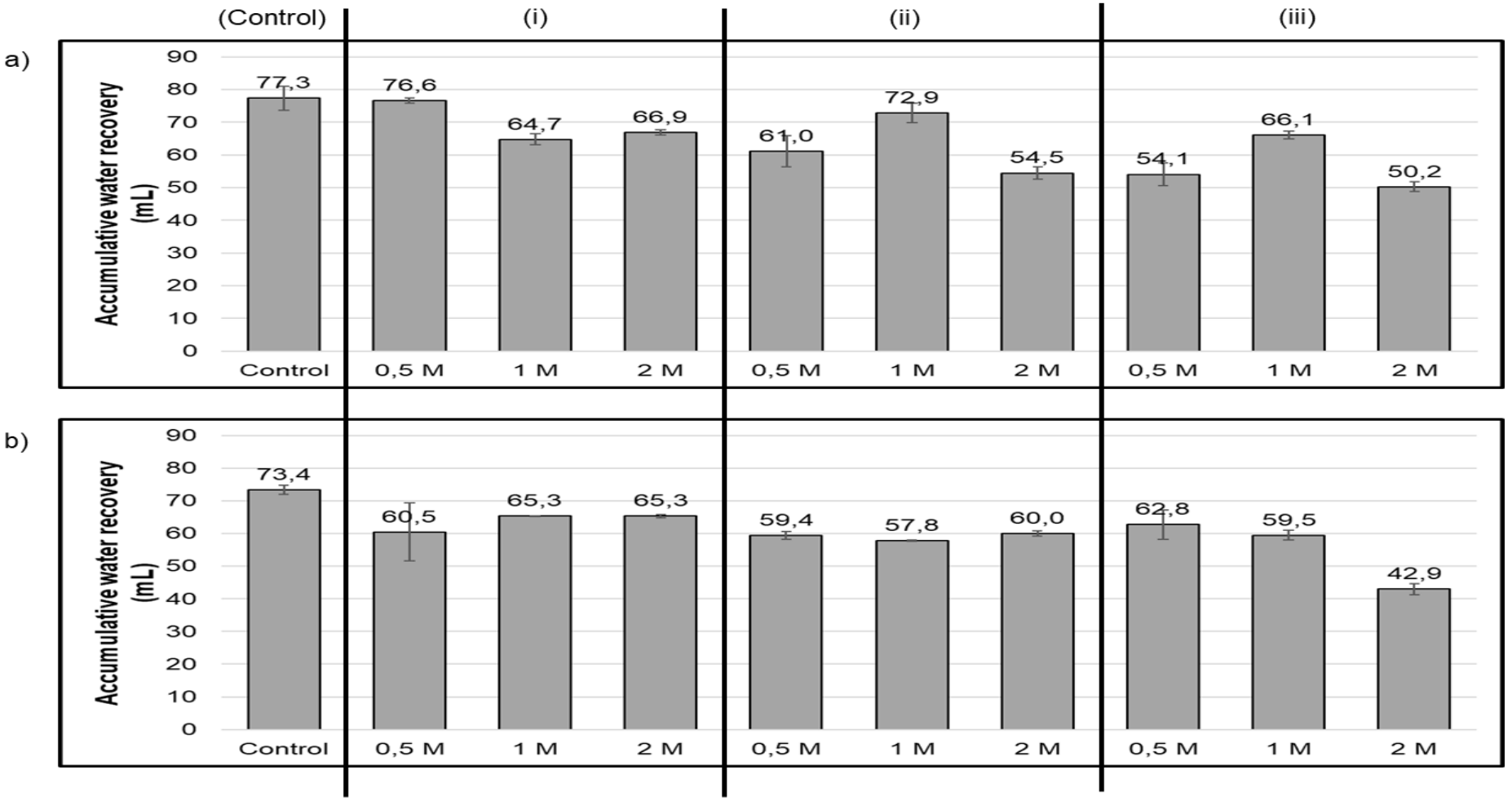

Figure 4.16: Accumulative water recoveries obtained during a 5 h operation for post-fertiliser membrane control experiments whilst operating in a) FO and b) PRO modes at a DS concentration of 1 M NaCl with DI water as the FS at a flow rate of 200 mL/min. (Note: All scaling test experiments was performed at this system conditions. The DS concentration of 0.5, 1 and 2 M at flow rates of i) 100, ii) 200 and iii) 400 mL/min as indicated are the conditions at which the FDFO experiments were performed).

4.6.1.1 High-resolution scanning electron microscope images of the forward osmosis membrane surfaces

Figure 4.17 illustrates a comparison of scanning electron microscope (SEM) images of the membrane active layer between a) new and b) used membrane at resolutions of i) 500, ii) 200, iii) 100 and iv) 20 µm, respectively. Comparing images from Figure 4.12 (a) to (b) (i) – (iv), no significant difference in the appearance of the active layer was observed for a new membrane compared to the re-used membrane used throughout the study. Figure 4.18 illustrates a comparison of SEM's of the membrane porous support layer between a) new and b) used membrane at resolutions of resolutions of i) 500, ii) 200, iii) 100 and iv) 20 µm, respectively. Comparing images from Figure 4.18 (a) to (b) (i) – (iv) also indicated insignificant changes in the porous support layer of a new and used membrane. However, closer inspection of Figure 4.13 (a) (iv) and (b) (iv), revealed a slight difference in the images of the membrane support layer. The body depicted in Figure 4.18 (a) (iv) is unknown, but, Figure 4.18 (b) (iv) might illustrate minute levels of fouling. This would confirm the assumption of membrane fouling as mentioned in section 4.6.1.

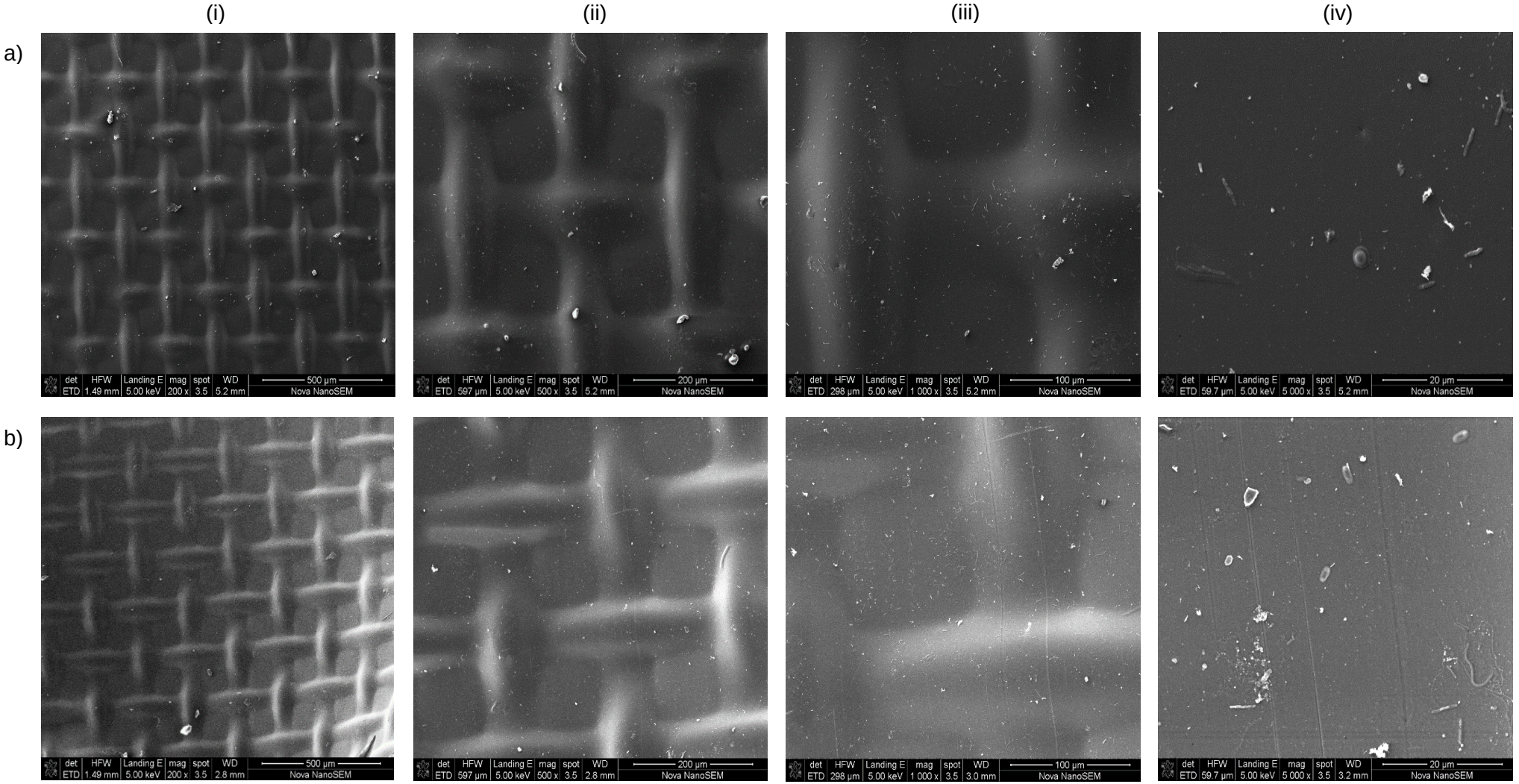

Figure 4.17: Membrane-active layer comparison between a) new and b) used membrane at resolutions of i) 500, ii) 200, iii) 100 and iv) 20 µm, respectively.

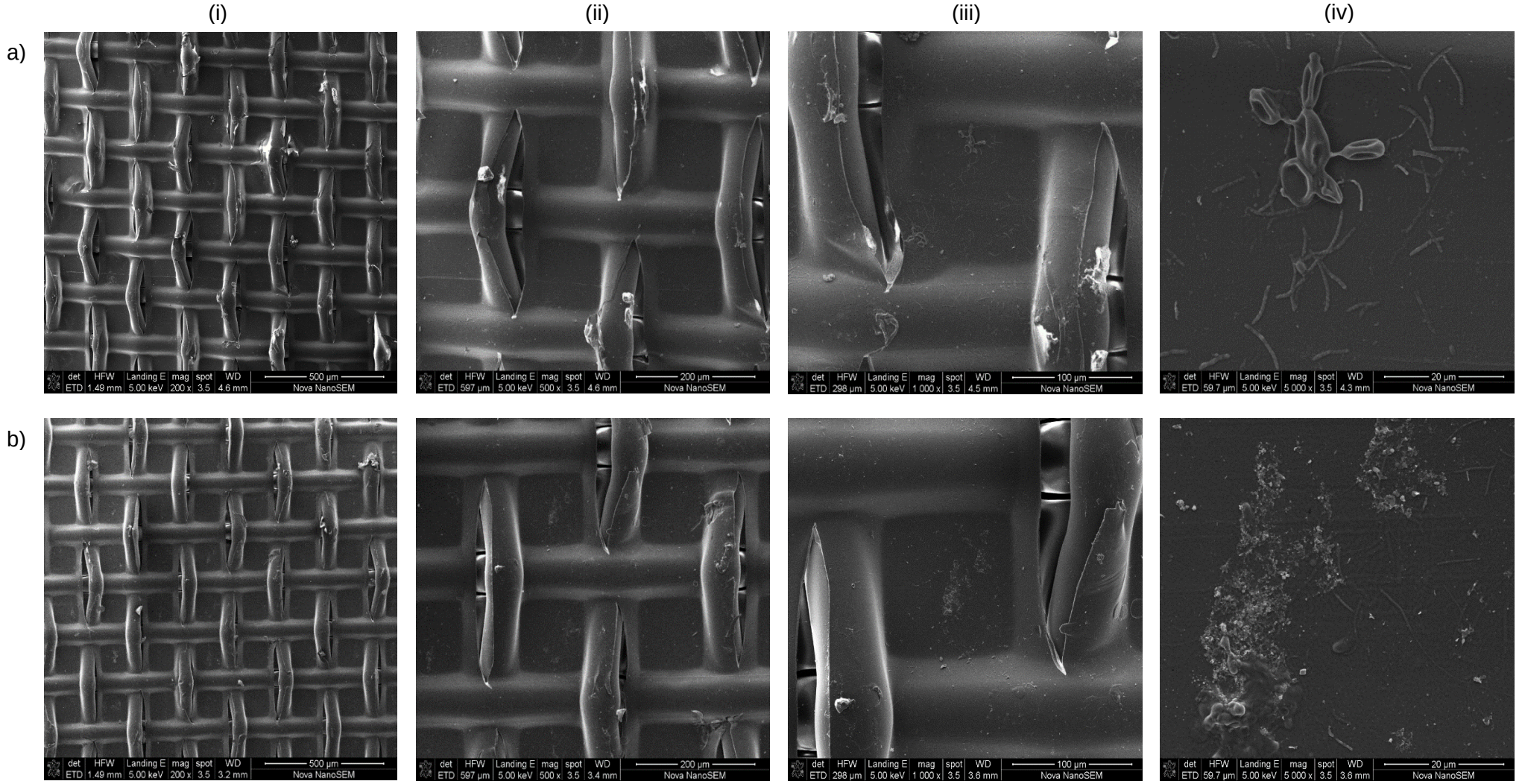

Figure 4.18: Membrane porous support layer comparison between a) new and b) used membrane at resolutions of i) 500, ii) 200, iii) 100 and iv) 20 µm, respectively.

4.6.2 The effects of membrane fouling on the fertiliser-drawn forward osmosis system energy consumption

Membrane fouling is a major factor affecting any membrane separation process in view of generating resistance to water flux and consequently water recovery. Membrane fouling, therefore, has significant impacts on a systems SEC as it reduces water recoveries which in turn increase SEC thus resulting in a less economical system. However, the findings of this study did not find a direct correlation between membrane fouling and SEC due to inconclusive water recovery results obtained from the post-FDFO membrane control experiments

4.7 Electrical power consumption for membrane cleaning

The membrane was subjected to a physical cleaning procedure at regular intervals (see Table 3.2). The procedure continued for 30 min and consumed ±0.044 kWh electrical power units per procedure.

CHAPTER 5
CONCLUSIONS AND RECOMMENDATIONS

5.1 Conclusion

This study investigated the effects of membrane orientation, flow rate, DS concentration and membrane fouling on an FDFO systems performance and energy consumption. The FDFO system performance was investigated by evaluating water flux, RSF and water recovery whilst system energy consumption was evaluated in terms of SEC. The effects of membrane fouling were studied by assessing water recoveries obtained from pre- and post- FDFO membrane control experiments.

(i) Draw solution concentration

The parameter which largely contributed to an improved system performance, as well as a reduction in SEC, was the increase in DS concentration. Water fluxes increased approximately threefold for a DS concentration alteration of 0.5 to 1 M. An additional 30 to 50 % rise in water fluxes was achieved at a DS concentration increase of 1 to 2 M. Unfortunately, due to the method used to estimate RSF, no definitive increase in RSF could be identified with a DS alteration. A significant improvement in SEC was also noted as greater water recoveries were obtained. In the FO mode, the SEC reduced by approximately 58 % for a DS concentration increase of 0.5 to 1 M whilst an additional 35 % reduction was achieved for a DS concentration increase from 1 to 2 M. For the PRO mode similar reductions were observed. At this point, SEC reduced by 53 % for a DS concentration increase of 0.5 to 1 M which reduced by an additional 37 % at a DS concentration increase from 1 to 2 M.

(ii) Membrane orientation

Altering the membrane orientation from FO to PRO mode did not significantly improved system performances as water fluxes, RSF's and water recoveries were nearly identical. Similarly, membrane orientation also did not contribute to a significant reduction in SEC. However, it was noted at a DS concentration of 0.5 M the PRO mode obtained approximately 5.3 % greater water recoveries compared to the FO mode. Conversely, at DS concentrations of 1 and 2 M, the FO mode obtained about 5.4 and 7.0 % greater water recoveries compared to the PRO mode. The only test during which a significant difference in performance was noted was at a DS concentration of 2 M and flow rate of 400 mL/min. At this point, the FO mode produced a greater water flux and so a water recovery compared to the PRO mode. For the same test, the RSF was also estimated to have been greater during the PRO mode than the FO mode.

(iii) Flow rate

The increase in flow rate also did not contribute to a significant FDFO system performance as water fluxes, RSF's and water recoveries were fairly similar. However, it was observed at a DS concentration of 2 M, water fluxes, RSF's and water recoveries were affected the greatest by a flow rate alteration. The increase in flow rate did affect the FDFO SEC due to the fluctuation in pump power consumption. A decrease in pump power consumption was observed at a flow rate increase from 100 to 200 mL/min followed by an increase in power consumption from a flow rate of 200 to 400 mL/min. It was suggested that this non-linear pump power consumption was as a result of regular tubing replacement due to wear.

(iv) Membrane fouling

Throughout the study, no membrane fouling was observed, however, on closer inspection of the membrane surface SEM's, the images indicated possible minute traces fouling. Additionally, by comparing pre- and post-FDFO membrane control water recoveries, a reduction in water recoveries were observed which indicate possible membrane fouling. However, the extent of the membrane fouling of the FDFO was unknown as no correlation between post-FDFO membrane control water recoveries could be linked to irregular FDFO performances.

(v) General

To conclude, the increase of DS concentration significantly improved the FDFO system performance as well as the SEC. However, final fertiliser concentration might exceed the concentration limit for direct fertigation, thus will require further dilution before use. Altering the membrane orientation did not contribute to a significant improvement in system performance nor energy consumption. However, FO mode should be considered to be the most viable orientation as potential fouling can more easily be removed from the membrane surface than in the PRO mode. Also, the increase in flow rate did not contribute a beneficial system performance, however, it did affect the FDFO system energy consumption. Therefore, a low flow rate should be considered in order to save on operational costs as low flow rates will result in similar system performances as higher flow rates. No membrane fouling was observed throughout the study. However, based on the post-FDFO membrane control water recoveries and membrane surface SEM's, minute levels of membrane fouling might have occurred.

5.2 Recommendations

The following recommendations are based on challenges experienced and results obtained from this study.

1. Although no membrane damage was found on a single membrane throughout the study, it is highly recommended not to re-use a membrane to test FO and PRO modes. A new membrane should be used for each designed experiment to prevent defective results. If membranes need to be re-used, membranes should be subjected to a chemical as well as physical cleaning procedure before re-use.

2. The use of flow meters to accurately control flow rate is a necessity as flow rates might become impaired due to tubing wear within a peristaltic pump head which in turn will create a pressure difference ($\Delta P \neq 0$) in the membrane cell which can potentially favour the FS or DS side which could increase or decrease water fluxes.

3. In order to accurately investigate an FDFO systems power consumption a gear, lobe or centrifugal pump etc. should be considered as power consumption data was affected by replacement tubing as well as tubing wear within the peristaltic pump head. Also, the correct pump size for the system should be used.

4. The use of a magnetic stirrer should be considered for both FS and DS to ensure a homogenous solution, thus, ensuring a constant solution EC and OP readings.

5. When investigating RSF whilst using an FS and DS containing solutes, FS samples should be taken at intervals to analysis in order to accurately determine RSF. Conductivity curves can only be used to determined RSF if an FS comprise of deionised water.

6. To more accurately investigate the effects of fouling on an FDFO system by comparing pre- and post-FDFO membrane control water recoveries, it is advisable that control experiments operate longer in order to achieve greater water recoveries which will more useful to investigate the effects of membrane fouling on the FDFO system performance. In addition, real FS's should be considered when investigating the effects of fouling on performance and energy consumptions as it would be more relevant to real-world scenarios.

REFERENCES

Achilli, A., Cath, T. Y. and Childress, A. E. 2009. Power generation with pressure retarded osmosis: An experimental and theoretical investigation. *Journal of Membrane Science*, 343(1–2):42–52.

Achilli, A., Cath, T. Y. and Childress, A. E. 2010. Selection of inorganic-based draw solutions for forward osmosis applications. *Journal of Membrane Science*, 364(1–2):233–241.

AgriSETA 2010. *Sector Analysis Agriculture*. Available at: http://www.agriseta.co.za/downloads/news/AGRISETA_Sector_Analysis_290610-version_2.pdf [1 June 2017].

Akther, N., Sodiq, A., Giwa, A., Daer, S., Arafat, H. A. and Hasan, S. W. 2015. Recent advancements in forward osmosis desalination: A review. *Chemical Engineering Journal*, 281:502–522.

Alexander, M. (ed.) 1981. *Advances in Microbial Ecology*. 1st edn. New York: Plenum Press.

Altaee, A., Zaragoza, G. and van Tonningen, H. R. 2014. Comparison between Forward Osmosis-Reverse Osmosis and Reverse Osmosis processes for seawater desalination. *Desalination*, 336(1):50–57.

Augustine, R. 2017. *Forward osmosis membranes for direct fertigation within the South African wine industry*. Cape Peninsula University of Technology.

Bahar, R., Hawlader, M. N. A. and Woei, L. S. 2004. Performance evaluation of a mechanical vapor compression desalination system. *Desalination*, 166:123–127.

Bitaw, T. N., Park, K. and Yang, D. R. 2016. Optimization on a new hybrid Forward Osmosis-Electrodialysis-Reverse osmosis seawater desalination process. *Desalination*, 398:265–281.

Cai, Y. and Hu, X. M. 2016. A critical review on draw solutes development for forward osmosis. *Desalination*, 391:16–29.

Cath, T. Y., Childress, A. E. and Elimelech, M. 2006. Forward osmosis: Principles, applications, and recent developments. *Journal of Membrane Science*, 281(1–2):70–87.

Chung, T.-S., Li, X., Ong, R. C., Ge, Q., Wang, H. and Han, G. 2012. Emerging forward osmosis (FO) technologies and challenges ahead for clean water and clean energy applications. *Current Opinion in Chemical Engineering*, 1(3):246–257.

Chung, T. S., Luo, L., Wan, C. F., Cui, Y. and Amy, G. 2015. What is next for forward osmosis (FO) and pressure retarded osmosis (PRO). *Separation and Purification Technology*,

156:856–860.

Dabaghian, Z. and Rahimpour, A. 2015. Carboxylated carbon nanofibers as hydrophilic porous material to modification of cellulosic membranes for forward osmosis desalination. *Chemical Engineering Research and Design*, 104:647–657.

Gray, G. T., McCutcheon, J. R. and Elimelech, M. 2006. Internal concentration polarization in forward osmosis: Role of membrane orientation. *Desalination*, 197(1–3):1–8.

Hawari, A. H., Kamal, N. and Altaee, A. 2016. Combined influence of temperature and flow rate of feeds on the performance of forward osmosis. *Desalination*, 398:98–105.

Korenak, J., Basu, S., Balakrishnan, M., Hélix-nielsen, C. and Petrinic, I. 2017. Forward Osmosis in Wastewater Treatment Processes. *Acta Chimica. Slovenica*, 64(1):83–94.

Kumar, R. and Pal, P. 2015. A novel forward osmosis-nano filtration integrated system for coke-oven wastewater reclamation. *Chemical Engineering Research and Design*, 100:542–553.

Larcher, W. 2003. *Physiology Plant ecology: ecophysiology and stress physiology of functional groups*. 4th edn. New York: Springer.

Ling, M. M., Wang, K. Y. and Chung, T. S. 2010. Highly water-soluble magnetic nanoparticles as novel draw solutes in forward osmosis for water reuse. *Industrial and Engineering Chemistry Research*, 49(12):5869–5876.

Lotfi, F., Phuntsho, S., Majeed, T., Kim, K., Han, D. S., Abdel-Wahab, A. and Shon, H. K. 2015. Thin film composite hollow fibre forward osmosis membrane module for the desalination of brackish groundwater for fertigation. *Desalination*, 364:108–118.

Majeed, T., Sahebi, S., Lotfi, F., Kim, J. E., Phuntsho, S., Tijing, L. D. and Shon, H. K. 2015. Fertilizer-drawn forward osmosis for irrigation of tomatoes. *Desalination and Water Treatment*, 53(10):2746–2759.

Mazlan, N. M., Peshev, D. and Livingston, A. G. 2016. Energy consumption for desalination - A comparison of forward osmosis with reverse osmosis, and the potential for perfect membranes. *Desalination*, 377:138–151.

McCutcheon, J. R. and Elimelech, M. 2006. Influence of concentrative and dilutive internal concentration polarization on flux behavior in forward osmosis. *Journal of Membrane Science*, 284(1–2):237–247.

McCutcheon, J. R., McGinnis, R. L. and Elimelech, M. 2006. Desalination by ammonia-carbon dioxide forward osmosis: Influence of draw and feed solution concentrations on process performance. *Journal of Membrane Science*, 278(1–2):114–123.

McGovern, R. K. and Lienhard, J. H. 2014. On the potential of forward osmosis to energetically outperform reverse osmosis desalination. *Journal of Membrane Science*, 469:245–250.

Mi, B. and Elimelech, M. 2008. Chemical and physical aspects of organic fouling of forward osmosis membranes. *Journal of Membrane Science*, 320(1–2):292–302.

National Geographic 2012. *Earth's Freshwater - National Geographic Society*. Available at: https://www.nationalgeographic.org/media/earths-fresh-water/ [4 May 2017].

Pardeshi, P. M., Mungray, A. A. and Mungray, A. K. 2016. Determination of optimum conditions in forward osmosis using a combined Taguchi-neural approach. *Chemical Engineering Research and Design*, 109:215–225.

Park, M., Lee, J. J., Lee, S. and Kim, J. H. 2011. Determination of a constant membrane structure parameter in forward osmosis processes. *Journal of Membrane Science*, 375(1–2):241–248.

Phillip, W. A., Yong, J. S. and Elimelech, M. 2010. Reverse draw solute permeation in forward osmosis: modeling and experiments. *Environmental Science and Technology*, 44(13):5170–5176.

Phuntsho, S., Kim, J. E., Johir, M. A. H., Hong, S., Li, Z., Ghaffour, N., Leiknes, T. O. and Shon, H. K. 2016. Fertiliser drawn forward osmosis process: Pilot-scale desalination of mine impaired water for fertigation. *Journal of Membrane Science*, 508:22–31.

Phuntsho, S., Lotfi, F., Hong, S., Shaffer, D. L., Elimelech, M. and Shon, H. K. 2014. Membrane scaling and flux decline during fertiliser-drawn forward osmosis desalination of brackish groundwater. *Water Research*, 57:172–182.

Phuntsho, S., Sahebi, S., Majeed, T., Lotfi, F., Kim, J. E. and Shon, H. K. 2013. Assessing the major factors affecting the performances of forward osmosis and its implications on the desalination process. *Chemical Engineering Journal*, 231:484–496.

Phuntsho, S., Shon, H. K., Hong, S., Lee, S. and Vigneswaran, S. 2011. A novel low energy fertilizer driven forward osmosis desalination for direct fertigation: Evaluating the performance of fertilizer draw solutions. *Journal of Membrane Science*, 375(1–2):172–181.

Phuntsho, S., Shon, H. K., Hong, S., Lee, S., Vigneswaran, S. and Kandasamy, J. 2012a. Fertiliser drawn forward osmosis desalination: The concept, performance and limitations for fertigation. *Reviews in Environmental Science and Biotechnology*, 11(2):147–168.

Phuntsho, S., Vigneswaran, S., Kandasamy, J., Hong, S., Lee, S. and Shon, H. K. 2012b. Influence of temperature and temperature difference in the performance of forward osmosis desalination process. *Journal of Membrane Science*, 415–416:734–744.

Qasim, M., Darwish, N. A., Sarp, S. and Hilal, N. 2015. Water desalination by forward (direct) osmosis phenomenon: A comprehensive review. *Desalination*, 374:47–69.

Ren, L., Xu, G. and E.A. Kirkby 2015. *The Value of KCl as a Fertilizer with Particular Reference to Chloride: A Mini Review*.

Roberts, T. L. 2009. The role of fertilizer in growing the world's food. *Better Crops*, 93(2):12–15.

Seader, J. D., Henley, E. J. and Roper, D. K. 2011. *Separation Process Principles: Chemical and Biological Operations*. 3rd edn. Hoboken, NJ: John Wiley & Sons.

Shaffer, D. L., Werber, J. R., Jaramillo, H., Lin, S. and Elimelech, M. 2015. Forward osmosis: Where are we now? *Desalination*, 356:271–284.

Shaffer, D. L., Yip, N. Y., Gilron, J. and Elimelech, M. 2012. Seawater desalination for agriculture by integrated forward and reverse osmosis: Improved product water quality for potentially less energy. *Journal of Membrane Science*, 415–416:1–8.

Sinnott, R. K. 2005. *Chemical Engineering Design*. 4th ed. Oxford: Elsevier Butterworth-Heinemann.

Tiraferri, A., Yip, N. Y., Phillip, W. A., Schiffman, J. D. and Elimelech, M. 2011. Relating performance of thin-film composite forward osmosis membranes to support layer formation and structure. *Journal of Membrane Science*, 367(1–2):340–352.

Wang, K. Y., Ong, R. C. and Chung, T.-S. 2010. Double-skinned forward osmosis membranes for reducing internal concentration polarization within the porous sublayer. *Industrial and Engineering Chemistry Research*, 49(10):4824–4831.

Wang, Y., Zhang, M., Liu, Y., Xiao, Q. and Xu, S. 2016. Quantitative evaluation of concentration polarization under different operating conditions for forward osmosis process. *Desalination*, 398:106–113.

WWAP 2016. *(United Nations World Water Assessment Programme). The United Nations World Water Development Report 2016: Water and Jobs*. Paris, UNESCO.

WWAP 2017. *(United Nations World Water Assessment Programme). The United Nations World Water Development Report 2017. Wastewater: The Untapped Resource*. Paris, UNESCO.

WWF-SA 2016. *Water: facts and futures Rethinking South Africa's Water Future*. Cape Town, South Africa.

WWF-SA 2017. *Scenarios for the Future of Water in South Africa*. Cape Town, South Africa.

Xiang, X., Zou, S. and He, Z. 2017. Energy consumption of water recovery from wastewater in a submerged forward osmosis system using commercial liquid fertilizer as a draw solute. *Separation and Purification Technology*, 174:432–438.

Zhao, S. and Zou, L. 2011. Relating solution physicochemical properties to internal concentration polarization in forward osmosis. *Journal of Membrane Science*, 379(1–2):459–467.

Zou, S. and He, Z. 2016. Enhancing wastewater reuse by forward osmosis with self-diluted commercial fertilizers as draw solutes. *Water Research*, 99:235–243.

APPENDIXES

APPENDIX A: Feed and draw solution preparation procedures

All equipment was prepared and calibrated according to the manufacturer's instructions prior to any solution preparation. A 2 L glass laboratory beaker was cleaned thoroughly with soapy water, followed by rinsing with normal tap water to remove soap. This was then followed by additional rinsing with DI water three times to remove all traces of tap water. The beaker was then dried with a paper towel.

A1. Draw solution preparation procedure for the membrane control experiments

The DS utilized in the pre- and post-FDFO membrane control experiments comprised of a 1 M NaCl solution. For this experiment, 0.5 L DS was used. Therefore, the solution was prepared by dissolving 29.22 g of NaCl in 0.5 L DI water.

A2. Feed solution preparation procedure for the fertiliser-drawn forward osmosis experiment

The FS utilized in the FDFO experiment comprised of an SBW5 solution with a salt content of 5 g NaCl per litre of water. For this experiment, 2 L FS was used. Therefore, the solution was prepared by adding 10 g of NaCl to 2 L DI water and mixed until dissolved.

A3. Draw solution preparation procedure for the fertiliser-drawn forward osmosis experiment

The DS utilized in the FDFO experiment comprised of a KCl fertiliser solution. During the study concentrations of 0.5, 1 and 2 M was tested, which correspond to 37.28, 74.55 and 149.10 g KCl per litre of water. For this experiment, 0.5 litre DS was used. Therefore, the solution was prepared by dissolving 18.64 or 37.28 or 74.55 g KCl (Depending on the concentration being tested) into 0.5 L DI water.

APPENDIX B: Membrane damage dye identification procedure

All equipment was prepared and calibrated according to the manufacturer's instructions prior to any solution preparation. A 2 L glass laboratory beaker was cleaned thoroughly with soapy water, followed by rinsing with normal tap water to remove soap. This was then followed by additional rinsing with DI water three times to remove all traces of tap water. The beaker was then dried with a paper towel.

B1. Feed solution preparation procedure for the membrane damage dye identification procedure

The FS used in the membrane damage dye identification procedure comprised of a methyl violet dye solution. For this experiment, 0.5 L FS was used. The solution was prepared by adding 30 drops of a 0.01% methyl violet dye solution (6 drops per 100 mL FS) to 0.5 L DI water and mixed thoroughly.

B2. Draw solution preparation procedure for the membrane damage dye identification procedure

The DS used for the membrane damage dye identification procedure consisted of a 2 M NaCl solution, therefore 58.44 g NaCl was dissolved in 0.5 L DI water.

APPENDIX C: Forward osmosis membrane preparation

The CTA membranes were supplied in 40 cm x 40 cm sheets and required an adjustment in order to fit within the FO membrane cell (membrane size 42 cm^2). The membrane was cut using a pair of scissors and with the aid of a plastic membrane stencil (Sterlitech^{TM} Co., Washington, USA). Latex laboratory gloves were worn to prevent possible damage to the membrane during the cutting process. A membrane sheet was positioned onto a clean working surface followed by tracing the membrane using the membrane stencil followed by cutting the membrane. Thereafter, the cut membrane was positioned into a clean ziplock plastic bag followed by the addition of 20 mL DI water to prevent the membrane from drying out. The bag was closed and positioned flat into a laboratory refrigerator at 5 ^{0}C for storage.

APPENDIX D: Custom build equipment

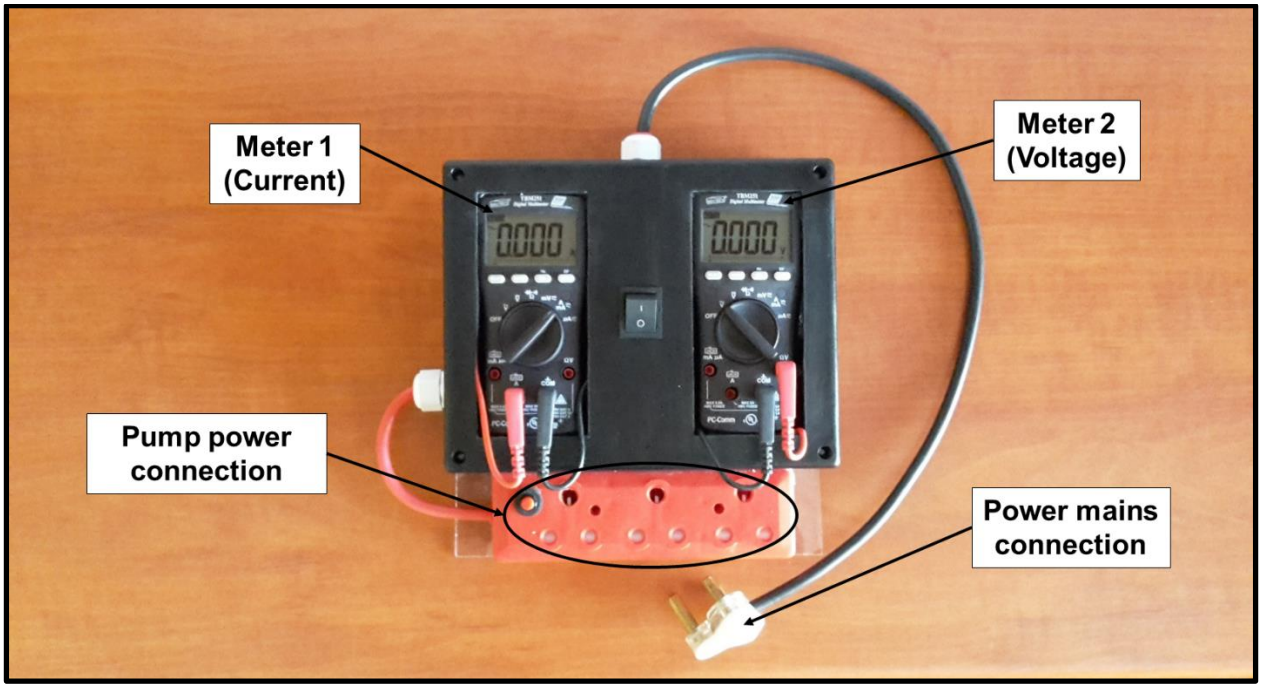

Figure D1: Custom build electrical multimeter used to determine pump power consumption

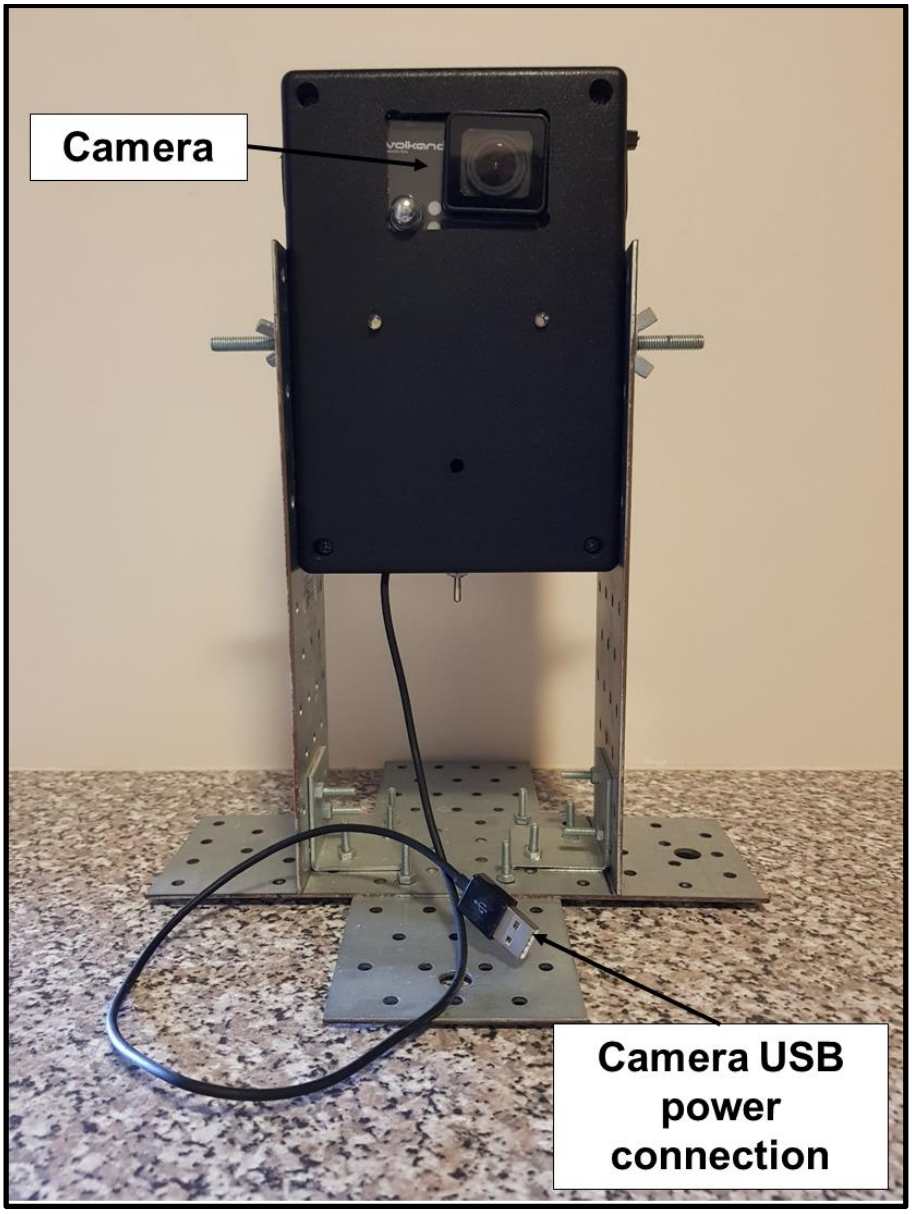

Figure D2: Custom build portable camera used for data capture

APPENDIX E: Forward osmosis membrane damage example images

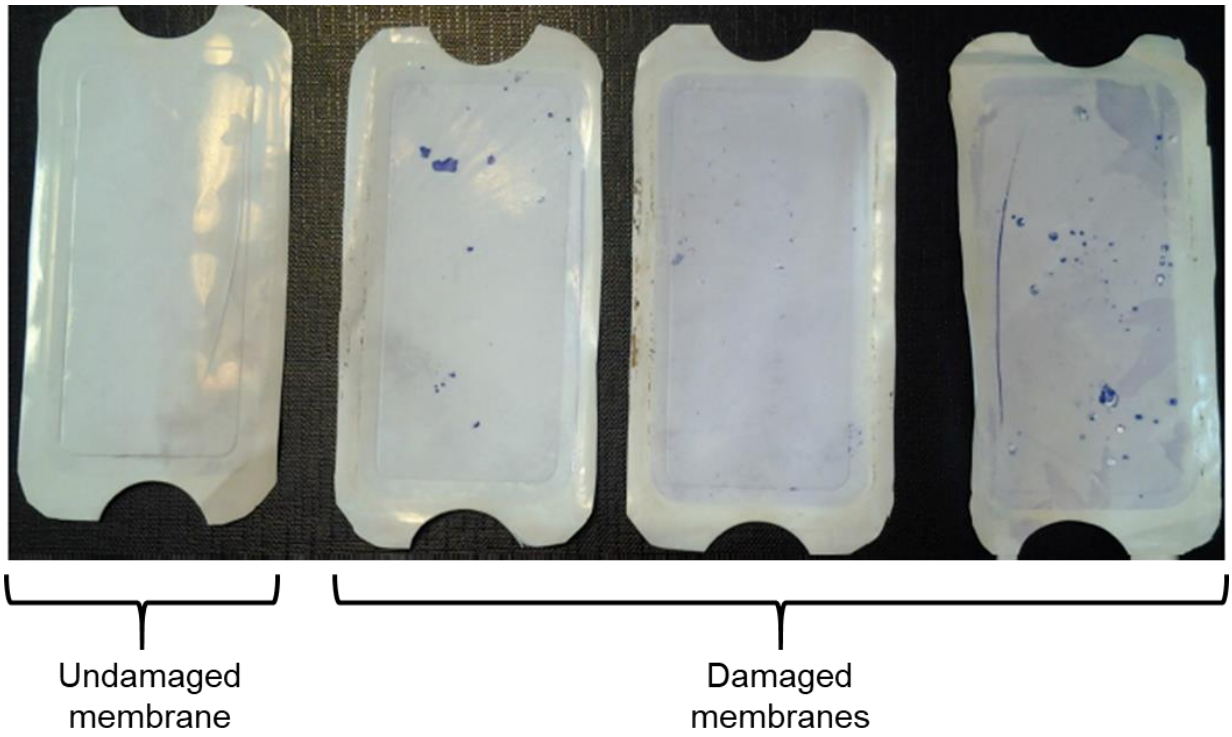

Figure E1: Comparison between undamaged and damaged FO membranes using a methyl violet dye solution

APPENDIX F: Sample calculations

F1. Osmotic pressure sample calculation

$$\frac{1\,Osmole}{kg}H_2O = 2.48\,MPa$$

$$\frac{1\,mOsmole}{1\,kg}H_2O = \frac{0.001\,Osmole}{kg}H_2O$$

$$\frac{1\,mOsmole}{kg}H_2O = 2.48\,kPa$$

$1\,mOsmole = 2.48\,kPa$

$1883\,mOsmole = x$

$\underline{x = 4669.84 \approx 4670\,kPa}$

F2. Water flux sample calculation

$$J_W = \frac{m_{DS_{t_2}} - m_{DS_{t_1}}}{\rho \cdot A_m \cdot (t_2 - t_1)}$$

It is assumed that the change in mass of the DS is mainly attributed to the permeation of pure water. Therefore, the density (ρ = 1000 g/L) of water was used.

Calculating water flux

$J_w = ?\,L/m^2.h$

$m_{DS_{t_1}} = 473.4\,g$

$m_{DS_{t_2}} = 482.6\,g$

$\rho = 1000\,g/L$

$A_m = 0.0042\,m^2$

$t_1 = 0\,h$

$t_2 = 1\,h$

$J_w = Water\ flux\ (L/m^2.h)$

$m_{DS_{t_1}} = Mass\ of\ DS\ at\ time\ interval\ 1\ (g)$

$m_{DS_{t_2}} = Mass\ of\ DS\ at\ time\ interval\ 2\ (g)$

$\rho = Density\ (g/L)$

$A_m = Effective\ membrane\ area\ (m^2)$

$t_1 = Time\ interval\ 1\ (h)$

$t_2 = Time\ interval\ 2\ (h)$

$$J_W = \frac{(482.6 - 473.4)}{(1000) \cdot (0.0042) \cdot (1 - 0)}$$

$$J_W = 2.19\ L/m^2.h$$

F3. Reverse solute flux sample calculation

$$J_S = \frac{V_{FS_{t_2}} . C_{FS_{t_2}} - V_{FS_{t_1}} . C_{FS_{t_1}}}{A_m \cdot (t_2 - t_1)}$$

Calculating RSF

$J_S = ?\ g/m^2.h$

$V_{FS_{t_1}} = 1.95\ L$

$V_{FS_{t_2}} = 1.94\ L$

$C_{FS_{t_1}} = 0.072\ g/L$

$C_{FS_{t_2}} = 0.073\ g/L$

$A_m = 0.0042\ m^2$

$t_1 = 0\ h$

$t_2 = 1\ h$

$$J_S = \frac{(1.94) \cdot (0.073) - (1.95) \cdot (0.072)}{0.0042 \cdot (1 - 0)}$$

$$J_S = 0.29\ g/m^2.h$$

$J_S = RSF\ (g/m^2.h)$

$V_{FS_{t_1}} = Volume\ of\ the\ FS\ at\ time\ interval\ 1\ (L)$

$V_{FS_{t_2}} = Volume\ of\ the\ FS\ at\ time\ interval\ 2\ (L)$

$C_{FS_{t_1}} = Mass\ concentration\ of\ the\ FS\ at\ time\ interval\ 1\ (g/L)$

$C_{FS_{t_2}} = Mass\ concentration\ of\ the\ FS\ at\ time\ interval\ 2\ (g/L)$

$A_m = Effective\ membrane\ area\ (m^2)$

$t_1 = Time\ interval\ 1\ (h)$

$t_2 = Time\ interval\ 2\ (h)$

F4. Volume water recovery sample calculation

$$Volume\ water\ recovery = V_{FS_{t_1}} - \left(V_{FS_{t_1}} - \left(\frac{m_{DS_{t_2}} - m_{DS_{t_1}}}{\rho} \right) \right)$$

Calculating volume water recovered

$Volume\ water\ recovery = ?\ mL$

$V_{FS_{t_1}} = 1.95\ L$

$m_{DS_{t_1}} = 462.3\ g$

$m_{DS_{t_2}} = 567.7\ g$

$\rho = 1000\ g/L$

$V_{FS_{t_1}} = Volume\ of\ the\ FS\ at\ time\ interval\ 1\ (L)$

$m_{DS_{t_1}} = Mass\ of\ DS\ at\ time\ interval\ 1\ (g)$

$m_{DS_{t_2}} = Mass\ of\ DS\ at\ time\ interval\ 2\ (g)$

$\rho = Density\ (g/L)$

$$Volume\ water\ recovery = 1.95 - \left(1.95 - \left(\frac{567.7 - 462.3}{1000} \right) \right)$$

$$Volume\ water\ recovery = 0.1054\ L \approx 105.4\ mL$$

F5. System specific energy consumption sample calculation

$$SEC = \frac{(PF \cdot V_{Volt} \cdot I_{Amp}) \cdot (Total\ hours\ of\ operation)}{(1000) \cdot (Total\ volume\ recovered\ for\ hours\ of\ operation)}$$

Calculating SEC

$SEC = ?\ kWh/m^3$

$PF = 1$

$V_{Volt} = 229.80\ W/A$

$I_{Amp} = 0.049\ A$

$SEC = Specific\ energy\ consumption\ (kWh/m^3)$

$V_{Volt} = Voltage\ (W/A)$

$I_{Amp} = Current\ (A)$

$PF = Power\ factor\ (Dimentionless)$

$Total\ hours\ of\ operation = 24$

$Total\ volume\ recoverd\ in\ 24\ hours\ of\ operation = 370\ mL \approx 3.7x10^{-4}\ m^3$

$$SEC = \frac{(1)\cdot(229.80)\cdot(0.049)\cdot(24)}{(1000)\cdot(3.7x10^{-4})}$$

$$\underline{SEC = 730.4\ kWh/m^3}$$